THE STRUCTURAL BEHAVIOR AND CRACK PATTERNS OF HIGHER STRENGTH CONCRETE BEAMS

BY

ABDEL-AZIZ A. MAKKAWY

B.S., CAIRO UNIVERSITY, 1979

205

A MASTER'S THESIS

SUBMITTED IN PARTIAL FULFILLMENT

OF THE REQUIREMENTS FOR THE DEGREE

MASTER OF SCIENCE

DEPARTMENT OF CIVIL ENGINEERING

KANSAS STATE UNIVERSITY

MANHATTAN, KANSAS

1986

APPROVED BY

Stuart E Swartz

MAJOR PROFESSOR

TABLE OF CONTENTS

TABLE OF CONTENTS CONTINUED...

TABLE OF CONTENTS CONTINUED...

TABLE OF CONTENTS CONTINUED...

LIST OF TABLES

LIST OF TABLES CONTINUED...

LIST OF TABLES CONTINUED...

LIST OF FIGURES

LIST OF FIGURES CONTINUED...

LIST OF FIGURES CONTINUED...

LIST OF FIGURES CONTINUED...

LIST OF FIGURES CONTINUED...

CHAPTER 1

INTRODUCTION

Dnriug the last century the mechauical strength of coucrete varied little. Researchers paid more attention to decreasiug the design safety factor rather than increasing the nltimate strength of concrete. The ratio betweeu nltimate stress and service stress has decreased dne to a greater knowledge of the mechanical properties of the materials used and also better quality staudards of these materials.

In the last decade there has beeu a rapid growth in the intrest of higher streugth coucrete. Because of the development of high rauge water-rednciug admixtnres aud reliable machinery for mixiug and trausporting, high strength coucrete has become a field product rather than a laboratory prodnct (24).

The developmeut of higher strength coucrete has spawned a rise iu many uses for a more viable prodnct. Dnriug 1982, water reducing chemical admixtnres of all types, inclndiug high range water-redneiug admixtnres, were used in an estimated 112 million cubic yards (85 million cnbic meters) of concrete in the United States. This is the equivalent of abont 71 percent of all concrete nsed in this conntry (15).

In this investigation, the classification of higher strength concrete according to its nniaxial compressive strength is as follows:

6,000 --> 12,000 psi (41.4 --> 82.7 MPa)	Higher Strength Concrete
Greater than 12,000 psi (>82.7 MPa)	High Strength Concrete

Higher Strength Conorete Usage

Builders were quick to see the advantages of using higher strength concrete. High rise bnildings and long span bridges have especially benefited from the latest resesrch and designs. The cost faotor is also advantageons. Examples are as follows.

1. In tall concrete bnildings the nse of higher strength concrete provides the following:

   a. It prodnces smaller columns in lower floors. Conseqnently there is more income-prodncing floor area.

   b. It rednces the total bnilding weight and height for a given nnmber of stories. These reduotions are significant in seismic design where mass and height are critical variables.

2. For long-span bridges, the combination of high-strength concrete reduces dead load and with prestressing to control deflection, has extended the range of concrete bridge spans to over 900 feet (274 m) (24).

Research Basis and Objectives

Important design equations found in the ACI 318-83 Code (32) are derived from tests of materials and members for which the compressive strengths were mostly less than 6,000 psi (24). Caution should be exercised in extrapolating data from lower strength to higher strength concrete (38). This problem led to an enlarged research area for studying the mechanical properties as well as the structural behavior of higher strength concrete.

Several research programs have been carried out in different universities around the country. The research reported herein is part of an extensive program at Kansas State University. The objectives of this work are the following:

1. To study the compressive stress block of higher strength concrete beams with different steel ratios, made using locally - available aggregates. The nominal compressive strength is 12,000 psi (87.2 MPa).

2. To determine the strain corresponding to the nltimate compressive strength f'_c .

3. To stndy the changes in the maximum bottom crack width and crack propagation at different load increments.

4. To verify the validity of different formnlas that oalcnlate vertical deflection and maximum crack width (based on normal strength concrete) for higher strength concrete.

CHAPTER 2

SELECTION OF MATERIALS

Introduction

Strength, cost, and field performance are the governing factors in developing the optimum mixture for higher atrength conorete (5). It reqnires the highest qnality of materials which should be pnrchaaed locally for economic reasons. Becanse of the variance in day to day nse of materiala in the field, carefnl consideration mnst be taken with quality control (35).

In designing higher atrength concrete atructural elements, it is more appropriste to uae steel reinforcing bars with a higher grade. This combination increases the load carrying capaoity of the strnctural element.

Steel Reinforcing Bara

Deformed bars of Grade 60 were considered for design. Samples of #3, #4, #7, and #9 bara were tested to find the yield point. Reanlts are shown in Fignre 2.1 and Table 2.1.

Higher Strength Concrete Ingredients

Cement

There are many factors that are important when dealing with the control of quality and uniformity of cement production. Even though Portland Cement is the recommended choice for higher strength concrete, chemical composition (ASTM C-114), cement fineness (ASTM C-115), and cube strength (by ASTM C-109), are the most important for quality control.

Cement is one of the major factors attributed to concrete strength. Various cements have different effects on concrete compressive strength. This is shown in Figure 2.2. Experiments such as Blick's (2) show results indicating that there is an agreement between the compressive strength values for mortar cubes and concrete cubes when using the same type of cement. Even with these test results, it is recommended that periodic sampling and testing be done during the course of a project.

Coarse Aggregates

Coarse aggregates occupy a relatively large portion of concrete volume and therefore their selection is important. Different types of aggregates with the same mix proportion resulted in variations of the compressive strength as much as twenty nine percent (12).

The basis for aelecting cosrae aggregates for higher strength concrete is different from that of normal strength concrete. In normal strength concrete, the quality of hsrdened cement paate has a grester effect on the compressive strength than coarse aggregatea (5). In higher strength concrete the cement psste and coarse aggrsgstes have almoat the same compressive strength.

The following are important factors to be conaidered when selecting coarse aggregstes for higher strength concrete:

1. strength
2. particle shape and surfsce textnre
3. maximum size snd gradation
4. mineralogy and formation
5. aggregate-paste bond

Strength

In normsl strength concrete, the mechsnical interlocking of the coarse sggregatea contributes to the compressive strength of the concrete (12). This is verified by the shape of the fsilure snrface which is highly irregular and inclndea a large smonnt of bond failure (7).

In higher strength concrete cosrse aggregates with a compressive strength eqnal to or greater than that of the hardened cement are required.

Most qnality aggregates available today have a crnshing strength of over 12,000 psi (82.7 MPa).

<u>Particle Shape and Surface Texture</u>

The workability of fresh concrete and the mechanical interlock of hardened concrete are affected by the particle shape of the coarse aggregates. Crnshed stone aggregates with a cnbic angnlar shape and a minimum content of flat and elongated particles, are the best choice for higher strength concrete (35). Crnshed stone coarse aggregates prodnce stronger concrete than a ronnded coarse aggregates. Fignre 2.3 showa a comparison between two types of conrse aggregates on the basis of compressive strength.

Changes in particle shape and textnre also affect the mixing water reqnirement. Freedman (8) proposed the nae of the void content as an index of differnce in particle shape and textnre of aggregates of the same grading.

<u>Maximum Size and Gradation</u>

The water reqnirement for the concrete mix is affected by the snrface area of coarse aggregates which is a fnnction or the maximum aggregate size. Several researchers (3,4,and 14) have conclnded that in higher strength concrete mixtures, the compressive strength increases as the aggregate size decreases. There must be some limitations to this conclusion in order to avoid excessive secondary effects such as shrinkage and creep.

At each strength level there is an optimum size for the different types of aggregates. It is recommended that trial batches be performed for each specific job application. A maximum value of 0.4 in. (10 mm) is usually acceptable for most applications (39). Figure 2.4 shows the maximum size aggregate for strength efficiency envelope.

A uniform grading is preferable to obtain the densest mix and enhanse the degree of compaction. It is important to have the coarse aggregates free from detrimental dust coatings that may affect the water requirements of the mix and also the strength. It is always recommended that the crushed stone aggregates be washed before use (36).

Mineralogy and Formation

Parrot (21) concluded that the rock formation has an effect on the compressive strength of concrete. As the Concrete ages, the effect is more pronounced. An example of the mineralogy effect on concrete strength was a test using granite rock. A concrete strength of 17,000 psi (117 MPa) was achieved (28).

Aggregate-Paste Bond

Bond strength depends on the paste strength as well as aggregate properties. Better bonding is usually obtained with softer, porous and mineralogically heterogeneous aggregate particles. Bond strength is also affected by the chemical properties of the aggregates.

A stronger aggregate-paste bond is necessary in producing higher strength concrete. The use of quality crushed stone meeting ASTM C-33 requirements provides adequate bond strength properties (36). Alexander (1) concluded that the use of angular shaped crushed stone aggregates with a maximum size of 1/2 inch produces the best results of bond strength.

In this investigation, quartzite stone with 3/4 inch maximum size, from Lincoln, Kansas was used. A previous study involving the sieve analysis and physical properties of quartzite was completed by Nikaeen (18) at Kansas State University.

Fine Aggregates

The use of fine aggregates in higher strength concrete is necessary to improve workability and surface finishing. This is important because the crushed stone commonly used for aggregates reduces workabality and results in a rough surface.

Rounded and smoother particles of sand are more appropriate than sharp, angular, and rough sands for higher strength concrete (16). Natural sands are better than manufactured sand because they produce higher strengths in concrete (5).

Gradation of fine aggregates for higher strength concrete is governed by the effect on water requirements of the mix (38). Aggregates with a fineness modulus of 2.7 - 3.2 have been most satisfactorly used in higher strength concrete (29). In this investigation, Kaw River sand passed through sieve number four was used. The characteristics of this sand were reported by Nikaeen (18).

Water

Water quality requirements are the same for both higher strength and conventional concrete (38). Mixing water is specified to be of potable quality. At times when mixing water of a poor quality must be used, specimens made with this water should be compression tested at seven and twenty eight days. The water is acceptable if the loss of compressive strength does not exceed ten percent of the strength of specimens made using distilled water (ASTM 94), (34).

Water-Reducing Admixtures

Water reducing admixtures reduce the water requirements of the concrete mix or increase the slump of freshly mixed concrete. Superplasticizers, (high-range water-reducing admixtures) are commonly used in the production of higher strength concrete. Their use greatly reduces the water required to produce a fresh concrete mix. This is particularly important in higher strength concrete due to the requirement of a low water-cement ratio and the use of crushed stones in the mixture. The above requirements decrease the workability of fresh concrete mix.

It is recommended that testing of trial mixes be conducted to determine the amount of superplasticizer to be used in higher strength concrete. Superplasticizers must be used with caution due to side effects with some types of cement (33). In this investigation, a Sikament type superplasticizer was used.

CHAPTER 3

MIX PROPORTIONING

Introduction

The mix proportion is more important in higher strength than in normal atrength concrete (38). The two major factora that direct higher strength concrete mix design are the workability of the fresh concrete and the compressive strength of hardened concrete. A very low water-cement ratio is nsnally nsed to satisfy the atrength reqnirement. The use of snperplasticizers is necesaary to maintain the workability and for compaction pnrposes.

The mix design must satiafy both strength and workability requirements. Cement content, water content and aggregate proportion are factors that affect the final mix characteristics. Many trial batches of concrete are often reqnired to identify optimum mix proportions.

Cement Content

In each mix design there is an optimum cement content. The strength of concrete may decrease if the cement content is lower or higher than the optimum value. This valne dependa on aggregate type, aggregate size, mixing conditions, cost, slump level, cement fineness, and the amount of entrained air (5).

Water-Cement Ratio

The relationship between water-cement ratio and compressive strength for lower strength concrete is valid for higher strength concrete. A rednction in the water-cement ratio increases the compressive strength. However, the minimum valne of the water-cemcnt ratio is governed by the minimum amonnt of water reqnired for the hydration process and the workability reqnired for good compaction (5).

The nse of snperplacticizers has provided for the nse of lower water-cement ratios and higher slumps. Water-cement ratioa, by weight, have ranged from 0.27 to 0.5 (38). The water-cement ratio sometimes inclndea the qnantity of snperplasticizer nsed.

Aggregate Proportions

Fine aggregates have considerably more impact on the mix proportions of higher strength conorete than coarse aggregatea. The particle shape and gradation of fine aggregates play an important role in the properties of fresh as well as hardened concrete. The amonnt of sand nsed in the concrete mix providea for the necessary workability and the highest strength for a givcn paste (38).

The proportion of fine to coarse aggregates has a direct qnantitative effect on the paste reqnired. The optimum amonnt and size of coarse aggregates for a given sand dependa to a great extent on the fineness modulus of the aand (38).

In conclnsion, aggregate content and the fine to coarse aggregate ratio for a given mix are determined so that the required characteristics of fresh concrete as well as hardened concrete are satisfied. Trial batches are recommended as the best way to find these ratios.

Research Investigation of the Mix Proportions

Previons investigations (10,17,18,and 23), have yielded four mix proportions that successfnlly satiafied strength reqnirements ranging from 8,400 to 12,000 psi (57.9 to 82.7 MPa). Table 3.1 shows the different mix proportions used for the concrete strength levels. In this research, the aame types of materials were used to provide for similar concrete strength levels (12,000 psi) which was required.

The change in the properties of mix ingredients with age made it necessary to determine the mix proportions by making trial batches. The mix proportions preaented in table 3.1 for the atrength level of 12,000 psi were appropriate values to begin with.

Ten trial mixes were created using the same cement, quartzite, and sand content. Assorted water-cement ratios were used for different trials. Different amounts of superplasticizer (included in water-cement ratio calculation) were also used. The water-cement ratio in the mix trials ranged from 0.28 to 0.3. The ratio of superplasticizer to the water content ranged from 0.12 to 0.17, by weight.

A reduction in the slump from 2.75 in. to 0.25 in. was observed as the water-cement ratio decreased from 0.3 to 0.28. During this time the 3-day cylinder compressive strength indicated an increase of 5,300 to 6,100 psi, (36.5 to 42 MPa), as the water-cement ratio decreased from 0.3 to 0.28.

The water content was slightly adjusted to meet workability requirements due to the difference in characteristics between the small mixer used in trial mixes and the large mixer used for the test specimens. The water content was also adjusted due to the different conditions of temprature, humidity, etc. The mix proportions used for different beam test specimens are presented in Table 3.2. The 3-day cylinder test results are shown in Table 3.3.

CHAPTER 4

DISCUSSION OF TEST PURPOSE AND DESIGN

Introduction

Extensive experimentation at several research centers have provided a fundamental understanding of the behavior of higher strength concrete. However, different conclusions have been obtained at different phases of experimentation. Because of this, it seemed likely that further work needed to be done in this field to verify the different conclusions. The ultimate compressive strain and the shape of the compressive stress block are two of the questionable areas for study.

Strain at Ultimate Stress

The ultimate strain value of 0.003 in./in. specified by the ACI Code (32) is based on testing concrete of normal strength. Different values for ultimate strain have been obtained for higher strength concrete. Hognestad (11) reported that with increasing concrete strengths, the maximum concrete strain becomes progressively smaller. Wang, Shah, and Naaman (30) observed that the maximum concrete compressive strain was always higher than 0.003. Carrasquillo, Nilson and Slate (6) reached the same conclusion. The state-of-the-art report on higher strength concrete (38) conclnded that 0.003 in./in. seemed to represent satisfactorly the nltimate compressive atrain of higher strength concrete, althongh it is not a oonservative valne for the nltimate oompressive strain. Other researchers (10, 17, and 23) have recommended that 0.0025 in./in. is a good estimate for nse.

The above mentioned differences may be conclnded from the nse of different types of mix ingredients which will definitely change the concrete characteriatics. However, the stndy of the nltimate compressive strain was part of this research.

Shape of the Compressive Stress Block

A rectangnlar compressive stress block with a β_1 factor varying from 0.85 to 0.65 waa specified by the ACI Code (32). β_1 haa a specified constant valne for all concretes with compresaive strength above 8,000 psi (55.1 MPa). It was this fact that enconraged reaearchers to investigate the validity of the rectangnlar stress block for higher atrength concrete. Different investigators made different snggestions for the shape of the compressive stresa block for higher strength concrete.

Lealie, Rajagopalan, and Everard (13) snggested that the triangnlar streas block will predict the behavior of over-reinforced beams better than the ACI Bnilding Code. Narayanan (17) snggested a parabolic streas block for over-reinforced beams. The parabolic stress block was also suggested by Hiremagalur (10) and Refai (23). The triangular stress block was suggested by Nikaeen (18).

Wang, Shah, and Naaman (30) concluded that the rectangular stress distribution gave a sufficiently accurate prediction of the ultimate loads and moments for reinforced concrete beams and columns made with higher strength concrete. Based on the wide variety of conclusions and suggestions, the shape of the compressive stress block was chosen to be investigated in this research.

Vertical Deflection

The ACI Code formula for vertical deflection is based on the effective moment of inertia of a concrete section and also concrete elastic modulus. The effective moment of inertia is a function of the modulus of rupture of the concrete. Zia (31) suggested that the ACI formula for estimating vertical deflecton is valid for higher strength concrete but needs the use of appropriate expressions for the elastic modulus and the modulus of rupture of concrete. These expressions are results of research at Cornell University (6).

$$E_c = 40{,}000 \sqrt{f'_c} + 1{,}000{,}000 \text{ psi} \quad \ldots\ldots (4.1)$$

for 3,000 psi $< f'_c <$ 12,000 psi

or

$(E_c = 3320\sqrt{f'_c} + 6900$ MPa

for 21 MPa $< f'_c <$ 83 MPa)

$f_r = 11.7\ \sqrt{f'_c}$ psi . . . . (4.2)

for 3,000 psi $< f'_c <$ 12,000 psi

or

$(f_r = 0.94\ \sqrt{f'_c}$ MPa

for 21 MPa $< f'_c <$ 83 MPa)

Pretorins (22) has presented a simplified approach based on the cracked moment of inertia. His expression for the short-term deflection of singly reinforced beams was:

$\Delta = K \cdot M_{max} \cdot L^2 / (E_c \cdot I_{cr})$ . . . . . (4.3)

where

Δ = midspan vertical deflection, in.

K = 23 / 216

M_{max} = maximum moment, in.-K

L = span length, in.

E_c = modulna of elasticity of concrete, ksi

I_{cr} = cracked monemt of inertia, in.^{4}

It is intended here to compare the vertical deflections naing test data against thoae calcnlated valnes nsing both the ACI Code and the Pretorins simplified approach.

Maximum Bottom Crack Width

Gergely and Lutz (9) suggested an expression for the maximum bottom crack width for concrete:

$$w = 0.091 \cdot \sqrt[3]{t_b A} \cdot R \cdot (f_s - 5) \; . \; . \; . \; . \; . \; . \; (4.4)$$

where

w = maximum bottom crack width, in. x 10^{-3}

t_b = bottom clear cover, in.

A = A_e / m

A_e = 2 b (t - d), in.^{2}

m = no. of steel bars

R = h_2 / h_1

f_s = steel stress, ksi

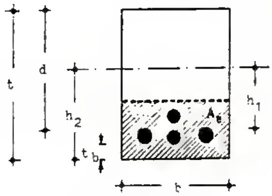

Dimensional Notation

This expression was based on specimens made of normal strength concrete. The validity of the expression for higher strength concrete is investigated in this research.

Based on the previous discussion, the research has been organized into the following functional steps:

1. To design four beams with different steel ratios, (0.75 ρ_b, 0.5 ρ_b, 0.25 ρ_b, and 200/f_y).
2. To test the beams under symmetric loading at the third points and collect strain data at each loading stage.

3. To measure the vertical deflection at the center line of each test specimen for each different load stage.

4. To trace the crack propagation and measnre the maximum crack width on both sides of the test specimen at each load stage.

Test Elements and Techniqnes Used

The availability of a wooden form shown in Fignre 4.1 and also a steel loading beam shown in Fignre 4.2, made it convenient to choose rectangnlar beams with a total length of 7.5 ft. (2286 mm) and cross-sectional dimensions of 8 x 12 in. (203 x 305 mm).

The beams were designed with the above mentioned ateel ratios. The stndy of the bending behavior of nnder-reinforced beams was the target of this investigation. Stirrnps were nsed in the onter thirds of the beam to avoid diagonal tension failnre.

The preliminary beam design based on the nse of grade 60 steel is reported in Table 4.1. Fignre 4.3 shows the reinforcement details of beam #1 with a steel ratio of 0.75 ρ_b. Fignre 4.4 shows the reinforcement details of beam #2 with a steel ratio of 0.5 ρ_b. Fignre 4.5 shows the reinforcement details of beam #3 with a steel ratio of 0.25 ρ_b. Fignre 4.6 ahows the reinforcement details of beam #4 with a steel ratio of 0.07 ρ_b.

The calcnlation waa revised based on the actnal yield stress of different steel reinforcing bars. Table 4.2

presents the revised design calculation. The revised value for the stirrup spacing for beam #2 turned out to be smaller than the actual value used for the beam. Because of this, a diagonal tension failure was predicted for this beam.

The revised value of the steel ratio for beam #1 was equal to ρ_b. The revised stirrup spacing was slightly smaller than the actual spacing used for this beam. A balanced failure (simultaneous compressive-tensile failure), or a diagonal tension failure was predicted for beam #1. Both preliminary and revised calculations are shown in Appendix II.

Strain values were measured with electrical resistance strain gages, type EA-06-240LZ-120. The characteristics of this type of gage are shown in ref. (37). The same arrangement of twenty four gages shown in Figure 4.7 was used for all test beams. Two, short,gage-length gages were placed 2.5 in. apart at each gage location. This was done to avoid the effect of coarse aggregate size which could provide misleading data if a longer gage was used. During the testing operation, strain gages were connected to a high-speed data aqnisition system in order to record the strain data at each load stage.

Figure 4.8 shows the test setup and loading arrangement that was used for different beams. With the assemblage of the strain data for the whole testing course, a complete pictnre of the actual straiu distribntion at the test specimeu's center line can be visnalized.

To measure the compressive streugth of coucrete, 3 in. x 6 in. cylinders were used. A dial gage was used to measure the strain correspondiug to different stress levels.

A magnifying measnriug tool with an accuracy of 0.02 mm (0.0008 in.) wss nsed to measnre the maximum crack width at different losd stages. Auother tool with a relatively smaller magnificstion factor was used to trace the propagations of cracks at each load stage.

Focns on Aualysis Goals

The previons seotion discnssed different techniques nsed to obtain the necessary data ueeded for analysis. The analytical part of this research was based iu part on statisticsl sualysis usiug the Statistical Aualysis System (SAS) available on the main frame compnter at Kausas Stste University.

The maiu goals of analysis were, to obtain a mathematical model for the stress-straiu relationship as a basis for stress-strain transformations, to find reasonable regressiou models for both strain and stress distribntions for differeut loading stages, and to compare with resnlts obtaiued from different expressions for vertical deflection and maximum bottom crack width.

Strain Regression Model

An important part of the snalyais wss to fit a straight line model nsing least sqnsre regression throngh the actnsl strain data obtained at esch load stage for different test beams. This step is important becanse s straight line strain distribntion ia a bssic assnmption for all formnlas of analysis in this ares.

Compressive Stress Block Regression Model

A part of this resesrch was to find the compressive stress block based on the actnal strsin dats and the stress-strain model derived from testing cylinders, and also to find a regression model for the compressive atreas block based on the straight line strain regression models and the stress-strsin model derived from cylinder testing. It is clear that both rectangnlar and triangnlar stress diatribntions can be obtained provided one finds the position of the nentral axis from the strain straight line regression model snd determines the nltimate compressive stress f'_c fonnd in the compressive stress block regression model. Valnes corresponding to each load level csn be derived nsing thia process.

Moment Calculation Based on Test Data

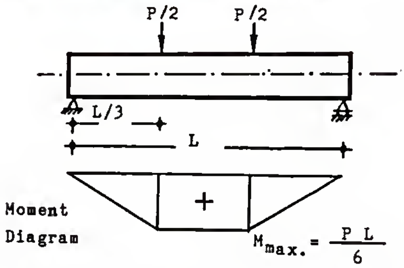

The Figure above shows that the maximum moment at each load stage is PL/6. A linear load-monemt relation is obtained for all loading stages based on test data.

Moment Calculation Using Compressive Stress Block Regression Model

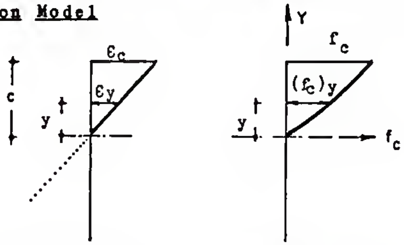

Linear Strain
Reg. Model

Stress Cubic
Reg. Model

The calculation of moments using the compressive stress block regression model was based on integrating the functions obtained by regression in order to find the resultant force. The line of action of this force was determined by integrating the first moment of area of the stress block around the neutral axis. The lever arm then can be determined and consequently the internal moment value. More details about this procedure are in Appendix II.

Moment Calculation Using Rectangular Stress Block

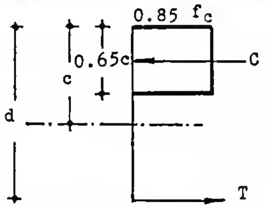

Rectangular Stress Distribution

The ACI Code 318-83 (32) suggests the rectangular stress block for moment calculation. In the illustration figure above, the value of c can be obtained from the strain regression model. The value of the compressive stress at the top fibers, can be obtained from the compressive stress block regression model. Then the following equation can be used to evaluate the compressive force C.

$$C = (0.85\ f_c) \cdot (0.65\ c) \cdot b \qquad \ldots (4.5)$$

Also the moment can be calculated using this formula:

$$M = (d - 0.325\ c) \cdot C \qquad \ldots\ldots (4.6)$$

Moment Calculation Using Triangular Stress Block

The stress-strain relationship is more linear for higher strength concrete (19). Consequently, a more linear compressive stress block can be predicted. Then, the use of a triangular stress block is a convenient and simple approach. A triangular stress block yields a smaller value of the compressive force C than a parabolic stress block does. However, it also slightly increases the lever arm in moment calculation.

The following equations are used to obtain the compressive force C and the moment M, using a triangular stress block.

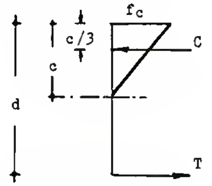

Triangular Stress Distribution

$$C = 0.5\ f_c \cdot c \cdot b \qquad \ldots\ldots\ldots \quad (4.7)$$

where

f_c = compressive stress at the top surface obtained by regression

c = depth of the neutral axis obtained by regression

$$M = (d - 0.33\ c) \cdot C \qquad \ldots\ldots \quad (4.8)$$

Vertical Deflection at Midspan

The test data obtained for vertical deflection were intended to be compared with calculated values using the ACI Code formula (32) and also Pretorius' simplified approach (22). The ACI equation is as follows:

$$\Delta_{max} = \beta_a \cdot M_{max} \cdot L^2 / (E_c \cdot I_e) \quad \text{in.} \quad \ldots (4.9)$$

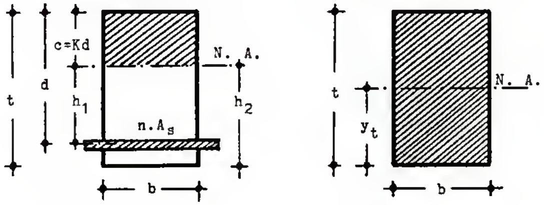

Cracked Section Notation

Gross Section Notation

where

β_a = 23/216

M_{max} = maximum moment, in.-K

M_{max} = PL / 6

I_e = effective moment of inertia, in.^{4}

$$= \left(\frac{M_{cr}}{M_{max}}\right)^3 \cdot I_g + \left[1 - \left(\frac{M_{cr}}{M_{max}}\right)^3\right] \cdot I_{cr} \leq I_g$$

M_{cr} = cracking moment, in.-K

$= f_r \cdot I_g / y_t$

f_r = modulus of rupture of concrete, ksi

$= 7.5 \sqrt{f'_c}$

I_g = gross moment of inertia, in.^{4}

$= b \cdot t^3 / 12$

I_{cr} = cracking moment of inertia, in.^{4}

$= b \cdot c^3 / 3 + n \cdot A_s \cdot h_1^2$

n = modular ratio

$= E_s / E_c$

E_c = modulus of elasticity of concrete, ksi

The ACI Code equation for deflection can also be written as follows:

$$\Delta_{max} = \beta_a \cdot P \cdot L^3 / 6 (E_c \cdot I_e) \quad . . (4.10)$$

Pretorius equation (4.3) is the same as the ACI Code equation (4.10) except that Pretorius used the cracked moment of inertia rather than the effective moment of inertia.

Maximum bottom crack width

The use of the Gergely and Lutz equation (4.4), provides values of the maximum bottom crack width to compare with those observed during testing.

CHAPTER 5

EXPERIMENTAL WORK AND TEST RESULTS

Preparation for the experimental work involved building the steel cages for different beams. The fine aggregates were placed in the oven for three days to evaporate the surface moisture. Special consideration was taken to remove dust and fine particles from the coarse aggregates. Trial mix batches were tested to determine the optimum mix design. The mix ingredients were weighed directly before casting to avoid any change in moisture content that might affect the mix characteristics.

A weekly casting program was planned so that all beams would be casted within one month. There were no acute weather conditions during the casting of different beams.

The experimental process before testing included mixing, placing, and curing of concrete. The fixing of the strain gages was usually performed immediatly prior to the testing of the beam.

Mixing and Placing

The mixer used had a capacity of three cubic feet. The volume of concrete required for each beam was greater than five feet. Two batches were mixed for each beam. A regular mixing procedure was implemented. Dry ingredients were firat mixed and then water was added slowly. The rate of adding water proved to have a direct effect on the consistency of the mix. A good oompaction was achieved by naing a rod vibrator.

A alump test was performed for each batch and 3 in. x 6 in. cylinder samplea were prodnced and vibrated dnring the same time period. The concrete top snrface waa smoothed with the nse of a trowl.

Cnring

The framework was removed after twenty fonr honra. A cnring techniqne was maintained by covering the beam with a plastic sheet with holes pnnched ont. A continnons water flow was applied throngh the pnnched ont sheet. Thia cnring proceaa lasted two months. Then the beams were pnt in a room where the humidity is maintained at 75 percent. Beams were nsnally removed to a room with normal humidity abont a week before testing in order to affix the strain gages. A similar cnring process was provided for the matching oylinders.

Test Setnp

A nniversal testing machine (Tinins Olsen) with a maximum loading capacity of 200,000 lbs. (890 kN) was nsed for testing the beams. Two rocking, roller edges were nsed to snpport the beam. Two bearing plates of 3 in. x12 in. x1 in.

(76 x 305 x 25 mm) were placed between the beam edges and the roller supports to avoid stress concentration.

Hydro-stone mortar was placed between the top snrface of the beam and the load application points of the steel loading beam. It was also placed between the bottom surface of the beam at the edges and the bearing plates. This was done to gnarantee a nniform and effective load transfer at these critical points and also to avoid any torsional effects dnring the testing.

The strain gages were connected to the data aquisition system. The efficiency of the strain gages was checked before testing the beam. The test setup is shown in Fignre 4.8.

Test Procedure

Predetermined nniform load intervals were applied. The loading intervals provided a fairly uniform increase in the measnred strain data. However, at nltimate stages this interval rate was decreased. The measnred strain data were printed by the data aqnisition system at each load increment. The vertical deflection was also reported at each load increment. A thorongh investigation of cracks was done at each load stage. The crack propagation was traced and the maximum width was carefnlly measnred after each load stage.

There were no serious problems during the testing procedures. The strain data obtained during the testing of cylinders using a dial gage were not accurate. For this reason, strain data for cylinders made with the same mix proportions and the same type of materials used in previous work were adapted for analysis use in this research. The plot of the stress-strain data and the cubic regression expression are shown in Figures 5.1 and 5.2.

Test Results, General Discussion

Cylinders for each beam were tested within the same twenty-four hour period. Compressive strength results of cylinders corresponding to beam #1 are reported in Table 5.1. Table 5.2 shows cylinder test results for beam #2. Results for cylinders of beam #3 are in Table 5.3. Results of cylinders for beam #4 are in Table 5.4.

Cylinder test results of beam #3 expressed the highest coefficient of variation of all the beams (4.6%). The compressive strength average values for beams #1, #2,and #3, (shown in Table 5.5) reasonably agree with the nominal compressive strength of 12,000 psi used in the primary design shown in Table 4.1.

Beam #1 had a compressive mode of failure in the pure bending zone (middle third). Beam #2 had a diagonal tension failure as predicted. Beam #3 had a tension mode failure with minor cracking in the outer thirds. Four major cracks occured in the middle third section of beam #4 without any cracks on the outer thirds.

Strain Data Analysis

The strain data was recorded for each load stage during testing. Table 5.6 reports the strain data obtained for beam #1. The strain values at zero load were subtracted from the corresponding strain data in order to get the absolute value of strain.

The absolute strain values were averaged for each side of the beam. Then an average of both sides was obtained. Table 5.7 presents the absolute average strain data for beam #1. Similar calculations were performed on the remaining three beams. The actual strain and the absolute average strain for beams #2, #3,and #4 are reported in Tables 5.8, 5.9, 5.10, 5.11, 5.12, and 5.13. The use of two, short,gage-length gages provided consistent data.

The strain distributions for each side of the beam and both sides together are diagramed. Figure 5.3 shows the average strain distribution for side one of beam #1. Figure 5.4 shows the distribution for side two of beam #1 and Figure 5.5 shows the strain distribution based on the average values of both sides for beam #1.

In order to validate the linear strain distribution which is a basic assumption, a straight line was fitted through the average strain data (average of both sides) for each load level. A least sqnare regression was nsed in this linear fitting. The compnter SAS package and its mannals (25, 26, and 27) were nsefnl for accomplishing the statistical work. Fignre 5.6 shows the average strain for beam #1 nsing the least sqnare straight line regression. The scattered valnea in this fignre represent the strain data provided from Fignre 5.6.

The aame analysia was performed on the data for the other three beama. Fignres 5.7, 5.8, 5.9, and 5.10 show the process for the atrain data on beam #2. Fignres 5.11, 5.12, 5.13, and 5.14 show the atrain data analysis of beam #3. The available strain data analysis for beam #4 is shown in Fignres 5.15, 5.16, 5.17, and 5.18. It waa observed that the actnal valnea of the maximum strain at the nltimate stress in the top snrface were always in the range of 0.0023 to 0.003 in./in.

Thronghont the strain straight line regression models, the depth of the nentral axis and the maximum strain were obtained for each load atage. These valnea are ahown in Tables 5.14, 5.15, 5.16, and 5.17 for beams #1, #2, #3, and #4.

Compreaaive Stresa Block

The cnbic expresaion ahown in Fignre 5.1 is the one that best fits the actnal cylinder data. The compressive strength of this cylinder was 11,500 psi. It was appropriate to use this cyliuder for analysis of beams #1, #2, and #3 becanse the average compressive strength of cylinders for these beams was close to the value of 11,500 psi.

A similar cubic expression with differeut coefficients was used for the analysis of dats for beam #4.

The geueral stress-straiu eqnatiou is as follows:

$$f_c = A1 \cdot (\epsilon) + A2 \cdot (\epsilon)^2 + A3 \cdot (\epsilon)^3 \text{ psi} \quad . . . (5.1)$$

where

ϵ = concrete straiu iu micro in./in.

The followiug coefficieuts (see Fignres 5.1 and 5.2) were used for the analysis of strain dsts for beams #1, #2, and #3:

A1 = 7.174513

A2 = - 0.000434

A3 = - 1.85455 x 10^{-7}

And the following coefficients were used for beam #4.

A1 = 6.582399

A2 = 0.000714

A3 = - 6.91179 x 10^{-7}

The above expression was nsed to calcnlate the stresses corresponding to the strain dsts provided in Fignre 5.5 for beam #1. The compressive stress distribntion using this analysis is showu in Figure 5.19.

The compressive stress block based on equation 5.1 and the linear strain data obtained by regression (Figure 5.6) is shown in Figure 5.20 for beam #1. A similar analysis was performed for the data of beams #2, #3, and #4. The results are shown in Figures 5.21, 5.22, 5.23, 5.24, 5.25, and 5.26.

Ultimate Moment Calculations

The ultimate moment was calculated using the test data, the rectangular stress block, the triangular stress block and the compressive stress block obtained by regression. The different methods of calculation are discussed in Chapter Four. An illustrative example is provided in Appendix II.

The moments calculated using different methods were plotted against the load value. Figures 5.27, 5.28, 5.29 and 5.30 show these plots for beams #1, #2, #3, and #4. The ratios between the test moment and the calculated moment using different methods are presented in Tables 5.18, 5.19, 5.20, and 5.21.

Midspan Vertical Deflection

Figures 5.31, 5.32, 5.33, and 5.34 show a comparison between the measured vertical deflection and the calculated values using the ACI Code and Pretorius approach for different beams. These methods are discussed in Chapter Four. It is concluded that both the ACI Code (32) approach and the Pretorius epproach ere somewhat nnconservetive in calcnleting the verticel deflection for these higher strength concrete beams.

The ratio between the measnred and celcnlated valnes for vertical deflection et midspan for the different beams are presented in Tables 5.22, 5.23, 5.24, and 5.25.

Crack Confignration

The stndy of cracks dnring the conrse of testing can be clessified into three cetegories: early crecks, middle stage crecks, and leter stege cracks.

Early Craoks

Initial crecks were alweys verticel and close to the center line of the beem. They elways started from the bottom snrface. The cracks had a rapid creck propegetion but there were minor changes in their meximum width. The meximum bottom width observed for the early cracks was abont 0.001 inch to 0.002 inch.

Middle Stage Cracks

New cracks were observed with each load increese. They were observed in both the middle third and the onter sides. Most cracks thet shaped the final crack pattern were created during the middle stage of loeding.

Later Stage Cracks

New sets of inclined cracks in the outer sides were observed in beam #1,#2, and #3. Few cracks were initiated in the middle third. At the nltimate load, there was a rapid increase in maximum crack width. Also a set of hair-line cracks initiated from the major cracks that spread in the tension zone.

It was noticed that the maximum bottom width for a new crack was very small as compared to its maximum width at the nltimate stage. On the other hand, the length of a new crack was, in most cases, greater than 50 percent of its total length at the nltimate stage.

Failnre Modes

In beam #1 (over-reinforced beam), a triangnlar wedge in the middle third (compressive zone) seperated from the beam to create a failure mechanism. This was accompanied by a horizontal set of cracks at the level of reinforcement. No cracks propagated through the compression failnre zone dnring the conrse of testing beam #1.

In beam #3 and #4 (under-reinforced beams), excessive crack propagation reached the top surface of the beam. Also excessive increases in the crack widths of the horizontal cracks were observed at the level of reinforcement for both beams.

For beam #2 (diagonal tension failure), the failure surface occured between one of the loading points and the support. No cracks at the level of the reinforcement accompanied failure. Appendix II includes calculations of the shear stress at ultimate load of beam #1 and beam #2.

The crack propogations and widths were investigated during most of the loading stages for the test beams. The complete details of the crack propagations and widths for the different loading stages of the beams are presented in Appendix III. Figures 5.35, to 5.58 cover this section of the investigation. The figures show the shape of the cracks using different symbols to distinguish crack propagation for each load stage. The load value and the measured maximum crack width are stated at the end of the crack propagation corresponding to each load stage.

In the middle third, crack propagations were always directed upward at the different load values. At the later stages, cracks close to the load application points propagated or turned towards these points.

In the outer thirds of the beam, some cracks initiated at the mid-depth. These cracks then extended at both ends during the different loading stages. The maximum widths of these cracks were in the middle section, not at the ends. All cracks propagated towards the loading point in the last loading stages.

A comparative study of the maximum crack width was based on the test data and the calculated values using the Gergely and Lutz formula as described in Chapter Four. Figures 5.59, 5.60, and 5.61 show that the Gergely and Lutz formula is more conservative in predicting the maximum crack width for higher strength concrete. Figure 5.62 shows the relationship between the load and the maximum bottom crack width for beam #4. The ratio between the measured and calculated values of the maximum bottom crack width for different beams are presented in Tables 5.26, 5.27, and 5.28.

The Ratio h_2 / h_1

Figure 5.63 shows the relationship between the maximum bottom crack width and the ratio h_2/h_1 for beam #1. The test data along with the calculated values using the Gergely and Lutz equation (4.4) are compared in this diagram. Similar diagrams for beams #2 and #3 are shown in Figures 5.64 and 5.65.

Figures 5.63 and 5.64 show that the rate of change in the calculated values for the maximum bottom crack width is greater than that of the measured values as the ratio h_2/h_1 decreased. This is true for the service stress testing margin. However, Figure 5.65 shows a similar rate of change in the maximum bottom crack width, with the variation of h_2/h_1 for both measured and calculated values of beam #3.

CHAPTER 6

SUMMARY AND CONCLUSIONS

Summary

Concrete with nominal compressive strength of 12,000 psi (82.7 MPa) was used to build four reinforced beams with different steel ratios. Beams were tested at the third points in order to study the structural behavior and crack propagation of higher strength concrete.

Conclusions

Analysis of the test data leads to the following conclusions:

1. The actual strain corresponding to the ultimate compressive stress was always in the range of 0.0023 to 0.003 in./in. for higher strength concrete.

2. The use of two, short,gage-length gages at each gage location provided more consistent strain data for analysis.

3. The rectangular stress distribution gives sufficiently accurate predictions of the moments of higher strength concrete beams. However, a parabolic or a triangular stress block is more realistic in predicting the moment at the ultimate load.

4. Both the ACI Code (32) approach and the Pretorius (22)

approach in calcnlating midspan vertical deflection provide valnes that are leas than the measnred test valnes. This indicates that the two methoda are not conaervative in evalnating vertical deflection for higher strength concrete. Thia also indicatea that the ACI Code formnlas for the modnlns of rnptnre and the effective moment of inertia need to be re-examined for higher strength concrete applications.

5. Steel ratio, ateel stress and reinforcement distribntions are major factors that govern crack patterns in higher strength concrete beama.

6. The data show that the maximum bottom crack width for the experimental beams is abont 40 - 70% of the calcnlated valnes naing the Gergely and Lntz eqnation. This indicates that this formnla is conservative in evalnating the maximum bottom crack width for higher atrength concrete.

APPENDIX I

REFERENCES

1. Alexander, K. M.," Faetors Controlling the Strength and the Shrinking of Conerete," Constrnetin Review, Vol. 33, No. 11, November 1960, pp. 19-29.

2. Bliek, Ronald L.,"Some Faetors Inflneneing High-Strength Conerete," Modern Conerete , April 1973,pp. 38-41, 47.

3. Bloem, D. L. and Gaynor, R. D., "Effeet of Aggregate Properties on High - Strength Conerete," ACI Jonrnal, Vol. 60, Oetober 1963, pp. 1429-1455.

4. Bnrgess, A. J., Ryell, J. and Bnnting, J., " High-Strength Conerete for Willows Bridge," ACI Jonrnal, Vol. 67. No. 8, Angnst 1970,p. 611.

5. Carrasqnillo, Ramon L.," The Prodnetion of High-Strength Conerete," Report No. 78-1, Department of Civil Engineering, Cornell University, Ithaea, N. Y., May 1978.

6. Carrasqnillo,Ramon L.,Nilson,A. H., and Slate, Floyd O., "properties of High Strength Conerete Snbjeet to Short Term Loading," ACI Jonrnal, May-Jnne 1981., pp. 177-178.

7. Carrasqnillo,Ramon L., Slate, Floyd O.,and Nilson,A. H., "Microeracking and Behavior of High Strength Snbjeet to Short - Term Loading," ACI Jonrnal, May-Jnne 1981., pp. 179-186.

8. Freedman, Sidney, "High-Strength Concrete," Modern Conerete, Vol. 34, No. 6, Oet. 1970, pp. 29-36, No. 7, Nov. 1970, pp. 28-32 ; No. 8, Dee. 1970,pp. 21-24 ; No. 9, Jan. 1971, pp. 15-22 ; and No. 10, Feb. 1971, pp. 16-23. Also Pnblieation No. FS176T,Portland Cement Association.

9. Gergely, P., and Lntz, L. A., "Maximum Craek Width in Reinforced Conerete Flexnral Members, Canses, Meehanism, and Control of Craeking in Concrete," Sp-20, Ameriean Conerete Institnte. Detroit 1968, pp. 87-117.

10. Hiremagalnr,N., "The Strnetnral Behavior of Higher Strength Conerete," Master's Thesis, Kansas State University, 1985.

11. Hognestad, Eivid., Hanson, N. W., and McHenry, Donglas, "Conerete Stress Distribntion in Ultimate Strength Design," Jonrnal of the American Conerete Institnte., Vol. 27, No. 4, Deeember 1955., pp. 455-479.

12. Keplan, M. F., "Flexnrel and Compressive Strength of Concrete as Affected by the Properties of Coarse Aggregate," American Concrete Institnte Jonrnal, Vol. 55, May 1959, pp. 1193-1208.

13. Leslie,Keith E., Rajagoplan,K. S., end Everard, Noel J., "Flexnral Behavior of High - Strength Concrete Beams." ACI Jonrnel, Vol. 73, No.9, September. 1976., pp. 517-521.

14. Mather, Katharine., "High - Strength, High Density Concrete," (ACI Summery Paper), ACI Jonrnal, Proceedings, Vol. 62, No 8, Angnst 1965, pp. 951-962.

15. Mielenz, Richard, "History of Chemical Admixtnres for Concrete," Concrete International, Vol. 6, No. 4, April 1984, pp. 40-53.

16. Morgan, Anstin H., "High - Strength Reedy - Mixed Concrete", paper presented to 41st Annnal Convention of the National Reedy Mixed Concrte Associetion, Jannery 1971, 18pp.

17. Nareyanen, P. ," Behavior of Reinforced Higher-Strength Concrete Beams in Bending end Shear," Master's Thesis, Kansas Stete Uinversity, 1985.

18. Nikaeen, Ali," The prodnction and Strnctnrel Behevior of Higher Strength Concrete," Master's Thesis, Kansas State University, 1982.

19. Nilson,Arthnr H., Slate, Floyd O.," Strnctnral Properties of Very High-Strength Concrete," Second Progress Report, Eng. 76-08752, Department of Strnctnrel Engineering, Cornell University, Ithaca, N. Y., Jannery 1979.

20. Orchard,D. F.," Concrete Mix Design and Qnality Control," Concrete Technology, Fonrth Edition., Vol. 1, Applied Science Pnblishers Ltd., London., 1079., p. 146.

21. Parrot, L. J., "The Selection of Constitnents end Proportions for prodncing Workable Concrete With a Compressive Cnbe Strength of 80 to 110 N/mm (11600 to 15900 lb./in.^{2})," Technical Reports, No. 416, Cement and Concrete Association, May 1969, pp. 12.

22. Pretorins, Pieter, C., "Deflections of Reinforced Concrete Members: A Simple Approech," Jonrnel of the American Concrete Institnte, Vol. 82, Proceedings, No. 6, Nov.-Dec. 1985, pp. 805-812.

23. Refei,T. M.," The Strnctnral Behavior of Higher Strength Concrete," Master's Thesis, Kensas Stete University,1984.

24. Russell, Heury G., "High Streugth Concrete," American Coucrete Iustitnte, SP-87, Detroit, Miehigan, 1985.

25. SAS/Graph User's Guide., SAS Institute Inc., Cary, North Carolina,1981.

26. SAS User's Gnide: Basies, 1982 Edition., SAS Institnte Iue., Cary, North Carolina, 1982.

27. SAS User'a Gnide: Statisties, 1981 Editiou., SAS Inatitnte Ine., Cary, North Caroliua, 1982.

28. Saneier, Kenueth L., "High Streugth Couerete, Paat, Preaent, Futnre," Couerete Internatioual, ACI, Vol. 2, No. 6, Juue 1980, pp. 46-50.

29. Smith, E. F., Tyneea, W. D., and Saneier, K. L., "High Compressive - Strength Couerete, Developmeut of Conerete Mixturea," Teehuieal Doeumeutary Report No TDR 63-3114, U. S. Army, Corps of Eugiueera, Waterways Experiment Statiou,Vieksbnrg, Mississippi, February, 1964, p. 44.

30. Waug, Pao-Tsan, Shah, Snreudra P., aud Naamau, A. E., "High-Strength Couerete iu Ultimate Strength Design," Jonrual of the Strnetnral Divisiou. ASCE, Vol. 104, No. ST11, 1978, pp. 1761-1773.

31. Zia, Paul., "Review of ACI Code for Design With High Streugth Couerete," Couerete Internatioual, Vol. 5, No.8, Augnst 1983, pp. 16-20.

32. "ACI 318-83, Bnilding Code Reqnirementa for Reinforced Coucrete," Amerieau Coucrete Inatitnte, Detroit, Mieh., 1983

33. "Admixtnrea for Couerete," Conerete Iuternatioual, Vol. 6, No. 4, April 1984, p. 56.

34. "Couerete aud Mineral Aggregates (iuelndiug Maunal of Couerete Teating)," Annnal Book of ASTM Standards, Part 14, 1974.

35. "High-Streugth Conerete," Firat Edition, Mauual of Coucrete Materials-Aggregates, National Crushed Stoue Associatiou, Jauuary, 1975, p. 16.

36. "High Streugth Conerete -- Crnshed Stoue Makes the Differeuce," Third Draft, preseuted at the Jauuary 1975 Natioual Crnshed Stoue Assoeiatiou Conveutiou iu Florida, November 1974, p. 31.

37. Micro Measnrements Division, Measurements Gronp, Catalog 400, Strain Gage Listings, Raleigh, N. C., Angnst 1, 1984.

38. "State-of-the-Art Report on High-Strength Concrete," Report by ACI Committee 363, ACI Jonrnal, Vol. 81, No. 4, July-Angust 1984, pp. 364-411.

39. "Tentative Interim Report on High-Strength Concrete", American Concrete Institnte Journal, Proceedings, Vol. 64, No. 9, September 1967, pp. 556-557.

APPENDIX II

DETAILS OF SOME CALCULATIONS

NUMERICAL EXAMPLE OF THE PRELIMINARY REINFORCEMENT DESIGN CALCULATIONS OF BEAM #1, TABLE 4.1

The purpose of these calculations is to design a cross section with a steel ratio of 0.75 ρ_b which is the maximum value accepted by the ACI Code 318-83 (32).

<u>DATA</u>

b = 8 in.

t = 12 in.

L = 84 in.

ϵ_{cu} = 0.0025 in./in. (assumed)

f'_c = 12 ksi (nominal)

f_y = 60 ksi

E_s = 29×10^3 ksi

The steel strain at the yield stress can be calculated as followed:

$$\epsilon_y = f_y / E_s$$
$$= 60 / 29 \times 10^3$$
$$= 0.002069 \text{ in./in.}$$

The strain distribution in a balanced section yields the following relation, (see figure).

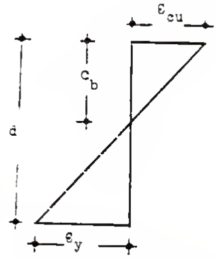

Strain Distribution in a Balanced Section

$$c_b / d = 0.0025 / (0.0025 + 0.002069)$$

or

$$c_b = 0.547\, d \quad . \quad . \quad . \quad . \quad . \quad . \quad \text{(II.1)}$$

From the equilibrium of the balanced section and using a triangular stress block, the balanced steel ratio can be obtained as follows:

$$A_s \cdot f_y = 0.5\ f'_c \cdot c_b \cdot b$$

$$60\ A_s = 0.5\ (12).(0.547)\ b \cdot d$$

$$A_s / b\ d = 0.0547$$

or

$$\rho_b = 0.0547 \quad \ldots \quad (II.2)$$

Assume that the depth of the beam is 10 in., reinforcing bars can be chosen as follows:

$$A_s = 0.75\ .(0.0547).(10).(8)$$

$$= 3.28\ in.^2$$

2#9 and 2#7 are the suitable steel bar choice. Their arrangement is shown in Figure 4.3.

$$A_s(actual) = 3.2\ in.^2$$

$$d\ (actual) = 9.8\ in.$$

The following calculations are to find the beam ultimate carrying capacity of load, moment, and shear.

$$c = \frac{A_s \cdot f_y}{0.5 \cdot f'_c \cdot b}$$

$$= \frac{(3.2).(60)}{(0.5).(12).(8)} = 4.0\ in.$$

$$C = 0.5\ f'_c \cdot b \cdot c$$

$$= 0.5\ .(12).(8).(4)$$

$$= 192\ K$$

$$M_u = C \cdot \left(d - \frac{c}{3} \right)$$

$$= 192 \cdot (9.8 - 1.33)$$

$$= 1626 \text{ in.-K}$$

$$P_u = 6\, M_u / L$$

$$= 6 \cdot (1626) / 84$$

$$= 116 \text{ K}$$

$$V_u = P_u / 2$$

$$= 58 \text{ K}$$

$$V_c = 2\sqrt{f'_c}\ b \cdot d / 1000$$

$$= 2 \sqrt{12{,}000}\ (8) \cdot (9.8) / 1000$$

$$= 17.2 \text{ K}$$

$$V_s = 58 - 17.2$$

$$= 40.8 \text{ K}$$

Using #3 stirrups with a cross sectional area of 0.11 in.^{2} and yield stress of 50 ksi, the stirrup spacing can be obtained.

$$A_s \text{ (stirrup)} = 2 \times 0.11$$

$$= 0.22 \text{ in.}^2 \text{ (two branches)}$$

$$s = A_v \cdot f_y \cdot d / V_s$$

$$= 0.22 \cdot (50) \cdot (9.8) / 40.8$$

$$= 2.6 \text{ in.}$$

$$s \text{ used} = 2.5 \text{ in.}$$

NUMERICAL EXAMPLE OF THE REVISED REINFORCEMENT DESIGN CALCULATIONS FOR BEAM #1,TABLE 4.2

The revised calcnlations are based on the data provided by testing cylinders, steel bars, and beam specimen.

<u>DATA</u>

ϵ_{cn} = 2,272 micro in./in., Table 5.7

f'_c = 11,400 psi, Table 5.5

E_s (#9) = 30.9×10^6 psi

E_s (#7) = 30.2×10^6 psi

A_s = 3.2 in.^{2}, (2#9, 2#7)

d = 9.8 in.

b = 8 in.

t = 12 in.

f_y (#9) = 64 ksi, Table 2.1

f_y (#7) = 70 ksi, Table 2.1

L = 84 in.

Steel bars nsed for beam #1 are 2#9 and 2#7

A_s (2#9) = 2 in.^{2}

A_s (2#7) = 1.2 in.^{2}

For the steel nsed in beam #1

$$E_s = (30.9 \times 2 + 30.2 \times 1.2) \times 10^6 / 3.2$$

$$= 30.6 \times 10^6 \text{ psi}$$

$$\epsilon_y = f_y / E_s$$

$$= 70{,}000 / (30.6 \times 10^6)$$

$$= 2{,}288 \text{ micro in./in.}$$

$c_b \;=\; d \cdot \epsilon_{cu} \;/\; (\epsilon_{cu} + \epsilon_y)$

$\;= 9.8 \times 2{,}272 \;/\; 4{,}560$

$\;= 4.9$ in.

Using a triangular stress block

$C = 0.5 \cdot f'_c \cdot c_b \cdot b$

$= 0.5\ (11.4) \cdot (4.9) \cdot (8)$

$= 224$ K

A_s(bal.) $= C \;/\; f_y = 3.2$ in.^{2}

$\rho_b = A_s$ (bal.) / (b . d)

$= 3.2 \;/\; (8 \times 9.8)$

$= 0.0408$

$M_u = C \cdot (d - 1.63)$

$= 224\ (9.8 - 1.63)$

$= 1830$ in.-K

$P_u = 6\ M_u \;/\; L$

$= 6 \cdot (1830) \;/\; 84 = 131$ K

$V_u = 131 \;/\; 2 = 65$ K

$V_c = 2 \sqrt{f'_c} \cdot b \cdot d$

$= 2 \sqrt{11{,}400} \times 8 \times 9.8 \;/\; 1000$

$= 17$ K

$V_s = 65 - 17 = 48$ K

Using #3 stirrups with steel area of 0.11 in. and f_y of 50 ksi

$s = A_v \cdot f_y \cdot d \;/\; V_s$

$= 0.22 \cdot (50) \cdot (9.8) \;/\; 48$

$= 2.2$ in.

s used $= 2.5$ in.

NUMERICAL EXAMPLE FOR THE CALCULATION OF MOMENT, DEFLECTION, AND MAX. CRACK WIDTH OF BEAM #1 AT THE LOAD LEVEL OF 87,300 LBS.

DATA

b = 8 in.	ϵ_c = 992 micro in./in.
d = 9.8 in.	A_s = 3.2 in.
t = 12 in.	E_s = 30.6×10^6 psi
c = 4.82 in.	f'_c = 11,400 psi
h_1 = 4.98 in.	β_a = 0.1065
h_2 = 7.18 in.	
y_t = 6 in.	

The values of ϵ_c, c, h_1, and h_2 are found in Table 5.14. These values are based on the strain regression formula.

Moment Calculations

A. Using test data

$$M_{max} = PL / 6$$
$$= 87{,}300 \times 84 / (6 \times 1000)$$
$$= 1222 \text{ in.-K}$$

B. Using triangular stress distribution

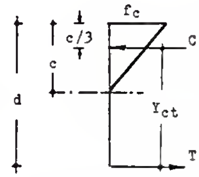

Triangular Stress Distribution

$$Y_{ct} = 9.8 - 0.33\ (4.82)$$
$$= 8.19 \text{ in.}$$

Using stress-strain eqnation 5.1,p. 37, the stress at the top fibers can be obtained.

$$f_c = A1 \;.(\epsilon) + A2 \;.(\epsilon)^2 + A3 \;.(\epsilon)^3 \quad . \;.\; . \quad psi$$

Snbstitnting the valne of 992 micro in./in.for C, f_c can be obtained.

f_c = 6,510 psi

M_{max} (tri.) = (8.19). 0.5 .(6.51).(4.82). (8)

= 1028 in.-K

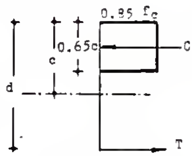

Rectangular Stress Distribution

C. <u>Using rectangular stress distribntion</u>

Y_{ct} = 9.8 - 0.325 .(4.82)

= 8.23 in.

M_{max} (rect.)= 8.23 .(0.85).(6.51).(0.65).(4.82).(8)

= 1141 in.-K

D. <u>Using stress distribntion obtained by regression</u>

The expression for the compressive stress block can be derived from eqnation 5.1 as follows:

$$(f_c)_y = Z1.(y) + Z2.(y)^2 + Z3.(y)^3 \quad . \;. \quad psi$$

where y is an arbitrary distance measnred from the nentral axis, and the valnes of Z1, Z2, and Z3 can be obtained as follows:

$$Z1 = A1 \cdot \epsilon_c / c$$
$$= (7.174513).(992) / 4.82$$
$$= 1477.2$$

$$Z2 = A2 \cdot (\epsilon_c)^2 / c^2$$
$$= -(0.000434).(992)^2 / (4.82)^2$$
$$= -18.4$$

$$Z3 = A3 \cdot (\epsilon_c)^3 / c^3$$
$$= -(1.85455 \times 10^{-7}).(992)^3 / (4.82)^3$$
$$= -1.6$$

By integration the compressive force can be expressed as follows:

$$C = b.\int_0^c (Z1 \cdot y + Z2 \cdot y^2 + Z3 \cdot y^3).\, dy$$
$$= 8 .[0.5 .(Z1).c^2 + 0.33 .(Z2).c^3 + 0.25 .(Z3).c^4]$$
$$= 130 \text{ K}$$

By integration, the line of action can be obtained:

$$\bar{y} = 8 .\int_0^c (Z1.y^2 + Z2.y^3 + Z3.y^4).\, dy / 130,000$$
$$= [0.33 .(Z1).c^3 + 0.25 .(Z2).c^4 + 0.2 .(Z3).c^5]/16250$$
$$= 3.19 \text{ in.}$$

$$Y_{ct} = d - (c - \bar{y})$$
$$= 9.8 - (4.82 - 3.19)$$
$$= 8.17 \text{ in.}$$

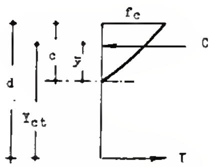

Comp. Stress Block
Using Reg. Anslysis

$$M_{max} \text{ (model)} = 8.17 \times 130$$
$$= 1062 \text{ in.-K}$$

The ratios between the teat moment and different calcnlated valnea are as follows:

M_{max} (teat) / M_{max} (tri.) = 1.19

M_{max} (test) / M_{max} (rect.) = 1.07

M_{max} (teat) / M_{max} (model) = 1.15

These values are reported in Table 5.18, for the load 87,300 lbs.

Midspan Vertical Deflection Calculation

A. Test Data

Measnred vertical deflection at the load 87,300 lba. is 340 in. x 10^{-3}, Table 5.22

B. ACI Code Approach

The following calcnlationa are to obtain the modnlar ratio n.

$0.45\ f'_c = 0.45\ .(11{,}430)$

$= 5{,}144$ psi

The correaponding strain for thia stress value is 764 micro in./in., (Fignre 5.1). Then the modnlua of elasticity of concrete (the secant modulns) can be calculated aa follows:

$E_c = 0.45\ f'_c\ /\ \epsilon_c$ (corresponding)

$= 5{,}144\ /\ (764 \times 10^{-6})$

$= 6.734 \times 10^{6}$ psi

Then the modnlar ratio can be obtained.

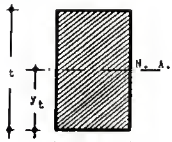

Gross Section
Notation

$$n = E_s / E_c$$

$$= 30.6 / 6.734 = 4.545$$

$$n \, . \, A_s = 14.54 \text{ in.}^2$$

$$f_r = 7.5\sqrt{f'_c} = 802 \text{ psi}$$

$$I_g = 8 \times 12^3 / 12 = 1152 \text{ in.}^4$$

$$I_{cr} = 8 \, .(4.82)^3 / 3 + 14.54 \, .(9.8 - 4.82)^2$$

$$= 659 \text{ in.}^4$$

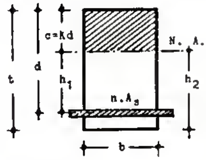

Cracked Section
Notation

$$M_{cr} = f_r \, . \, I_g / y_t$$

$$= 802 \, .(1152)/(6 \times 1000)$$

$$= 154 \text{ in.-K}$$

$$I_e = \left(\frac{M_{cr}}{M_{max}}\right)^3 . \, I_g + \left[1 - \left(\frac{M_{cr}}{M_{max}}\right)^3 \right] . \, I_{cr} \leq I_g$$

Snbstitnting for M_{max} = 1222 in.-K

$$I_e = 660 \text{ in.}^4$$

$$\Delta(\text{ACI}) = \beta_a \, . \, M_{max} \, . \, L^2 / (E_c \, . \, I_e)$$

$$= \frac{(0.1065).(1222).(84)^2}{(6.73).(10)^3.(660)}$$

$$= 206.5 \text{ in.} \times 10^{-3}$$

C. Pretorins Approach

$$K = \beta_a = 0.1065$$

Pretorins eqnation for short-term deflection:

$$\Delta(\text{Pret.}) = K \frac{M_{max} \, . \, L^2}{E_c \, . \, I_{cr}}$$

$$= 0.1065 \frac{1222 \times 84^2}{6.73 \times 10^3 \times 659}$$

$$= 207 \text{ in.} \times 10^{-3}$$

From the previous calculation, the ratio between the measured and calculated values are as follows:

Δ(test) / Δ(ACI) = 1.65

Δ(test) / Δ(Pret.) = 1.64

Comparative values for different beams are provided in Tables 5.22, 5.23, 5.24, and 5.25.

__Maximum bottom crack width__

A. __Measured test value__

The observed maximum bottom crack width of beam #1 at load level of 87,300 lbs. was 3.9 in. x 10^{-3}

B. __Calculated value__

Using the Gergely and Lutz expression (4.4), p. 21

$$w = 0.091 \,.\sqrt[3]{t_b \quad A} \quad R \,.(f_s - 5)$$

The maximum bottom crack width is calculated as follows:

t_b = 0.875 + 0.375 + 0.5 .(0.875)

= 1.69 in.

$A = A_e / m$

$A_e = 2\ b\ (t - d)$

$m = A_s / 1.0$

= 3.2

A = 2 .(8).(12 - 9.8)/ 3.2

= 11 in.^{2}

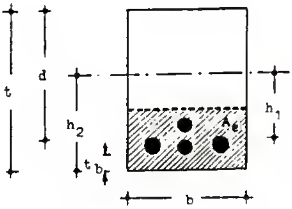

Dimensional Notation

$R = h_2 / h_1$

$= 7.18 / 4.98$

$= 1.44$, Table 5.14

$f_s = C / A_s$

$= 130 / 3.2$

$= 40.6$ ksi

$w = 0.091 . \sqrt[3]{(1.69).(11)} .(1.44).(40.6 - 5)$

$= 12.4$ in. x 10^{-3}

The ratio between measured and calculated values is as follows:

$w \text{ (test)} / w \text{ (G / L)} = 3.9/12.4$

$= 0.315$

A comparison between test data and calculated values are listed in Tables 5.26, 5.27, and 5.28 for beams #1, #2, and #3.

ULTIMATE SHEAR CAPACITY OF BEAM #1 AND BEAM #2

A. Beam #1

DATA

$b = 8$ in.

$d = 9.8$ in.

$s = 2.5$ in., Table 4.1

$A_v = 0.22$ in.^{2}

$P_u = 156{,}000$ lbs., Table 5.7

$V_u = 78{,}000$ lbs.

$f'_c = 11{,}400$ psi

According to the ACI equation 11.3

$$V_c = 2\sqrt{f'_c}\ b \cdot d$$
$$= 2\sqrt{11{,}400}\ .(8).(9.8)$$
$$= 17\ K$$

$$V_s = 78 - 17$$
$$= 61\ K$$

Using 2.5 in. spacing between #3 stirrups of beam #1, the shear reinforcement ultimate stress can be calculated as follows:

$$f_s\ (\text{ult.}) = \frac{s \cdot V_s}{A_v \cdot d}$$
$$= \frac{2.5 \times 61}{0.22 \times 9.8}$$
$$= 70.73\ \text{ksi}$$

This indicates that the shear reinforcement passed the yield point and was very close the its ultimate strength (72.72 ksi). Beam #1 failed in a compression failnre mode.

B. Beam #2

DATA

b = 8 in.

d = 10.13 in., Fignre 4.4

s = 4.0 in., Table 4.1

A_v = 0.22 in.^{2}

P_n = 112,600 lbs., Table 5.5

V_n = 56,300 lbs.

f'_c = 11,200 psi

According to ACI eqnation 11.3:

$$V_c = 2\sqrt{f'_c}\ b\ .\ d$$

$$= 2\sqrt{11{,}200}\ .(8).(10.13)$$

$$= 17\ K$$

$$V_s = 56.30 - 17.15$$

$$= 39.15\ K$$

Using 4 inch spacing between #3 closed stirrups, the stress of the shear reinforcement at ultimate load is as follows:

$$f_s\ (\text{nlt.}) = \frac{4 \times 39.15}{0.22 \times 10.13}$$

$$= 70.27\ \text{ksi}$$

A diagonal tension failnre occnred for this beam at the specified load.

APPENDIX III

TABLES AND FIGURES

TABLE 2.1 : Tensile Test Results for Steel Reinforcing Bars

DESCRIPTION	#3	#4	#7	#9
Cross Sectional Area (in.^{2})	0.11	0.20	0.60	1.00
Yield Load (lbs.)	5,500	11,300	42,000	64,000
Yield Stress (psi)	50,000	56,500	70,000	64,000
Ultimate Load (lbs.)	8,000	16,200	59,700	98,600
Ultimate Stress (psi)	72,720	81,000	99,500	98,600
Young's modulus (psi x10^6)	29.6	28.6	30.2	30.9

1 in. = 25.4 mm, 1 lb. = 4.45 N, 1 psi = 6.89 kPa

TABLE 3.1 : Review of Mix Proportions of Some Previous Work

(given weights per cubic foot)

REFERENCE NUMBER	MIX PROPORTION (weight in lbs.)		W/C	NOMINAL COMP. STRENGTH (psi)
18	cement	27.470	0.350	8400
	quartzite	49.650		
	sand	60.880		
	water	9.390		
	super-plasticizer	0.229		
23	cement	27.470	0.336	9600
	quartzite	49.650		
	sand	60.880		
	water	8.810		
	super-plasticizer	0.423		
10	cement	31.930	0.288	12000
	quartzite	49.650		
	sand	60.880		
	water	8.280		
	super-plasticizer	0.900		
17	cement	31.930	0.282	12000
	quartzite	49.650		
	sand	60.880		
	water	8.280		
	super-plasticizer	0.740		

1 in. = 25.4 mm, 1 lb. = 4.45 N, 1 psi = 6.89 kPa

TABLE 3.2: Mix Proportions Used for Different Beams*

(Weight in lbs. per cu. ft., Volume in cu. in.)

BEAM No.	MIX PROPORTIONS			SPECIFIC GRAVITY	W/C	SLUMP (in.)
	INGREDIENT	Weight	Volume**			
1	cement	31.93	285	2.432	0.292	3.8
	quartzite	49.65	519			
	sand	60.88	639			
	water	7.95	220			
	super-plasticizer	1.37	32			
	TOTAL	151.78	1695			
2	cement	31.93	285	2.432	0.292	3.5
	quartzite	49.65	519			
	sand	60.88	639			
	water	7.95	220			
	super-plasticizer	1.37	32			
	TOTAL	151.78	1695			
3	cement	31.93	285	2.432	0.291	1.2
	quartzite	49.65	519			
	sand	60.88	639			
	water	7.93	220			
	super-plasticizer	1.37	32			
	TOTAL	151.76	1695			
4	cement	31.93	285	2.427	0.301	2.9
	quartzite	49.65	519			
	sand	60.88	639			
	water	8.02	222			
	super-plasticizer	1.59	37			
	TOTAL	152.07	1702			

* Calculation is based on the following specific gravities: cement=3.1, quartzite=2.65, sand=2.64, superplasticizer=1.2

** 2 % air content for beams #1, #2, and #3. 1.5 % air content for beam #4

1 in. = 25.4 mm, 1 lb. = 4.45 N, 1 psi = 6.89 kPa

TABLE 3.3: 3 - Day Cylinder Test

For Different Beams

BEAM NO.	CYLINDER DATA: CYLINDER NO.	CYLINDER DATA: LOAD (lbs.)	CYLINDER DATA: COMPRESSIVE STRENGTH (psi)	AVERAGE STRENGTH (psi)
	1	40,500	5,700	
1	2	44,000	6,200	6,000
	3	42,200	6,000	
	1	46,000	5,500	
2	2	41,100	5,800	6,100
	3	43,200	6,100	
	1	41,200	5,800	
3	2	46,100	6,500	6,200
	3	43,200	6,200	
	1	37,100	5,300	
4	2	34,200	4,800	5,000
	3	35,200	5,000	

1 in. = 25.4 mm, 1 lb. = 4.45 N, 1 psi = 6.89 kPa

TABLE 4.1 : Preliminary Reinforcing Steel Design Calculations*

DESCRIPTION	B #1	B #2	B #3	B #4
ρ/ρ_b required	0.75	0.50	0.25	0.07**
A_s needed (in.^{2})	3.21	2.21	1.10	0.33
Bar choice	2#9+2#7	1#9+2#7	6#4	3#3
A_s actual (in.^{2})	3.20	2.20	1.18	0.33
Depth d (in.)	9.80	10.13	10.04	10.44
ρ used	0.0408	0.0271	0.0147	0.0040
ρ/ρ_b used	0.75	0.50	0.27	0.07
c (in.)	4.00	2.75	1.48	0.34
M_u (in.-K)	1626	1216	686	170
P_u (K)	116	87	49	12
V_u (K)	58.0	43.5	24.5	6.0
V_c (K)	17.2	17.8	17.6	18
V_s (K)	40.8	25.7	6.9	--
s calc. (in.)	2.6	4.34	20.4	--
s used (in.)	2.5	4.0	5.5	9.5

* Calculations are based on the use of grade 60 steel bars and also a triangular stress block assumption

** Minimum steel ratio = 200 / f_y

1 in. = 25.4 mm, 1 lb. = 4.45 N, 1 psi = 6.89 kPa
1 in.-K = 0.113 kN-m

TABLE 4.2 : Revised Desigu Calculations for Steel Reinforcing Bars Based on Actual Yield Stress of Steel*

DESCRIPTION	B #1	B #2	B #3	B #4
ϵ_{cu} (micro in./in.)**	2,272	2,810	2,414	2,500
f'_c (psi)	11,400	11,200	11,600	10,000
E_s (psi x 10^6)	30.6	30.5	28.6	29.6
ρ_b	0.0408	0.0456	0.0565	0.0597
ρ/ρ_b	1.000	0.594	0.260	0.067
c (iu.)	4.9	3.4	1.4	0.4
M_n (in.-K)	1,830	1,384	637	170
P_u (K)	131	99	46	12
V_u (K)	65	49	23	6
V_c (K)	17	17	17	17
V_s (K)	48	32	6	--
s calc. (in.)	2.2	3.5	20.2	--
s nsed (in.)	2.5	4.0	5.5	9.5

* Calculations are based a triangnlar stress block assumption

** C_{cu} of beam #1, #2, and #3 are obtained from Table 5.7, 5.9, and 5.11 respectively. The value is assumed for beam #4.

1 in. = 25.4 mm, 1 lb. = 4.45 N, 1 psi = 6.89 kPa
1 in.-K =0.113 kN-m

TABLE 5.1 : Compressive Strength Test Results of 3in. x 6in. Cylinders for Beam #1 (age = 108 days)

CYLINDER NUMBER	U1TIMATE LOAD (lbs)	ULTIMATE STRENGTH (psi)
1-1	80,000	11,300
1-2	86,000	12,200
1-3	80,200	11,400
1-4	81,150	11,500
1-5	77,000	10,900
1-6	79,700	11,300
1-7	79,300	11,200
1-8	82,700	11.700

1 in. = 25.4 mm

1 lb. = 4.45 N

1 psi = 6.89 kPa

TABLE 5.2: Compressive Strength Test Results of 3in. x 6in. Cylinders for Beam #2 (age = 108 days)

CYLINDER NUMBER	ULTIMATE LOAD (lbs)	ULTIMATE STRENGTH (psi)
2-1	76,000	10,800
2-2	80,100	11,300
2-3	77,200	10,900
2-4	77,600	11,000
2-5	80,300	11,400
2-6	83,600	11,300

1 in. = 25.4 mm

1 lb. = 4.45 N

1 psi = 6.89 kPa

TABLE 5.3: Compressive Strength Test Results of 3in. x 6in. Cylinders for Beam # 3 (age = 84 days)

CYLINDER NUMBER	ULTIMATE LOAD (lbs)	ULTIMATE STRENGTH (psi)
3-1	82,000	11,600
3-2	82,000	11,600
3-3	75,000	10,600
3-4	86,000	12,200
3-5	83,800	11,900
3-6	83,100	11,800

1 in. = 25.4 mm

1 lb. = 4.45 N

1 psi = 6.89 kPa

TABLE 5.4: Compressive Strength Test Results of 3in. x 6in. Cylinders for Beam #4 (age = 70 days)

CYLINDER NUMBER	ULTIMATE LOAD (lbs)	ULTIMATE STRENGTH (psi)
4-1	73,000	10,300
4-2	75,000	10,600
4-3	71,000	10,000
4-4	71,500	10,100
4-5	67,000	9,500
4-6	68,000	9,600
4-7*	105,000	9,500
4-8*	113,500	10,300

* 3.75 in. x 8 in. Cylinders cut from the beam after testing with area = 11.04 in.^{2}

1 in. = 25.4 mm

1 lb. = 4.45 N

1 psi = 6.89 kPa

TABLE 5.5: Average Compressive Strength Valnes for Different Beams

BEAM NUMBER	AVERAGE COMPRESSIVE (psi)	STANDARD DEVIATION (psi)	COEFFICIENT OF VARIATION
1	11,400	380	3.3%
2	11,200	360	3.2%
3	11,600	530	4.6%
4	10,000	420	4.2%

1 in. = 25.4 mm

1 lb. = 4.45 N

1 psi = 6.89 kPa

TABLE 5.6: Load vs. Strain Data for Beam #1

(strain data in micro in./in.)

LOAD No.	LOAD (lbs)	GAGE #1	GAGE #2	GAGE #3	GAGE #4	GAGE #5	GAGE #6	GAGE #7	GAGE #8
-	0	21	21	13	14	1	-18	31	28
1	7885	-57	-57	-45	-81	-72	-72	2	0
2	15700	-130	-130	-103	-179	-146	-124	-27	-21
3	23500	-202	-202	-161	-276	-217	-178	-47	-44
4	32450	-265	-265	-211	-353	-273	-219	-67	-61
5	39775	-326	-326	-272	-440	-340	-267	-89	-80
6	47650	-426	-426	-342	-544	-415	-321	-118	-110
7	55500	-510	-510	-404	-621	-476	-366	-135	-130
8	63450	-598	-598	-470	-703	-538	-416	-157	-150
9	71300	-696	-696	-552	-795	-616	-470	-186	-176
10	79400	-773	-773	-618	-871	-672	-517	-204	-194
11	87300	-864	-864	-702	-957	-741	-574	-228	-223
12	95300	-952	-952	-779	-1035	-805	-627	-252	-247
13	103500	-1066	-1066	-887	-1136	-886	-696	-283	-282
14	111200	-1155	-1155	-969	-1215	-946	-748	-307	-306
15	119000	-1254	-1254	-1080	-1303	-1022	-816	-338	-338
16	125650	-1311	-1311	-1135	-1353	-1060	-849	-350	-353
17	130800	-1424	-1424	-1248	-1453	-1132	-916	-378	-383
18	137500	-1587	-1587	-1376	-1587	-1187	-961	-344	-350
19	142200	-1985	-1985	-1671	-1808	-1256	-1018	-229	-254

TABLE 5.6: Continued

LOAD No.	LOAD (lbs)	GAGE #9	GAGE #10	GAGE #11	GAGE #12	GAGE #13	GAGE #14	GAGE #15	GAGE #16
-	0	20	29	85	69	-54	-19	-10	75
1	7885	-30	11	84	72	-150	-98	-78	-1
2	15700	-80	-2	81	70	-247	-183	-140	-75
3	23500	-118	-14	83	74	-359	-275	-210	-105
4	32450	-142	-17	84	80	-455	-351	-269	-178
5	39775	-167	-21	93	96	-575	-442	-334	-200
6	47650	-189	-33	85	94	-714	-544	-413	-49
7	55500	-195	-35	87	95	-838	-637	-477	-187
8	63450	-208	-41	83	83	-960	-727	-540	-259
9	71300	-247	-55	73	73	-1096	-838	-611	-312
10	79400	-262	-58	75	72	-1198	-926	-668	-378
11	87300	-298	-72	71	62	-1309	-1034	-773	-389
12	95300	-319	-81	71	61	-1416	-1128	- 792	-457
13	103500	-365	-102	56	40	-1556	-1259	- 864	-667
14	111200	-382	-105	56	39	-1676	-1359	- 924	-740
15	119000	-427	-124	52	34	-1828	-1488	- 986	-691
16	125650	-435	-126	52	38	-1909	-1555	-1026	-742
17	130800	-461	-136	50	30	-2082	-1698	-1089	-863
18	137500	-358	- 51	49	33	-2316	-1931	-1174	-1007
19	142200	-134	59	31	19	-2830	-2319	-1314	-1111

TABLE 5.6: Continued

LOAD No.	LOAD (lbs)	GAGE #17	GAGE #18	GAGE #19	GAGE #20	GAGE #21	GAGE #22	GAGE #23	GAGE #24
-	0	-17	-49	-32	14	18	7	70	21
1	7885	-60	-112	-84	-30	0	-11	70	19
2	15700	-92	-169	-114	-63	6	-14	93	54
3	23500	-128	-233	-159	-99	4	-18	99	191
4	32450	-161	-284	-198	-129	-3	-29	100	229
5	39775	-197	-348	-240	-172	-7	-40	102	312
6	47650	-242	-420	-297	-225	-26	-65	87	339
7	55500	-282	-480	-339	-264	-35	-72	87	404
8	63450	-321	-536	-379	-298	-40	-81	82	494
9	71300	-367	-608	-437	-351	-59	-96	79	543
10	79400	-404	-663	-473	-380	-60	-100	78	644
11	87300	-456	-731	-526	-432	-75	-113	78	678
12	95300	-495	-787	-560	-463	-77	-115	79	842
13	103500	-560	-876	-623	-522	-95	-130	72	839
14	111200	-611	-938	-664	-562	-103	-137	70	454
15	119000	-676	-1029	-732	-620	-125	-156	72	312
16	125650	-711	-1070	-756	-646	-130	-161	72	320
17	130800	-779	-1163	-819	-702	-145	-176	69	301
18	137500	-818	-1232	-788	-652	-72	71	64	82
19	142200	-871	-1336	-660	-493	-38	104	48	202

1 in. = 25.4 mm, 1 lb. = 4.45 N

TABLE 5.7: load vs. Absolute Average
Strain Data for Beam #1
(Average of Side 1 and Side 2)
(strain data in micro in./in.)

LOAD No.	LOAD (lbs.)	DEPTH FROM THE BEAM TOP SURFACE					
		0	1 in.	2 in.	3 in.	4 in.	5 in.
1	7885	-83	-74	-63	-38	-26	0
2	15700	-165	-147	-122	-67	-41	13
3	23500	-252	-211	-183	-98	-55	51
4	32450	-326	-276	-232	-124	-66	62
5	39775	-410	-335	-290	-156	-77	90
6	47650	-520	-360	-357	-198	-97	90
7	55500	-616	-445	-413	-227	-103	107
8	63450	-713	-516	-467	-256	-111	124
9	71300	-824	-591	-536	-298	-133	131
10	79400	-910	-657	-587	-323	-139	156
11	87300	-1010	-718	-651	-363	-158	161
12	95300	-1104	-789	-707	-391	-167	202
13	103500	-1229	-912	-786	-438	-192	191
14	111200	-1329	-985	-844	-470	-200	94
15	119000	-1448	-1038	-921	-517	-227	56
16	125650	-1514	-1087	-959	-537	-323	59
17	130800	-1647	-1186	-1036	-581	-248	51
18	137500	-1845	-1309	-1090	-544	-121	-4
19	142200	-2272	-1499	-1164	-419	7	14
20	156000			FAILURE			

1 in. = 25.4 mm, 1 lb. = 4.45 N

TABLE 5.8: Load vs. Strain Data for Beam #2

(strain data in micro in./in.)

LOAD No.	LOAD (lbs)	GAGE #1	GAGE #2	GAGE #3	GAGE #4	GAGE #5	GAGE #6	GAGE #7	GAGE #8
-	0	9	2	10	4	4	5	5	4
1	5850	-60	-53	-80	-48	-36	-27	-23	-19
2	12175	-139	-119	-183	-104	-80	-61	-52	-41
3	17985	-215	-179	-274	-161	-121	-94	-76	-60
4	23765	-297	-251	-377	-225	-165	-127	-97	-79
5	29675	-376	-323	-475	-287	-201	-158	-114	-92
6	35795	-444	-387	-572	-351	-238	-189	-126	-103
7	41645	-531	-471	-667	-421	-284	-225	-148	-120
8	47685	-611	-533	-758	-487	-326	-259	-167	-134
9	53325	-682	-615	-839	-557	-366	-294	-186	-150
10	59500	-758	-696	-922	-626	-407	-329	-205	-165
11	65580	-843	-780	-1004	-701	-454	-365	-227	-183
12	71535	-929	-865	-1094	-782	-506	-407	-251	-203
13	75515	-985	-923	-1143	-828	-533	-433	-259	-213
14	79450	-1036	-981	-1191	-873	-560	-455	-270	-223
15	83670	-1109	-1068	-1257	-935	-603	-487	-291	-328
16	87640	-1165	-1132	-1308	-989	-636	-514	-305	-251
17	91435	-1219	-1193	-1359	-1037	-668	-542	-317	-265
18	95260	-1275	-1255	-1410	-1087	-700	-570	-333	-276
19	99425	-1353	-1342	-1480	-1159	-745	-607	-356	-294
20	56400	-1363	-1507	-1445	-1162	-763	-640	-379	-316
21	105850	-2055	-2304	-1777	-1539	-716	-598	2	185
22	108250	-2491	-2843	-1993	-1820	-724	-604	59	841
23	109815	-2806	-3185	-2135	-1975	-659	-560	75	1069

TABLE 5.8: Continued

LOAD No.	LOAD (lbs)	GAGE #9	GAGE #10	GAGE #11	GAGE #12	GAGE #13	GAGE #14	GAGE #15	GAGE #16
-	0	8	4	4	4	5	6	0	-1
1	5850	-13	-15	-6	0	-59	-34	-51	-36
2	12175	-30	-29	-12	0	-133	-75	-103	-81
3	17985	-44	-40	-13	1	-208	-104	-158	-123
4	23765	-55	-36	-17	216	-296	-124	-219	-169
5	29675	-64	-23	-22	850	-382	-169	-276	-211
6	35795	-70	-20	-25	1309	-458	-209	-342	-254
7	41645	-82	-10	-30	2110	-546	-273	-410	-299
8	47685	-89	1	-30	2798	-631	-334	-472	-339
9	53325	-102	0	-32	3168	-708	-396	-532	-375
10	59500	-107	2	-22	3508	-795	-467	-603	-420
11	65580	-112	8	-5	3995	-887	-542	-667	-466
1	71535	-124	-1	14	4201	-987	-622	-751	-516
13	75515	-113	-3	27	4368	-1047	-672	-799	-545
14	79450	-105	-4	25	4551	-1103	-721	-838	-574
15	83670	-108	-13	19	4692	-1174	-782	-895	-589
16	87640	-107	-18	15	4847	-1235	-833	-936	-623
17	91435	-103	-22	10	4951	-1293	-885	-977	-654
18	95260	-101	-24	1	5103	-1351	-935	-1020	-684
19	99425	-100	-34	-5	5112	-1488	-1004	-1084	-725
20	56400	-90	-61	54	3553	-1468	-1099	-1088	-768
21	105850	1911	-41	53	13633	-2128	-1741	-1351	-954
22	108250	1409	-58	59	12873	-2490	-2126	-1539	-1082
23	109815	1156	66	58	12473	-2820	-2407	-1660	-1179

TABLE 5.8: Continued

LOAD No.	LOAD (lbs)	GAGE #17	GAGE #18	GAGE #19	GAGE #20	GAGE #21	GAGE #22	GAGE #23	GAGE #24
-	0	6	5	5	2	5	3	6	4
1	5850	-38	-17	-16	-27	-7	-4	6	3
2	12175	-88	-44	-41	-60	-21	-15	9	3
3	17985	-131	-67	-64	-95	-28	-22	12	3
4	23765	-177	-94	-83	-124	-27	-27	9	-7
5	29675	-220	-116	-101	-155	-23	-30	2	-14
6	35795	-264	-135	-117	-189	-11	-29	9	-2
7	41645	-307	-161	-133	-222	-8	-36	10	-1
8	47685	-342	-185	-146	-248	-4	-31	20	26
9	53325	-378	-209	-159	-274	0	-29	19	79
10	59500	-413	-236	-175	-302	2	-22	22	127
11	65580	-448	-264	-189	-327	-1	-13	17	216
12	71535	-488	-298	-214	-362	-12	-8	16	279
13	75515	-513	-320	-225	-380	-12	0	18	307
14	79450	-535	-338	-233	-393	-15	5	16	281
15	83670	-569	-364	-252	-418	-21	8	14	263
16	87640	-590	-387	-263	-434	-22	12	16	259
17	91435	-614	-410	-273	-446	-22	14	18	246
18	95260	-635	-430	-281	-459	-22	18	17	237
19	99425	-666	-458	-295	-480	-25	25	20	217
20	56400	-703	-489	-590	-476	-15	7	92	109
21	105850	-595	-338	1962	544	7	5872	41	48
22	108250	-546	-277	-204	762	11	14507	55	106
23	109815	-490	-203	203	825	7	9562	48	116

1 in. = 25.4 mm, 1 lb. = 4.45 N

TABLE 5.9: Load vs. Absolute Average Strain Data for Beam #2 (average of side 1 and side 2) (strain data in micro in./in.)

LOAD No.	LOAD (lbs.)	DEPTH FROM THE BEAM TOP SURFACE 0	1 in.	2 in.	3 in.	4 in.	5 in.
1	5850	-57	-57	-37	-25	-15	4
2	12175	-122	-121	-78	-53	-29	-5
3	17985	-182	-182	-115	-78	-39	-4
4	23765	-248	-251	-155	-100	-41	46
5	29675	-318	-316	-189	-120	-40	200
6	35795	-380	-383	-224	-138	-38	318
7	41645	-460	-453	-264	-160	-39	518
8	47685	-533	-517	-300	-178	-36	699
9	53325	-606	-579	-335	-196	-38	804
10	59500	-685	-646	-371	-216	-36	904
11	65580	-769	-713	-410	-235	-35	1051
12	71535	-856	-789	-454	-262	-41	1123
13	75515	-912	-832	-480	-273	-37	1176
14	79450	-966	-872	-503	-284	-35	1213
15	83670	-1038	-922	-539	-304	-39	1243
16	87640	-1096	-967	-567	-317	-39	1278
17	91435	-1153	-1010	-595	-330	-38	1301
18	95260	-1210	-1054	-621	-341	-37	1335
19	99425	-1302	-1115	-658	-360	-39	1332
20	103200	-1365	-1119	-684	-444	-45	948
21	105850	-2063	-1409	-596	669	1929	3439
22	108250	-2493	-1612	-573	361	3962	3269
23	109815	-2810	-1741	-508	539	2693	3169
24	112600			FAILURE			

1 in. = 25.4 mm, 1 lb. = 4.45 N

TABLE 5.10: Load vs. Strain Data for Beam #3

(strain data in micro in./in.)

LOAD No.	LOAD (lbs)	GAGE #1	GAGE #2	GAGE #3	GAGE #4	GAGE #5	GAGE #6	GAGE #7	GAGE #8
-	0	-17	-19	-42	-5	-7	1	-18	0
1	4000	-56	-60	-90	-31	-29	-19	-45	-20
2	8150	-100	-104	-138	-60	-52	-36	-76	-38
3	12100	-170	-175	-235	-109	-91	-64	-134	-71
4	15800	-241	-250	-305	-141	-118	-80	-149	-76
5	19865	-345	-362	-420	-198	-145	-100	-150	-79
6	23850	-420	-447	-433	-240	-169	-117	-154	-76
7	27775	-494	-523	-512	-282	-194	-131	-158	-76
8	31725	-568	-586	-355	-330	-225	-151	-164	-83
9	35650	-683	-703	-454	-407	-268	-185	-183	-102
10	39650	-707	-728	-479	-422	-274	-187	-177	-99
11	41750	-744	-766	-532	-450	-291	-200	-181	-1
12	43850	-784	-800	-664	-471	-303	-211	-182	-111
13	45750	-824	-844	-810	-501	-320	-225	-191	-117
14	46825	-839	-858	-874	-507	-323	-228	-187	-118
15	47825	-855	-875	-908	-519	-329	-236	-192	-122
16	48815	-873	-895	-940	-532	-337	-240	-195	-125
17	49925	-896	-920	-984	-550	-342	-246	-193	-124
18	50775	-919	-939	-1020	-561	-2	-251	-179	-124
19	51750	-1171	-1220	-1142	-636	-246	-163	-134	-86
20	52750	-1679	-1783	-1264	-726	-11	20	-90	-44
21	53700	-2275	-2244	-1161	-708	77	117	-58	-37
22	55650	-2620	-2505	-1104	-714	39	128	-47	-28

TABLE 5.10: Continued

LOAD No.	LOAD (lbs)	GAGE #9	GAGE #10	GAGE #11	GAGE #12	GAGE #13	GAGE #14	GAGE #15	GAGE #16
-	0	6	10	8	13	5	0	7	-3
1	4000	-9	0	1	9	-36	-39	-20	-36
2	8150	-25	-8	-8	7	-71	-75	-46	-69
3	12100	-45	-21	-8	7	-124	-128	-81	-116
4	15800	-34	-8	28	35	-180	-195	-119	-166
5	19865	34	24	109	73	-260	-295	-158	-220
6	23850	60	39	101	72	-330	-381	-188	-268
7	27775	62	43	82	64	-398	-461	-220	-317
8	31725	72	38	61	61	-468	-542	-254	-362
9	35650	73	36	33	56	-573	-655	-308	-430
10	39650	79	40	10	60	-598	-685	-314	-444
11	41750	83	41	9	62	-644	-733	-338	-474
12	43850	78	40	-12	59	-682	-772	-352	-495
13	45750	78	43	-19	62	-722	-804	-371	-518
14	46825	78	43	-22	63	-734	-811	-373	-523
15	47825	77	44	-24	64	-747	-822	-380	-529
16	48815	80	44	-27	67	-764	-836	-386	-538
17	49925	84	47	-31	67	-786	-856	-391	-549
18	50775	88	49	-35	68	-805	-868	-396	-554
19	51750	34	39	-75	50	-1027	-1075	-391	-545
20	52750	-4	22	-123	35	-1555	-1486	-335	-490
21	53700	-18	17	-126	37	-2203	-1864	-95	-371
22	55650	-5	25	-122	46	-2534	-2027	162	-321

TABLE 5.10: Continued

LOAD No.	LOAD (lbs)	GAGE #17	GAGE #18	GAGE #19	GAGE #20	GAGE #21	GAGE #22	GAGE #23	GAGE #24
-	0	15	10	11	16	22	21	32	24
1	4000	-15	-9	-7	-2	8	5	27	20
2	8150	-40	-25	-22	-15	-2	-7	26	21
3	12100	-71	-41	-37	-25	-2	-2	40	47
4	15800	-102	-62	-45	-36	1	9	57	83
5	19865	-109	-68	-22	15	26	443	34	696
6	23850	-120	-76	-10	54	35	629	36	713
7	27775	-132	-84	-3	107	42	405	62	813
8	31725	-154	-99	-6	157	43	302	66	763
9	35650	-182	-118	-3	206	54	234	36	570
10	39650	-181	-115	6	233	61	206	10	405
11	41750	-194	-127	6	248	61	199	-8	385
12	43850	-197	-132	16	281	51	194	-30	380
13	45750	-200	-141	20	320	61	192	-44	372
14	46825	-195	-140	27	372	76	188	-46	19
15	47825	-195	-139	29	402	76	187	-47	292
16	48815	-194	-141	31	436	77	186	-48	284
17	49925	-193	-141	35	510	71	180	-52	252
18	50775	-188	-140	39	566	68	176	-55	234
19	51750	-109	-22	2	596	21	129	-83	220
20	52750	-56	103	-21	521	-14	69	-108	210
21	53700	64	72	-25	495	-41	69	-109	201
22	55650	57	76	-21	491	-41	74	-103	192

1 in. = 25.4 mm, 1 lb. = 4.45 N

TABLE 5.11: Load vs. Absolute Average Strain Data for Beam #3 (average of side 1 and side 2) (strain data in micro in./in.)

LOAD No.	LOAD (lbs.)	DEPTH FROM THE BEAM TOP SURFACE 0	1 in.	2 in.	3 in.	4 in.	5 in.
1	4000	-40	-34	-23	-21	-14	-5
2	8150	-80	-68	-45	-40	-25	-8
3	12100	-142	-125	-76	-69	-32	2
4	15800	-209	-172	-103	-78	-23	32
5	19865	-308	-238	-120	-61	117	209
6	23850	-387	-272	-136	-49	176	211
7	27775	-461	-322	-154	-35	123	236
8	31725	-533	-315	-179	-26	99	219
9	35650	-646	-389	-212	-23	85	155
10	39650	-672	-404	-214	-12	82	102
11	41750	-714	-438	-229	16	81	93
12	43850	-752	-485	-247	-2	76	80
13	45750	-791	-539	-248	6	79	74
14	46825	-803	-559	-248	21	82	-16
15	47825	-817	-573	-251	27	81	52
16	48815	-834	-588	-255	35	82	50
17	49925	-857	-608	-257	55	81	40
18	50775	-875	-622	-86	73	81	34
19	51750	-1115	-668	-159	92	41	9
20	52750	-1618	-693	4	90	4	-16
21	53700	-1618	-573	70	92	-8	-19
22	55650	-2414	-484	50	97	-2	-16
23	56100		FAILURE				

1 in. = 25.4 mm, 1 lb. = 4.45 N

TABLE 5.12: Load vs. Available Strain Data for Beam #4*

(strain data in micro in./in.)

LOAD No.	LOAD (lbs)	GAGE #1	GAGE #2	GAGE #3	GAGE #4	GAGE #5	GAGE #6	GAGE #7	GAGE #8
-	0	-31	-13	0	-2	7	2	2	0
1	1000	-47	-26	-8	-15	-2	-7	-7	-8
2	2000	-63	-39	-15	-27	-9	-15	-14	-12
3	3230	-81	-51	-26	-39	-18	-24	-24	-22
4	4175	-157	-125	-42	-82	-27	-43	-27	-18
5	5800	-183	-149	-51	-97	-35	-57	-36	-22
6	6150	-194	-158	-56	-104	-39	-60	-39	-26
7	7150	-224	-182	-70	-124	-54	-71	-52	-34

TABLE 5.12: Continued

LOAD No.	LOAD (lbs.)	GAGE #9	GAGE #10	GAGE #11	GAGE #12	GAGE #13	GAGE #14	GAGE #15	GAGE #16
-	0	3	-5	-6	-32	-5	-26	-32	-9
1	1000	-4	-10	-11	-37	-17	-40	-44	-21
2	2000	-10	-14	-13	-40	-27	-55	-55	-32
3	3230	-13	-19	-18	-46	-42	-72	-69	-44
4	4175	-2	-5	-4	-26	-96	-176	-113	-110
5	5800	-1	-3	2	-17	-118	-213	-129	-130
6	6150	-6	-4	1	-17	-124	-225	-138	-139
7	7150	-8	-7	-5	-18	-143	-253	-157	-155

TABLE 5.12: Continued

LOAD No.	LOAD (lbs.)	GAGE #17	GAGE #18	GAGE #19	GAGE #20	GAGE #21	GAGE #22	GAGE #23	GAGE #24
-	0	-2	-4	-4	-40	0	-5	-22	-10
1	1000	-10	-16	-11	-48	-4	-11	-26	-16
2	2000	-17	-24	-18	-58	-5	-14	-32	-17
3	3230	-26	-34	-25	-65	-11	-18	-36	-19
4	4175	-44	-61	-26	-63	-2	3	-19	-26
5	5800	-55	-78	-33	-66	-2	5	-14	-19
6	6150	-58	-83	-36	-71	-4	5	-16	-19
7	7150	-61	-85	-47	-39	-6	2	-2	2

* Missing data due to printer malfunction.

1 in. = 25.4 mm, 1 lb. = 4.45 N

TABLE 5.13: Load vs. Absolute Average Strain Data for Beam #4 (average of side 1 and side 2) (strain data in micro in./in.)

LOAD No.	LOAD (lbs.)	DEPTH FROM THE BEAM TOP SURFACE					
		0	1in.	2in.	3in.	4in.	5in.
1	1000	-14	-11	-10	-8	-6	-5
2	2000	-27	-22	-17	-15	-9	-8
3	3230	-43	-34	-26	-24	-14	-12
4	4175	-120	-76	-42	-23	0	-1
5	5800	-147	-91	-53	-29	2	6
6	6150	-157	-99	-57	-33	-1	5
7	7150	-181	-116	-66	-33	-3	12

1 in. = 25.4 mm, 1 lb. = 4.45 N

TABLE 5.14 Properties of Cracked Section at Midspan of Beam #1 Based on Regression Analysis

load (lbs.)	c (in.)	h_1 (in.)	h_2 (in.)	$\frac{h_2}{h_1}$	f_s (ksi)	Top Surface ϵ_c *	Top Surface f_c(psi)
7885	5.83	3.97	6.17	1.55	4.52	87	619
15700	5.30	4.50	6.70	1.49	8.22	174	1234
23500	5.15	4.65	6.85	1.47	11.93	261	1841
32450	5.05	4.75	6.95	1.46	15.12	339	2377
39775	5.00	4.80	7.00	1.46	18.59	423	2941
47650	5.04	4.76	6.96	1.46	22.41	508	3508
55500	4.90	4.90	7.10	1.45	26.01	609	4169
63450	4.82	4.98	7.18	1.44	29.42	705	4780
71300	4.84	4.96	7.16	1.44	33.80	811	5437
79400	4.79	5.01	7.21	1.44	36.78	898	5961
87300	4.82	4.98	7.18	1.44	40.60	992	6509
95300	4.78	5.02	7.22	1.44	43.81	1086	7043
103500	4.79	5.01	7.21	1.44	48.88	1221	7776
111200	4.76	5.04	7.24	1.44	52.10	1320	8289
119000	4.80	5.00	7.20	1.44	56.16	1423	8799
125650	4.78	5.02	7.22	1.44	58.18	1489	9108
130800	4.76	5.04	7.24	1.44	62.32	1620	9697
137500	4.33	5.47	7.67	1.40	62.60	1824	10520
142200	3.90	5.90	8.10	1.37	65.19	2197	11703

* Strain in micro in. / in.

1 in. = 25.4 mm, 1 lb. = 4.45 N, 1 psi = 6.89 kPa

TABLE 5.15 Properties of Cracked Section at Midspan of Beam #2 Based on Regression Analysis

load (lbs.)	c (in.)	h_1 (in.)	h_2 (in.)	$\frac{h_2}{h_1}$	f_s (ksi)	Top Surface	
						ϵ_c *	f_c(psi)
5850	5.29	4.84	6.71	1.39	4.23	61	439
12175	5.24	4.89	6.76	1.38	8.91	131	932
17985	5.17	4.96	6.83	1.38	13.12	196	1389
23765	4.99	4.14	7.01	1.36	17.34	270	1898
29675	4.77	5.36	7.23	1.35	21.07	344	2409
35795	4.68	5.45	7.32	1.34	24.79	414	2883
41645	4.56	5.57	7.44	1.34	28.97	498	3444
47685	4.48	5.65	7.52	1.33	32.64	574	3942
53325	4.41	5.72	7.59	1.33	36.22	650	4430
59500	4.35	5.78	7.65	1.32	40.02	732	4945
65580	4.30	5.83	7.70	1.32	43.91	817	5473
71535	4.29	5.84	7.71	1.32	48.38	908	6017
75515	4.26	5.87	7.74	1.32	50.82	964	6350
79450	4.22	5.91	7.78	1.32	52.98	1019	6662
83670	4.21	5.92	7.79	1.32	56.29	1089	7061
87640	4.19	5.94	7.81	1.31	58.77	1148	7384
91435	4.17	5.96	7.83	1.31	61.17	1205	7690
95260	4.15	5.98	7.85	1.31	63.51	1263	7994
99425	4.12	6.01	7.88	1.31	66.88	1351	8445
103200	4.32	5.81	7.68	1.32	71.71	1383	8601
105850	2.44	7.69	9.56	1.24	59.54	2201	11713
108250	2.62	7.51	9.38	1.25	70.41	2519	12358
109815	2.50	7.63	9.50	1.25	72.15	2822	12626

* Strain in micro in. / in.

1 in. = 25.4 mm, 1 lb. = 4.45 N, 1 psi = 6.89 kPa

TABLE 5.16 Properties of Cracked Section at Midspan of Beam #3 Based on Regression Analysis

load (lbs.)	c (in.)	h_1 (in.)	h_2 (in.)	$\frac{h_2}{h_1}$	f_s (ksi)	Top Surface ϵ_c *	Top Surface f_c(psi)
4000	4.80	5.24	7.20	1.37	4.76	41	292
8150	4.68	5.36	7.32	1.37	9.28	82	584
12100	4.46	5.58	7.54	1.35	15.90	147	1047
15800	4.04	6.00	7.96	1.33	20.89	214	1516
19865	3.37	6.67	8.63	1.29	25.53	316	2220
23850	3.11	6.93	8.89	1.28	29.03	391	2725
27775	3.03	7.01	8.97	1.28	33.64	466	3229
31725	2.93	7.11	9.07	1.28	36.15	519	3583
35650	2.91	7.13	9.09	1.27	43.51	634	4329
39650	2.88	7.16	9.12	1.27	44.64	659	4487
41750	2.90	7.14	9.10	1.27	47.82	703	4764
43850	2.91	7.13	9.09	1.27	50.98	749	5052
45750	2.94	7.10	9.06	1.28	54.67	798	5352
46825	2.93	7.11	9.07	1.28	55.69	814	5454
47825	2.93	7.11	9.07	1.28	56.70	830	5550
48815	2.93	7.11	9.07	1.28	57.85	849	5662
49925	2.91	7.13	9.09	1.28	59.13	874	5816
50775	2.34	7.70	9.66	1.25	49.90	922	6102
51750	2.35	7.69	9.65	1.26	60.48	1126	7265
52750	1.95	8.09	10.05	1.24	67.68	1580	9522
53075	1.80	8.24	10.20	1.24	75.42	1985	11083
54250	1.81	8.23	10.19	1.24	82.67	2224	11772

* Strain in micro in. / in.

1 in. = 25.4 mm, 1 lb. = 4.45 N, 1 psi = 6.89 kPa

TABLE 5.17 Properties of Cracked Section at Midspan of Beam #4 Based on Regression Analysis

load (lbs.)	c (in.)	h_1 (in.)	h_2 (in.)	$\frac{h_2}{h_1}$	f_s (ksi)	Top Surface	
						ϵ_c *	f_c(psi)
1000	7.58	2.86	4.42	1.55	8.13	13	89
2000	6.70	3.74	5.30	1.42	13.96	26	172
3230	6.61	3.83	5.39	1.41	21.69	41	271
4175	4.32	6.13	7.69	1.25	36.00	104	690
5700	4.20	6.24	7.80	1.25	43.39	128	855
6075	4.26	6.18	7.74	1.25	47.18	138	918
7075	4.19	6.25	7.81	1.25	54.17	161	1072

* Strain in micro in. / in.

1 in. = 25.4 mm, 1 lb. = 4.45 N, 1 psi = 6.89 kPa

TABLE 5.18 Comparison Between Test Moment and Calculated Moment Using Different Methods for Beam #1

load (lbs)	M(test) / M(rect.)	M(test) / M(par.)	M(test) / M(tri.)
7885	0.88	0.97	0.97
15700	0.94	1.04	1.04
23500	0.97	1.07	1.07
32450	1.05	1.16	1.17
39775	1.05	1.15	1.16
47650	1.05	1.15	1.16
55500	1.05	1.15	1.16
63450	1.06	1.15	1.18
71300	1.04	1.13	1.16
79400	1.07	1.15	1.19
87300	1.07	1.15	1.19
95300	1.09	1.16	1.21
103500	1.07	1.13	1.19
111200	1.08	1.14	1.20
119000	1.08	1.14	1.20
125650	1.11	1.16	1.23
130800	1.09	1.13	1.21
137500	1.14	1.16	1.26
142200	1.16	1.13	1.28

1 lb. = 4.45 N

TABLE 5.19 Comparison Between Test Moment and Calculated Moment Using Different Methods for Beam #2

load (lbs.)	M(test) / M(rect.)	M(test) / M(par.)	M(test) / M(tri.)
5850	0.95	1.05	1.05
12175	0.94	1.04	1.04
17985	0.94	1.04	1.04
23765	0.93	1.03	1.04
29675	0.95	1.05	1.06
35795	0.98	1.07	1.08
41645	0.97	1.06	1.08
47685	0.99	1.08	1.09
53325	0.99	1.08	1.10
59500	1.00	1.09	1.12
65580	1.01	1.09	1.12
71535	1.01	1.08	1.12
75515	1.10	1.09	1.12
79450	1.02	1.10	1.13
83670	1.02	1.09	1.13
87640	1.02	1.09	1.14
91435	1.03	1.09	1.14
95260	1.04	1.10	1.15
99425	1.03	1.08	1.14
103200	1.01	1.06	1.12
105850	1.25	1.22	1.38
108250	1.14	1.06	1.26
109815	1.18	1.05	1.31

1 lb. = 4.45 N

TABLE 5.20 Comparison Between Test Moment and Calculated Moment Using Different Methods for Beam #3

load (lbs.)	M(test) / M(rect.)	M(test) / M(par.)	M(test) / M(tri.)
4000	1.06	1.18	1.18
8150	1.11	1.23	1.23
12100	0.95	1.06	1.06
15800	0.94	1.03	1.04
19865	0.94	1.04	1.04
23850	0.99	1.08	1.09
27775	0.99	1.09	1.10
31725	1.05	1.15	1.17
35650	0.99	1.07	1.09
39650	1.07	1.16	1.18
41750	1.05	1.14	1.17
43850	1.04	1.13	1.15
45750	1.01	1.10	1.12
46825	1.02	1.10	1.13
47825	1.02	1.11	1.13
48815	1.03	1.11	1.14
49925	1.03	1.11	1.14
50775	1.03	1.31	1.35
51750	1.03	1.10	1.14
52750	0.96	0.99	1.06
53075	0.89	0.89	0.99
54250	0.86	0.83	0.95

1 lb. = 4.45 N

TABLE 5.21 Comparison Between Test Moment and Calculated Moment Using Different Methods for Beam #4

load (lbs.)	M(test) / M(rect.)	M(test) / M(par.)	M(test) / M(tri.)
1000	0.59	0.66	0.66
2000	0.67	0.74	0.74
3230	0.69	0.77	0.77
4175	0.49	0.55	0.55
5700	0.55	0.62	0.62
6075	0.54	0.61	0.61
7075	0.55	0.61	0.61

1 lb. = 4.45 N

TABLE 5.22 Comparison Between Measured and Calculated Vertical Deflection at Midspan for Beam #1

(deflection in in. x 10^{-3})

load (lbs)	Δ (test)	Δ (ACI)	Δ (Pret.)	(test) / Δ(ACI)(32)	(test) / Δ(Pret.)(22)
7885	20	11	16	1.82	1.20
15700	48	29	35	1.66	1.35
23500	79	50	54	1.57	1.46
32450	114	73	75	1.55	1.50
39775	141	92	93	1.54	1.52
47650	175	110	111	1.59	1.58
55500	205	129	131	1.58	1.57
63450	237	150	150	1.58	1.58
71300	271	168	169	1.61	1.61
79400	306	188	188	1.63	1.62
87300	340	207	207	1.65	1.64
95300	376	226	226	1.66	1.66
103500	409	245	246	1.67	1.67
111200	450	264	264	1.70	1.70
119000	486	282	282	1.72	1.72
125650	522	298	298	1.75	1.75

1 in. = 25.4 mm, 1 lb. = 4.45 N

TABLE 5.23 Comparison Between Measured and Calculated Vertical Deflection at Midspan for Beam #2

(deflection in in. x 10^{-3})

load (lbs)	Δ (test)	Δ (ACI)	Δ (Pret.)	(test) / Δ(ACI)(32)	(test) / Δ(Pret.)(22)
5850	20	8	15	2.35	1.38
12175	42	19	31	2.19	1.36
17985	62	38	46	1.62	1.36
23765	86	57	62	1.50	1.38
29675	112	77	80	1.45	1.39
35795	141	95	98	1.48	1.44
41645	169	114	116	1.49	1.46
47685	197	132	133	1.49	1.48
53325	226	149	150	1.52	1.51
59500	262	167	168	1.57	1.55
65580	292	185	186	1.58	1.57
71535	324	202	203	1.60	1.59
75515	346	214	215	1.62	1.61
79450	366	226	226	1.62	1.61
83670	389	238	238	1.64	1.63
87640	410	249	250	1.64	1.64
91435	433	260	261	1.66	1.66
95260	458	272	272	1.69	1.69
99425	485	284	284	1.71	1.71

1 in. = 25.4 mm, 1 lb. = 4.45 N

TABLE 5.24 Comparison Between Measured and Calculated Vertical Deflection at Midspan for Beam #3

(deflection in in. x 10^{-3})

load (lbs)	Δ (test)	Δ (ACI)	Δ (Pret.)	(test) / Δ(ACI)(32)	(test) / Δ(Pret.)(22)
4000	13	5	14	2.39	0.90
8150	25	11	31	2.26	0.82
12100	44	19	48	2.27	0.91
15800	62	39	69	1.58	0.90
19865	95	66	95	1.43	0.99
23850	120	92	116	1.30	1.03
27775	150	116	135	1.29	1.11
31725	178	139	154	1.28	1.15
35650	207	161	173	1.28	1.19
39650	240	183	193	1.31	1.24
41750	257	194	203	1.32	1.26
43850	273	205	213	1.33	1.28
45750	287	215	223	1.33	1.29
46825	298	221	228	1.35	1.30
47825	305	226	233	1.35	1.31
48815	313	231	238	1.36	1.32
49925	320	237	243	1.35	1.32

1 in. = 25.4 mm, 1 lb. = 4.45 N

TABLE 5.25 Comparison Between Measured and Calculated Vertical Deflection at Midspan for Beam #4 (deflection in in. x 10^{-3})

load (lbs)	Δ (test)	Δ (ACI)	Δ (Pret.)	(test) / Δ(ACI)(32)	(test) / Δ(Pret.)(22)
1000	3.5	1	1.3	2.59	2.64
2000	6.0	3	3.8	2.22	1.59
3230	10.0	4	6.4	2.29	1.57
4175	23	6	24	2.66	0.95
5700	30	8	35	2.85	0.86
6075	31	8	36	2.80	0.86
7075	35	10	44	2.82	0.80

1 in. = 25.4 mm, 1 lb. = 4.45 N

TABLE 5.26 Comparison Between Measured and Calculated Maximum Bottom Crack Width for Beam #1*

LOAD (lbs.)	w (test) in.x10^{-3}	w (G / L) in.x10^{-3}	w (test) / w (G / L)
55500	1.6	4.8	0.33
79400	2.4	10.0	0.23
87300	3.9	12.4	0.32
142200	11.8	19.9	0.59

* Calculations are based on the Gergely and Lutz equation (4.4)

1 in. = 25.4 mm, 1 lb. = 4.45 N

TABLE 5.27 Comparison Between Measured and Calculated Maximum Bottom Crack Width for Beam #2*

LOAD (lbs.)	w (teat) in.x10^{-3}	w (G / L) in.x10^{-3}	w (test) / w (G / L)
29675	2.8	5.6	0.49
35795	3.1	6.9	0.46
41645	3.9	8.3	0.48
59500	5.5	12.0	0.46
79450	7.1	16.3	0.43
99425	31.5	21.0	1.50
105850	47.2	17.5	2.69

* Calculations are based on the Gergely and Lutz equation (4.4)

1 in. = 25.4 mm, 1 lb. = 4.45 N

TABLE 5.28 Comparison Between Measured and Calculated Maximum Bottom Crack Width for Beam #3*

LOAD (lbs.)	w (test) in.x10^{-3}	w (G / L) in.x10^{-3}	w (test) / w (G / L)
19865	2.4	4.8	0.49
23850	3.9	5.6	0.71
27775	4.7	6.6	0.71
31725	5.1	7.2	0.71
35650	5.5	8.9	0.62
39650	6.3	9.1	0.69
43850	7.7	10.6	0.72
47825	9.3	11.9	0.78

* Calculations are based on the Gergely and Lutz equation (4.4)

1 in. = 25.4 mm, 1 lb. = 4.45 N

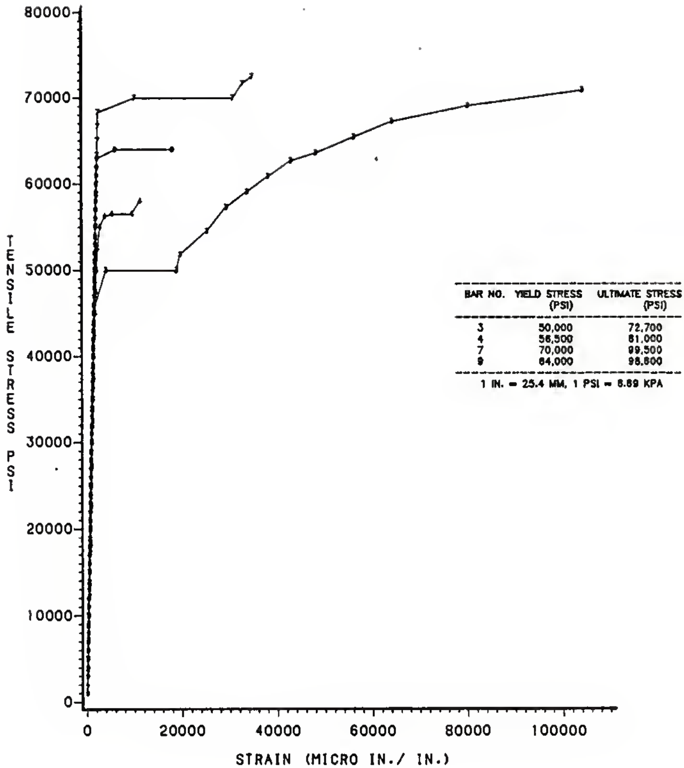

FIG. 2.1 STRESS–STRAIN CURVE FOR DIFFERENT STEEL REINFORCING BARS

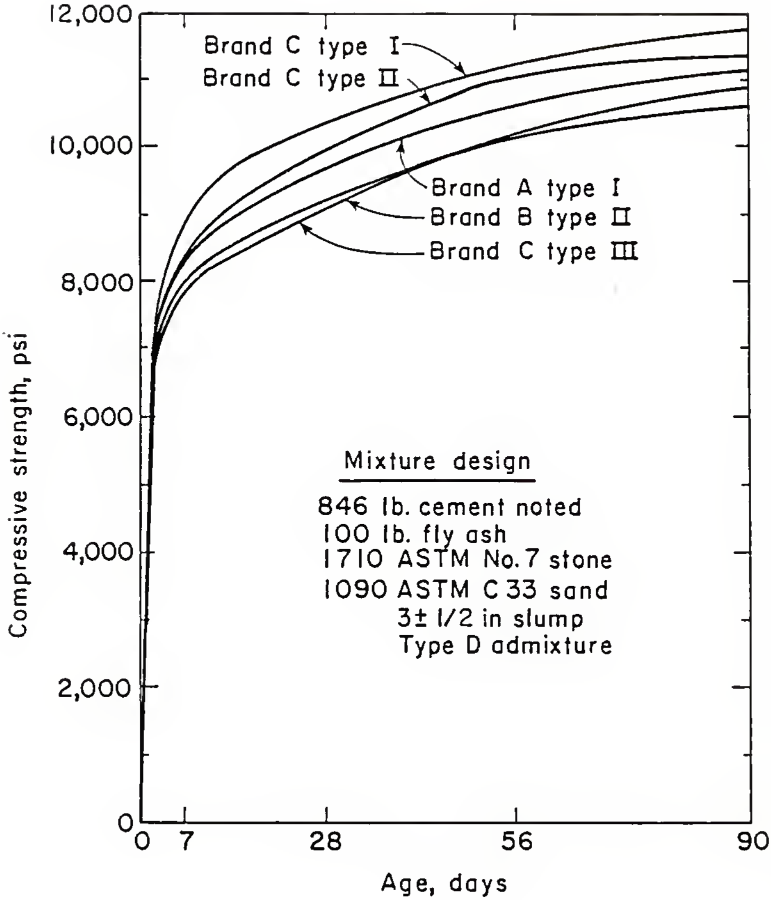

FIG. 2.2: EFFECT OF VARIOUS CEMENTS ON CONCRETE COMPRESSIVE STRENGTH (2)

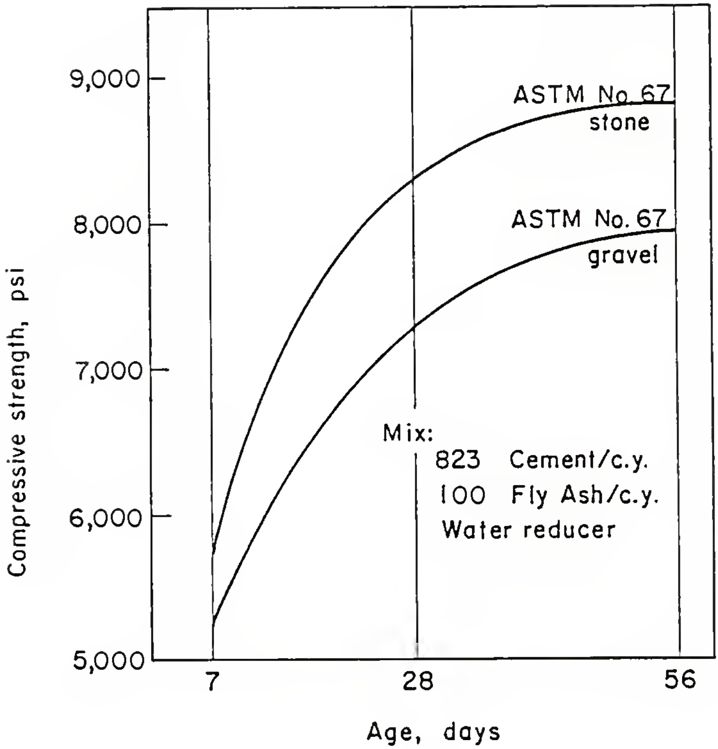

FIG. 2.3: COMPRESSIVE STRENGTH OF CONCRETE USING TWO SIZES AND TYPES OF COARSE AGGREGATES FOR 7,500 PSI CONCRETE (36)

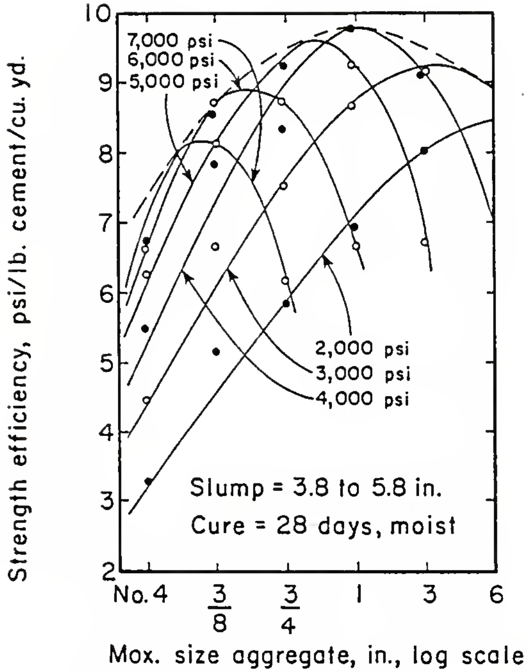

FIG. 2.4: MAXIMUM SIZE AGGREGATE FOR STRENGTH EFFICIENCY ENVELOPE (8)

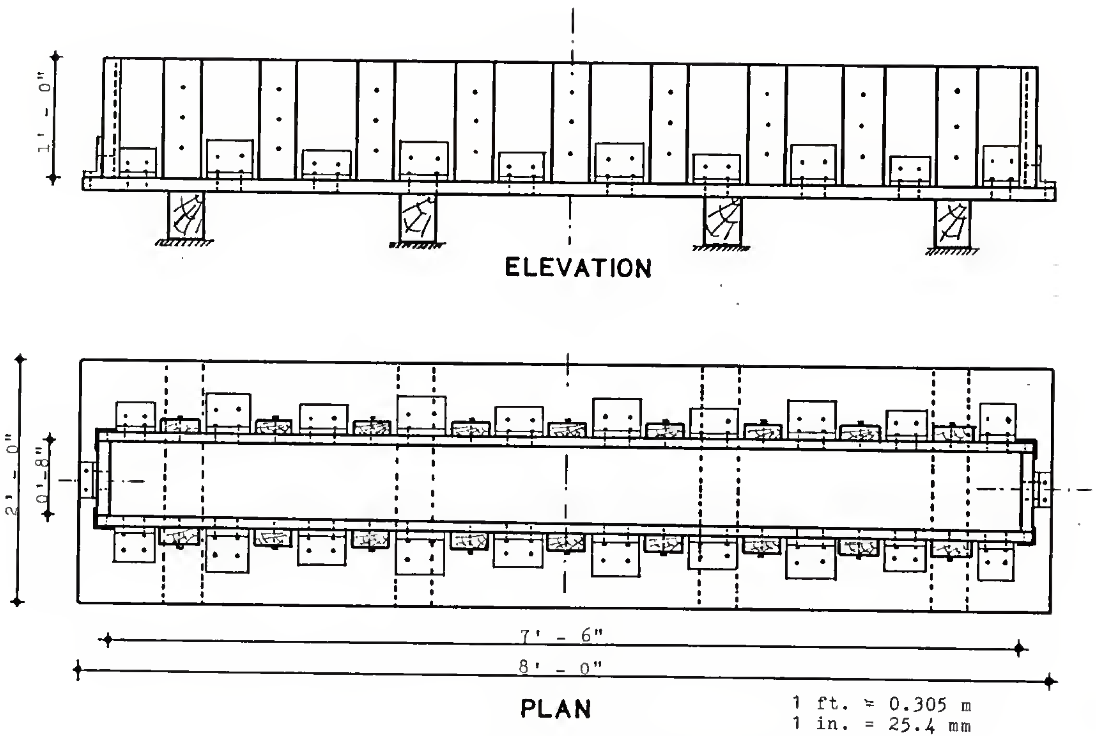

Fig. 4.1 : Wooden Form for Test Beams

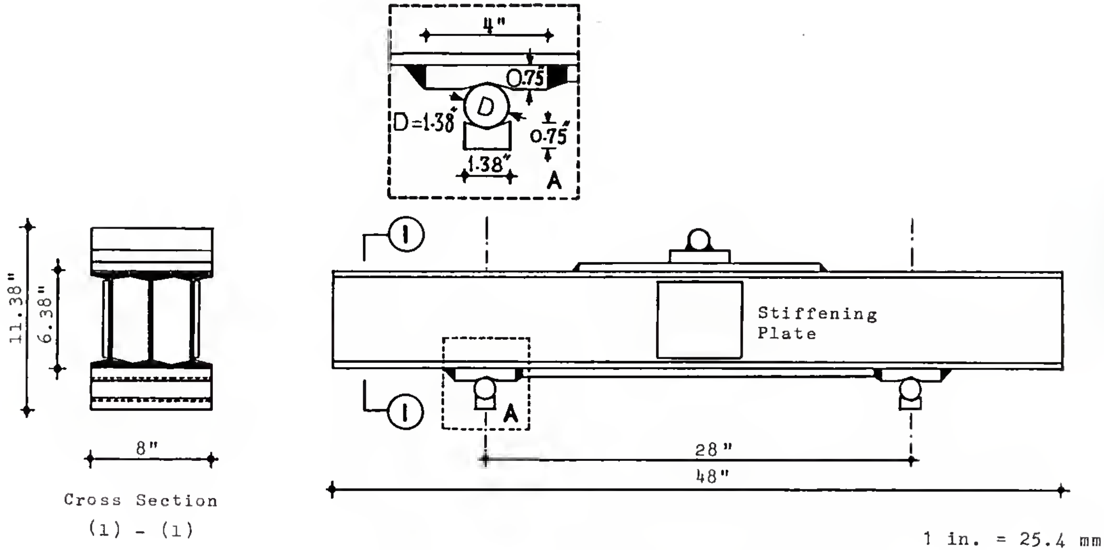

Fig. 4.2 : Details of the Loading Beam..

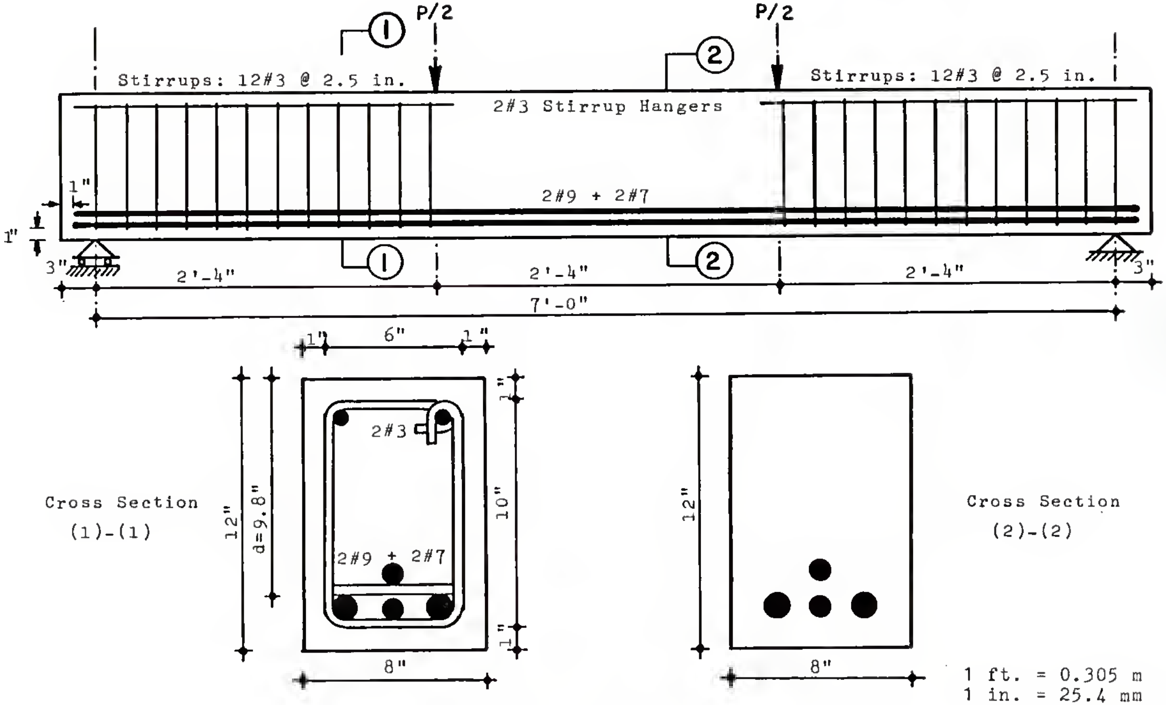

Fig. 4.3 : Reinforcement Details of Beam #1

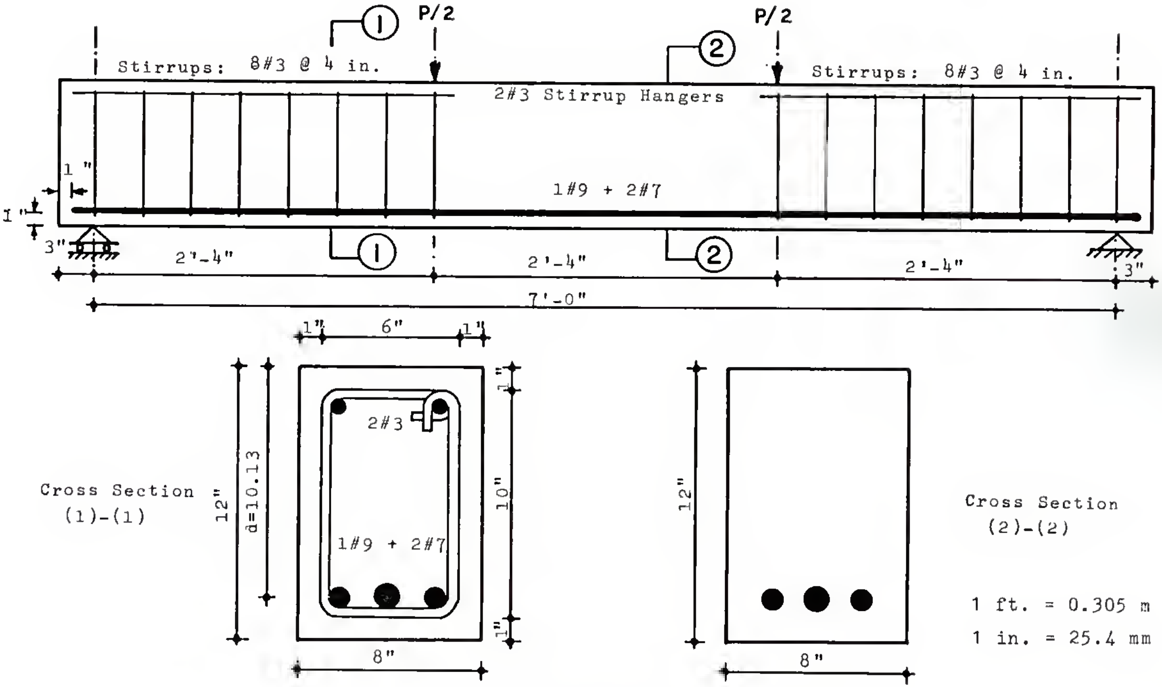

Fig. 4.4 : Reinforcement Details of Beam #2

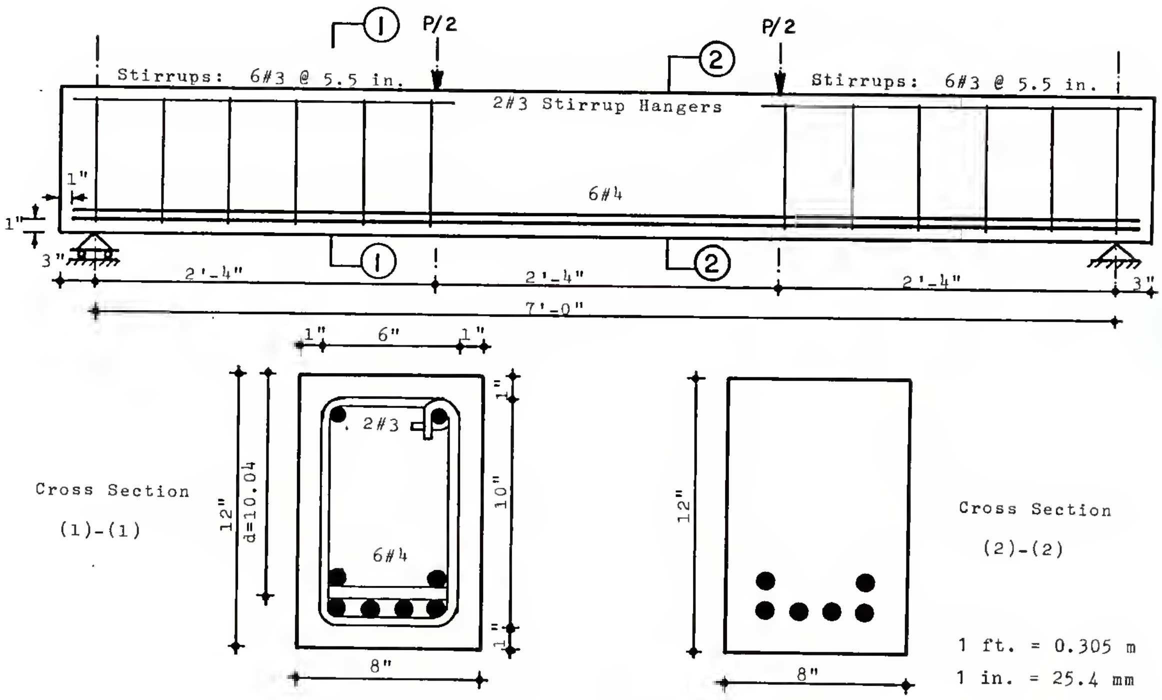

Fig. 4.5 : Reinforcement Details of Beam #3

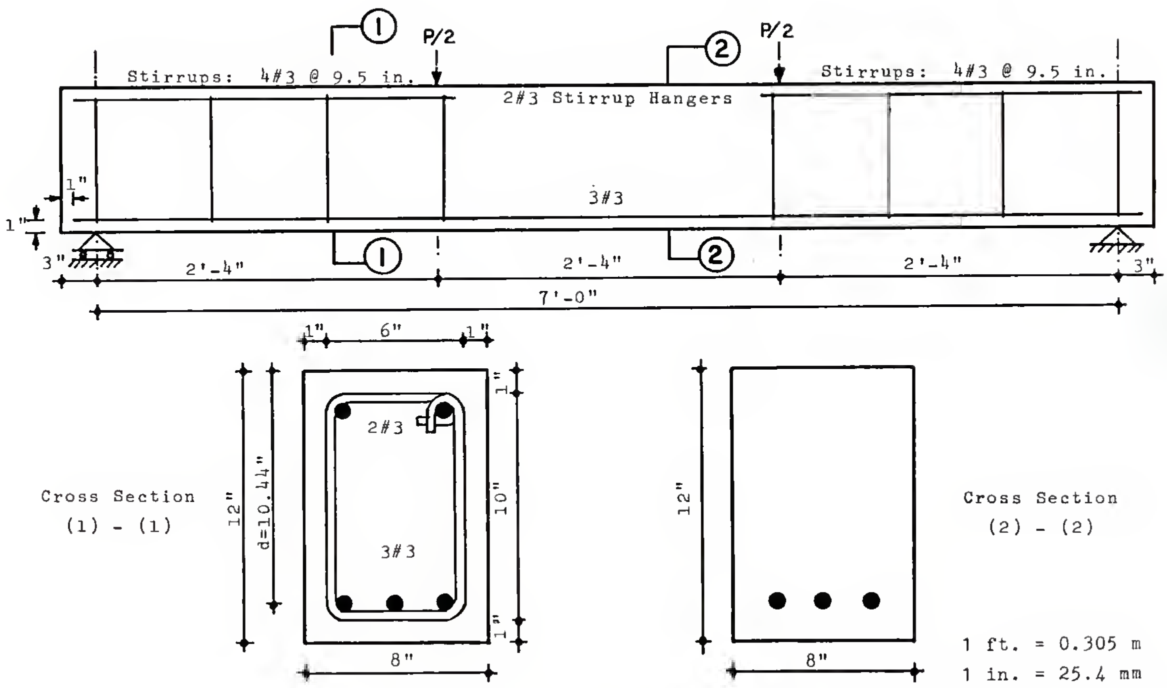

Fig. 4.6 : Reinforcement Details of Beam #4

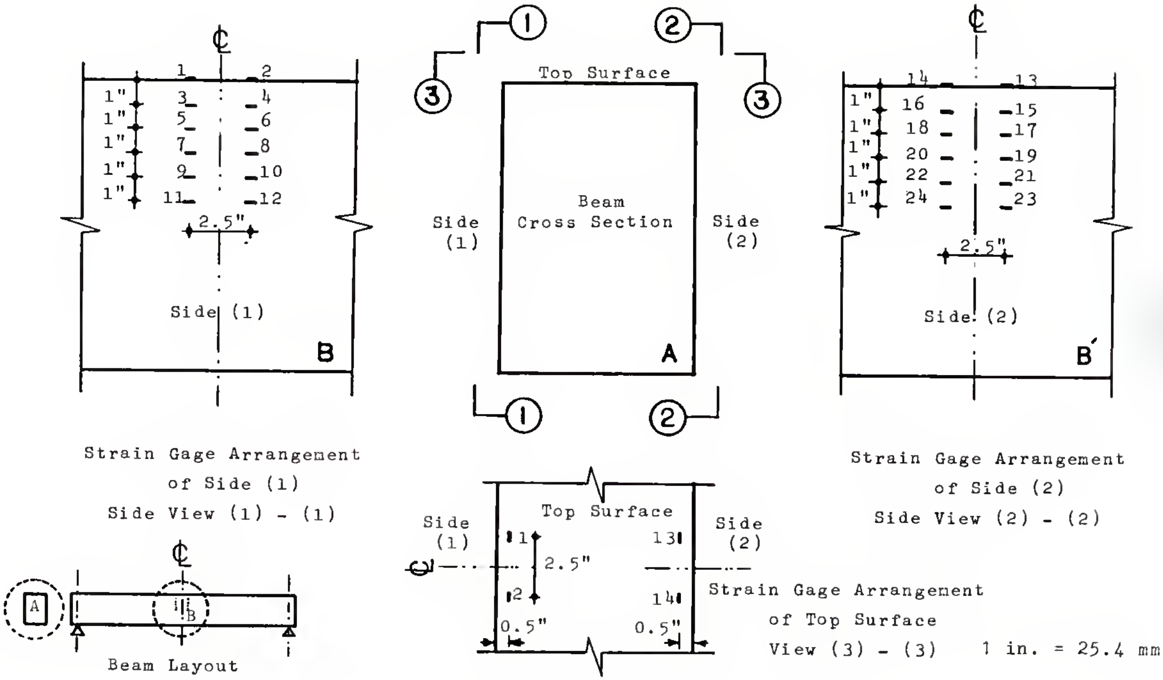

Fig. 4.7 : Strain Gage Arrangement of Test Beam

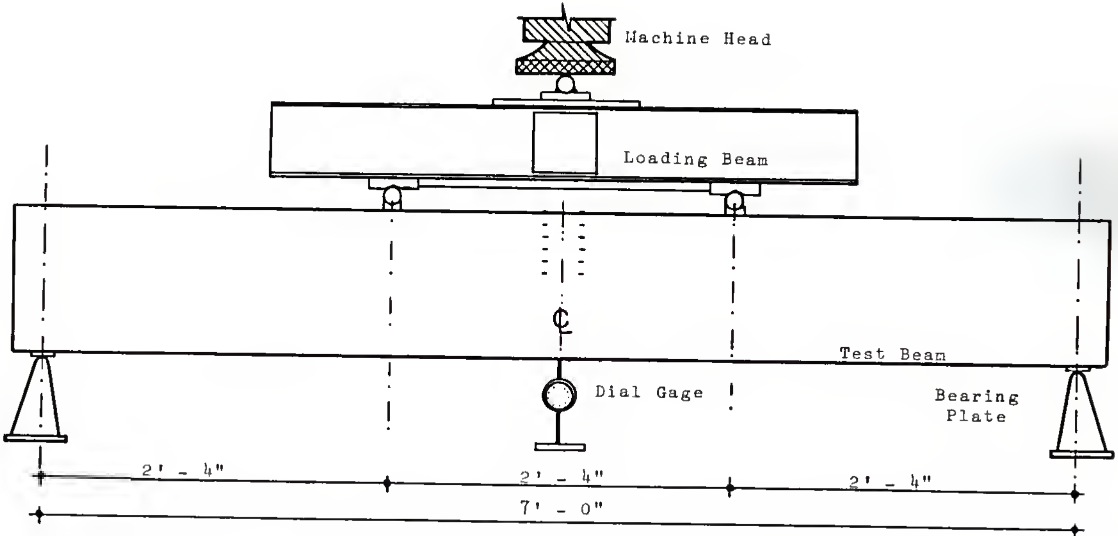

1 ft. = 0.35 m 1 in. = 25.4 mm

Fig. 4.8 : Test Setup and Loading Arrangement

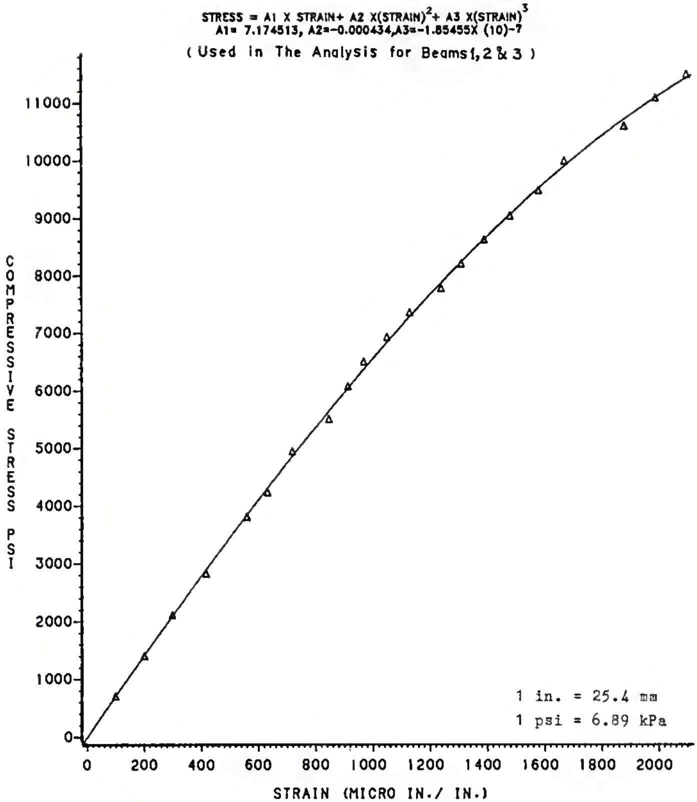

FIG. 5.1: STRESS–STRAIN CURVE BASED ON CYLINDER TEST DATA PRESENTED IN TABLE 5.11,REF. 10,P. 50

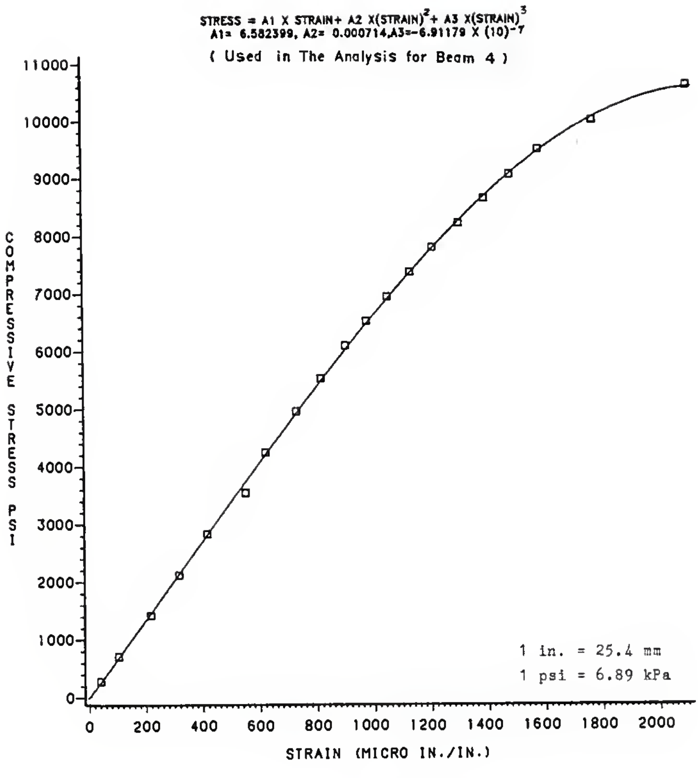

FIG. 5.2: STRESS-STRAIN CURVE BASED ON CYLINDER TEST OATA PRESENTEO IN TABLE 5.10,REF. 10,P. 48

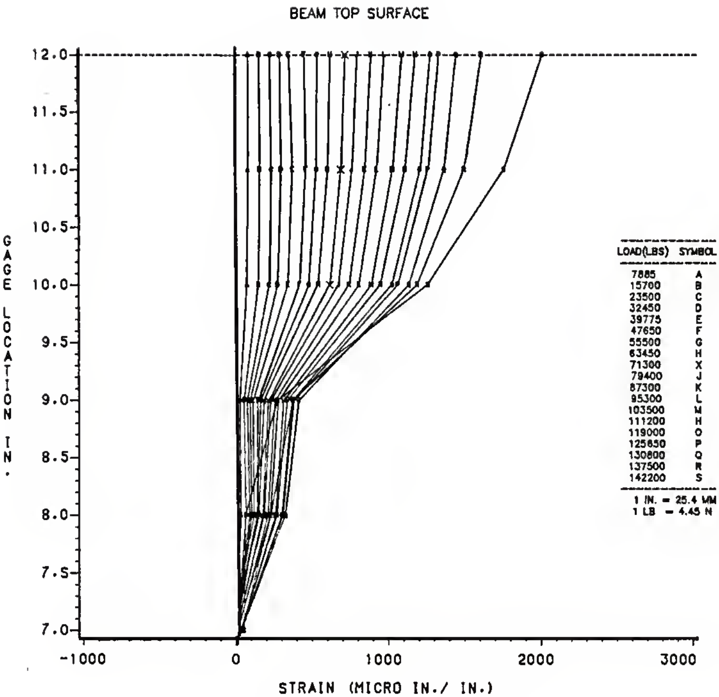

FIG. 5.3: GAGE LOCATIONS VS. STRAIN
FOR BEAM 1 SIDE 1

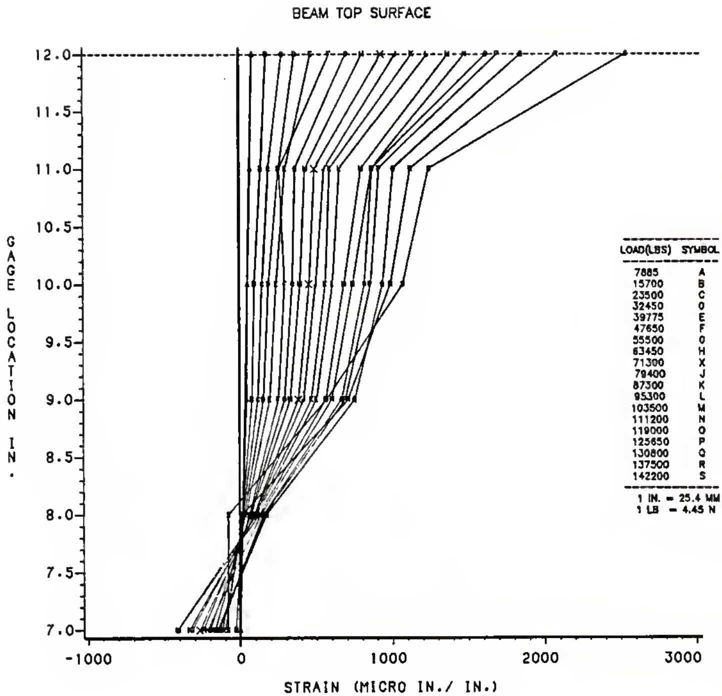

FIG. 5.4: GAGE LOCATIONS VS. STRAIN
FOR BEAM 1 SIDE 2

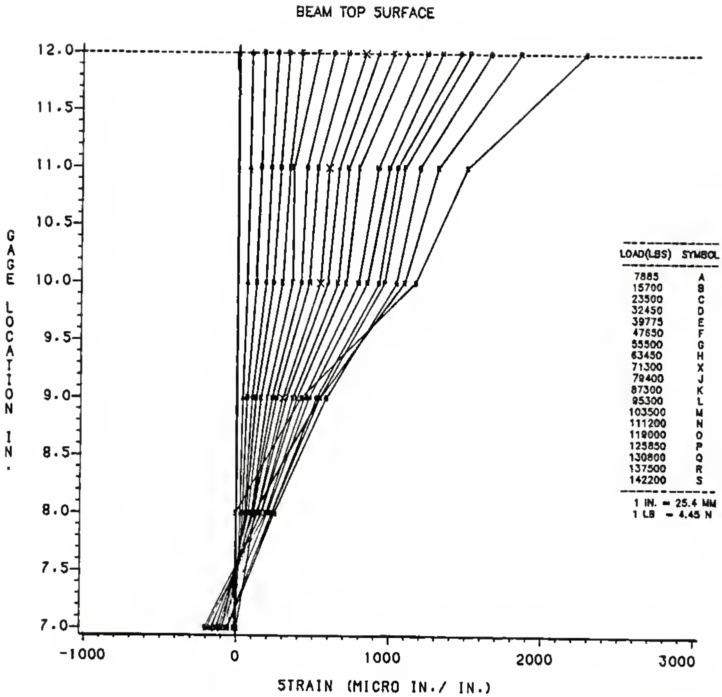

FIG 5.5: GAGE LOCATIONS VS. AVERAGE STRAIN
FOR BEAM 1
(AVERAGE OF SIDE 1 AND SIDE 2)

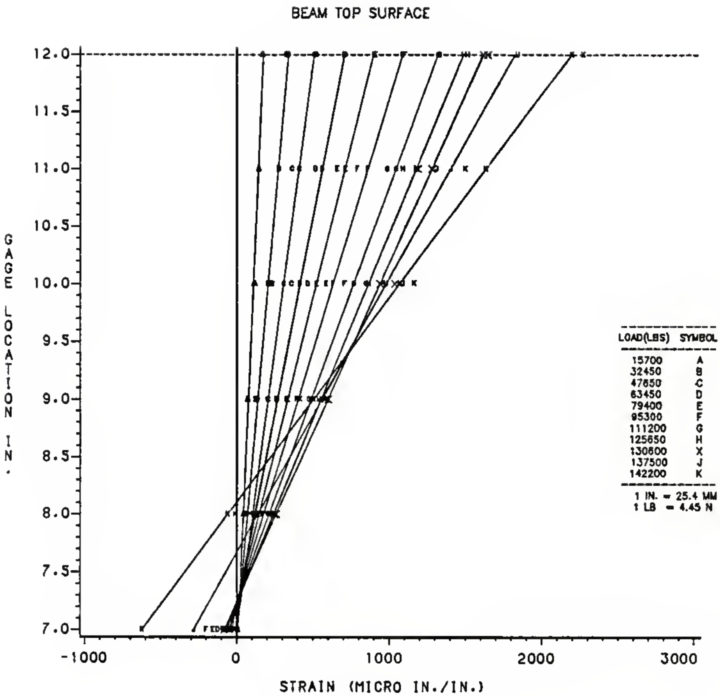

FIG. 5.6: GAGE LOCATIONS VS. AVERAGE STRAIN
FQR BEAM 1 USING LEAST SQUARE REGRESSION
(AVERAGE OF SIDE 1 AND SIDE 2)

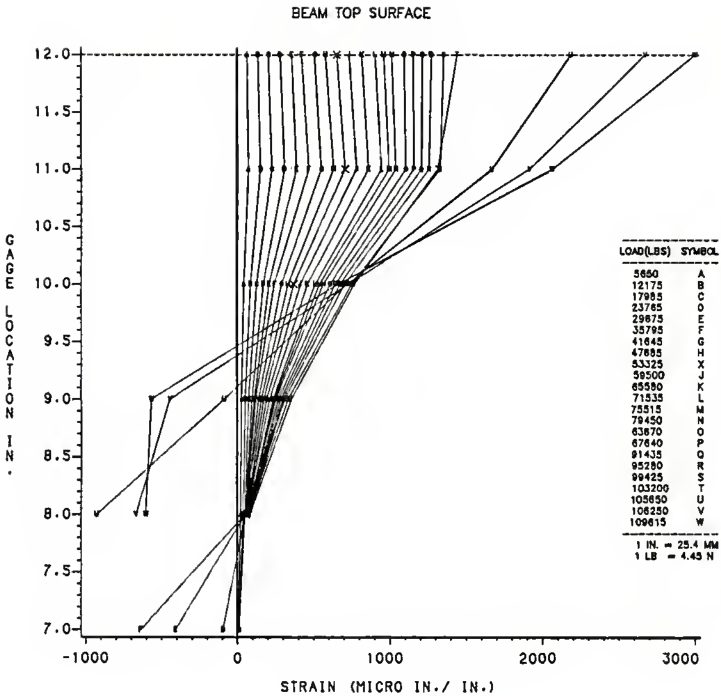

FIG. 5.7: GAGE LOCATIONS VS. STRAIN
FOR BEAM 2 SIDE 1

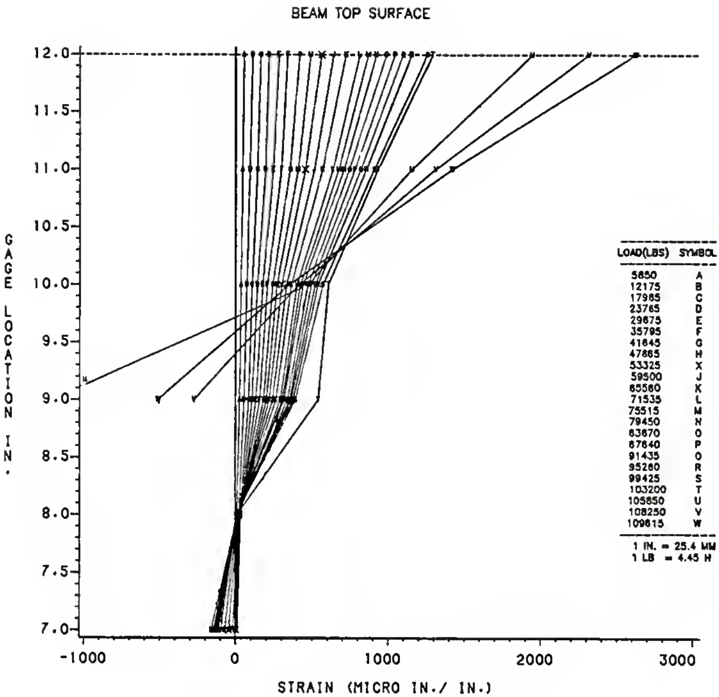

FIG. 5.8: GAGE LOCATIONS VS. STRAIN
FOR BEAM 2 SIDE 2

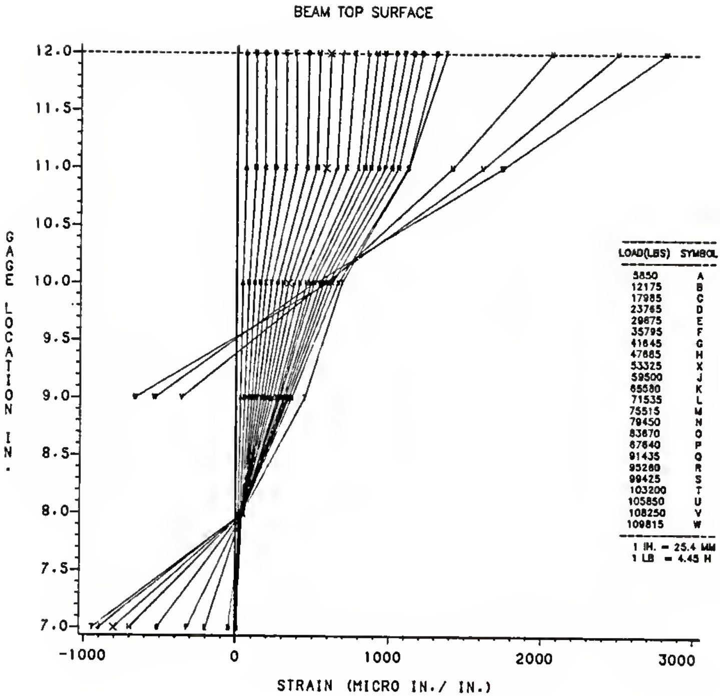

FIG. 5.9: GAGE LOCATIONS VS. AVERAGE STRAIN
FOR BEAM 2
(AVERAGE OF SIDE 1 AND SIDE 2)

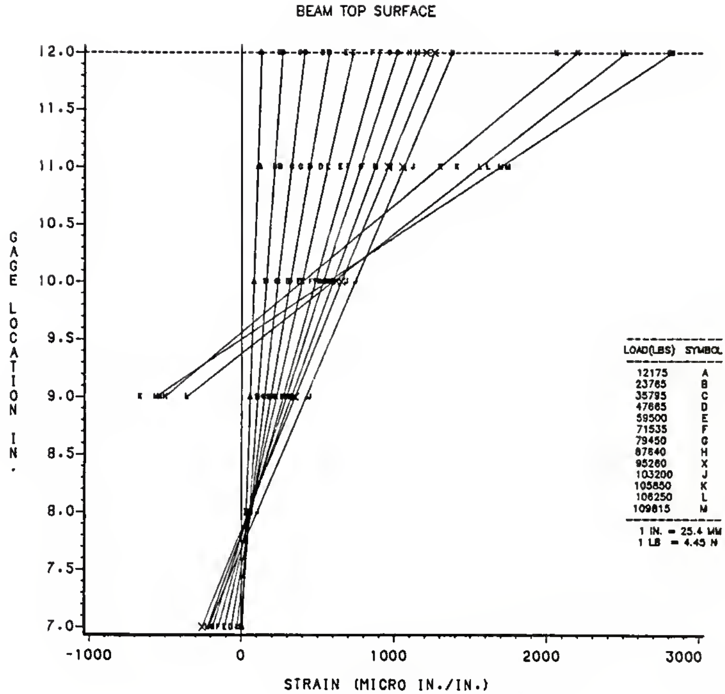

FIG. 5.10: GAGE LOCATIONS VS. AVERAGE STRAIN
FOR BEAM 2 USING LEAST SQUARE REGRESSION
(AVERAGE OF SIDE 1 AND SIDE 2)

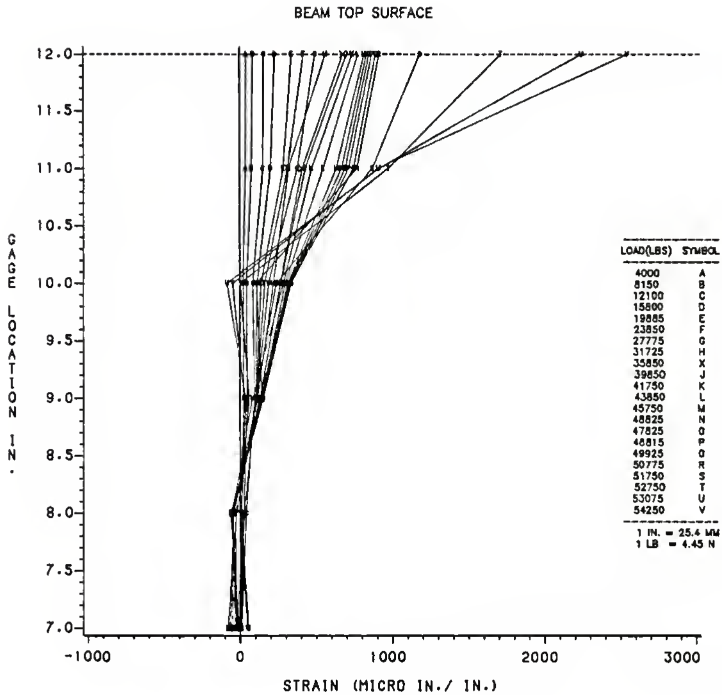

FIG. 5.11: GAGE LOCATIONS VS. STRAIN
FOR BEAM 3 SIDE 1

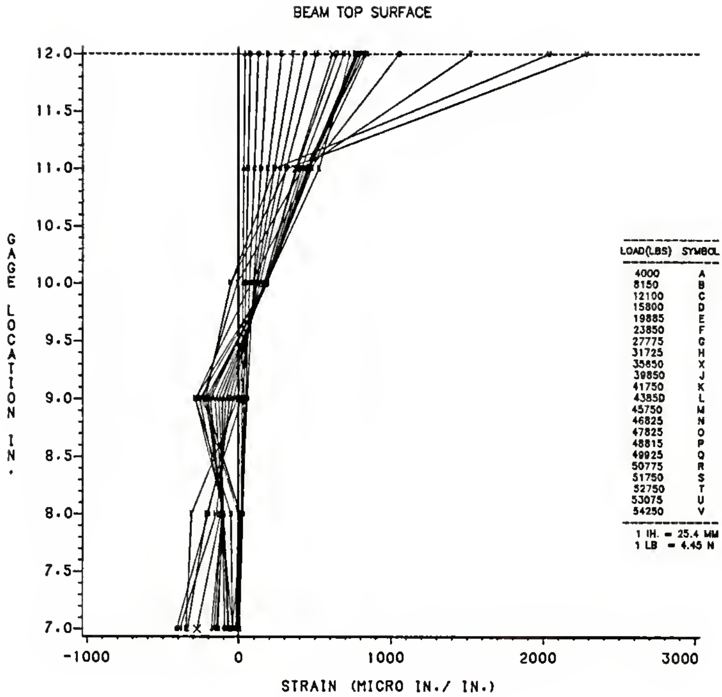

FIG. 5.12: GAGE LOCATIONS VS. STRAIN
FOR BEAM 3 SIDE 2

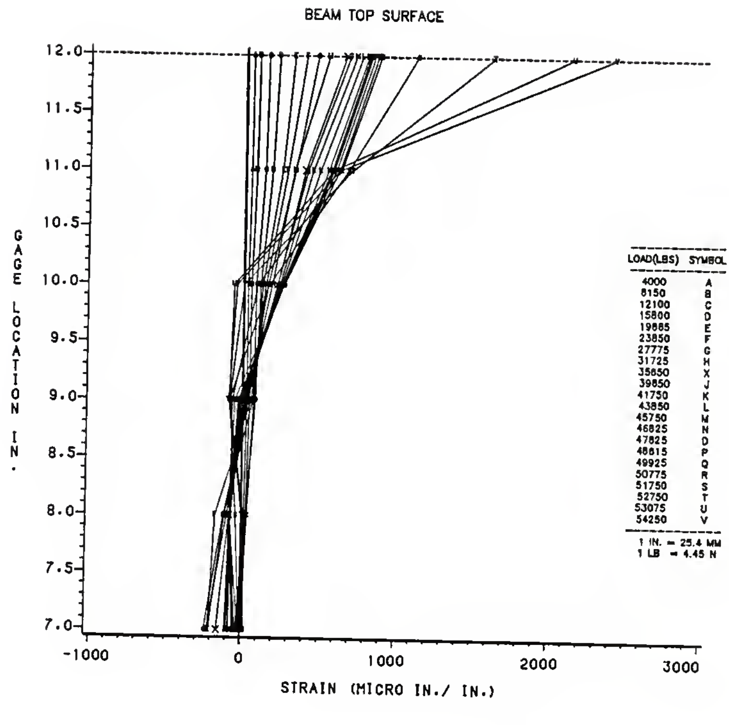

FIG. 5.13: GAGE LOCATIONS VS. AVERAGE STRAIN
FOR BEAM 3
(AVERAGE OF SIDE 1 AND SIDE 2)

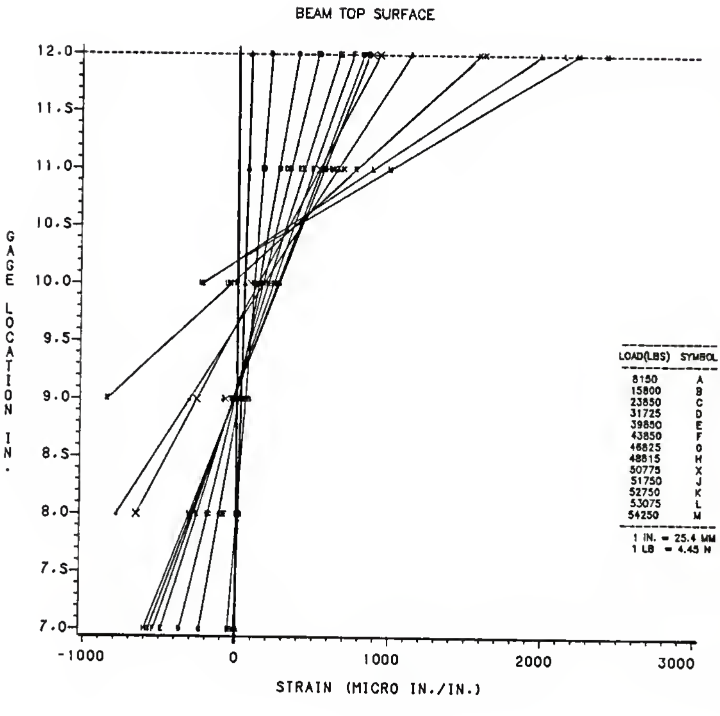

FIG. S.14: GAGE LOCATIONS VS. AVERAGE STRAIN
FOR BEAM 3 USING LEAST SQUARE REGRESSION
(AVERAGE OF SIDE 1 AND SIDE 2)

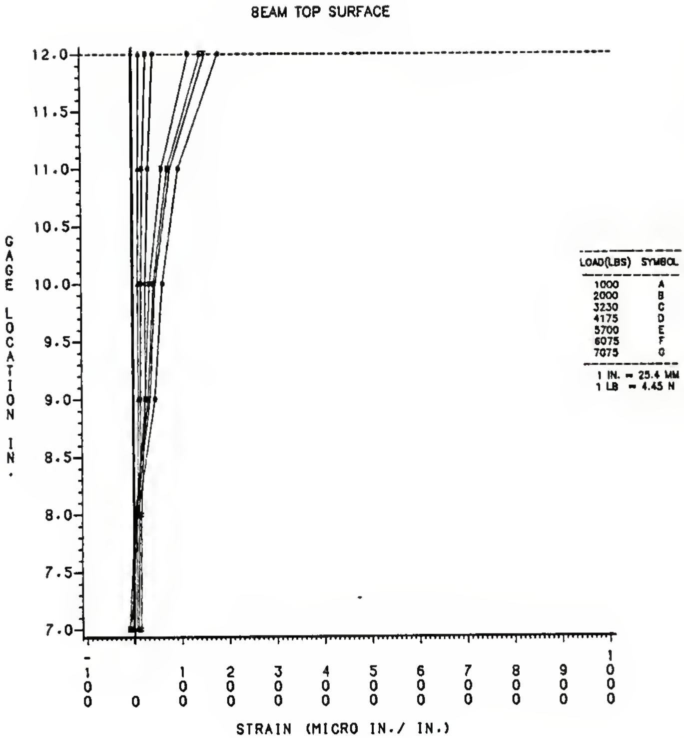

FIG. 5.15: GAGE LOCATIONS VS. AVAILABLE STRAIN DATA FOR BEAM 4 SIDE 1

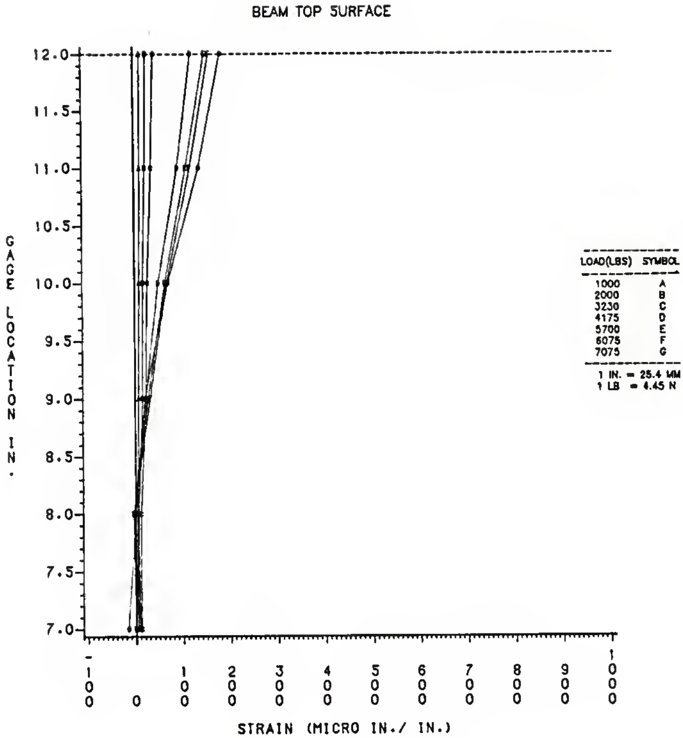

FIG. 5.16: GAGE LOCATIONS VS. AVAILABLE STRAIN OATA FOR 8EAM 4 5IOE 2

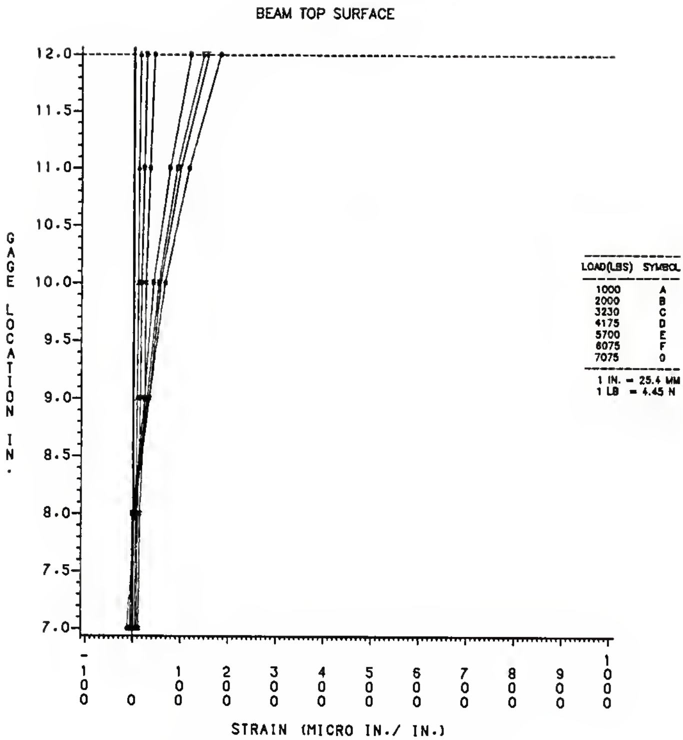

FIG. 5.17: GAGE LOCATIONS VS. AVAILABLE STRAIN
DATA FOR BEAM 4
(AVERAGE OF SIDE 1 AND SIDE 2)

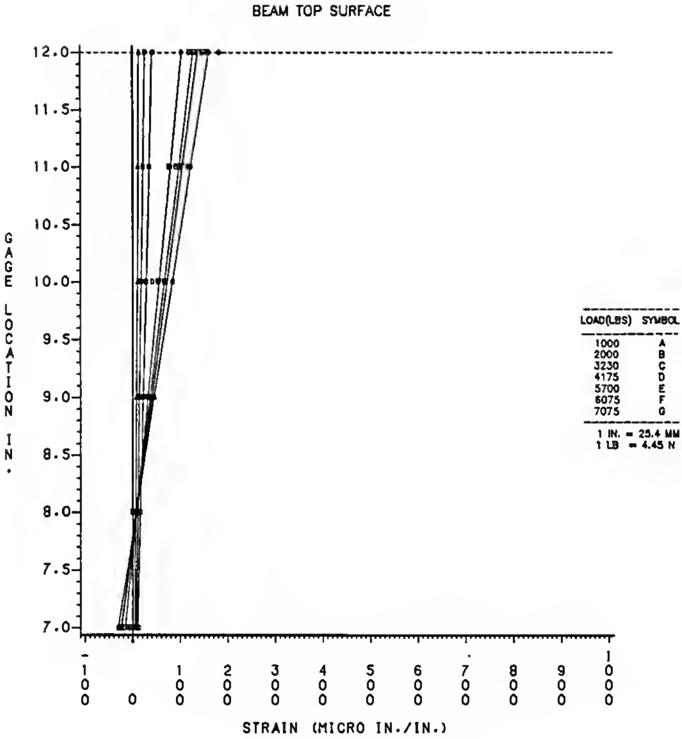

FIG. 5.18: GAGE LOCATIONS VS. AVERAGE STRAIN FOR BEAM 4 USING LEAST SQUARE REGRESSION (AVERAGE OF SIDE 1 AND SIDE 2)

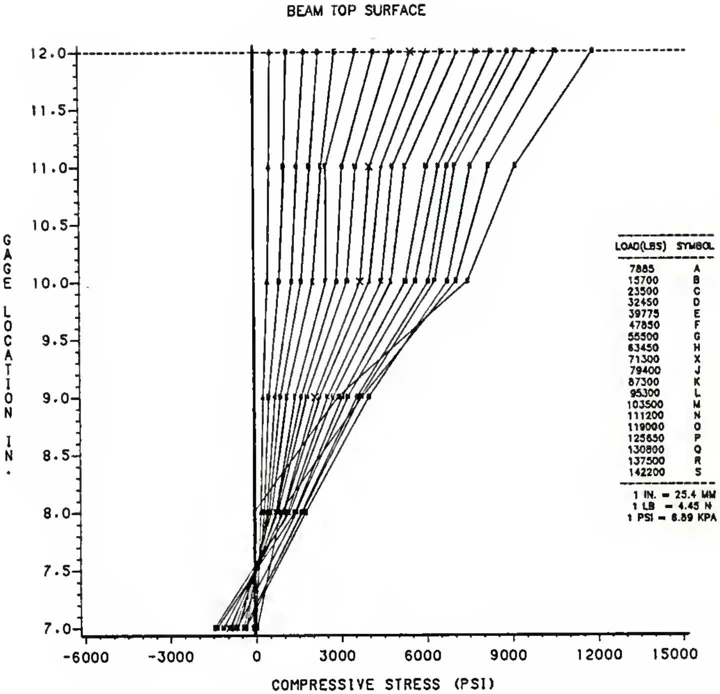

FIG. 5.19: GAGE LOCATIONS VS. AVERAGE COMPRESSIVE STRESS FOR BEAM 1 BASED ON CUBIC REGRESSION MODEL
(AVERAGE OF SIDE 1 AND SIDE 2)

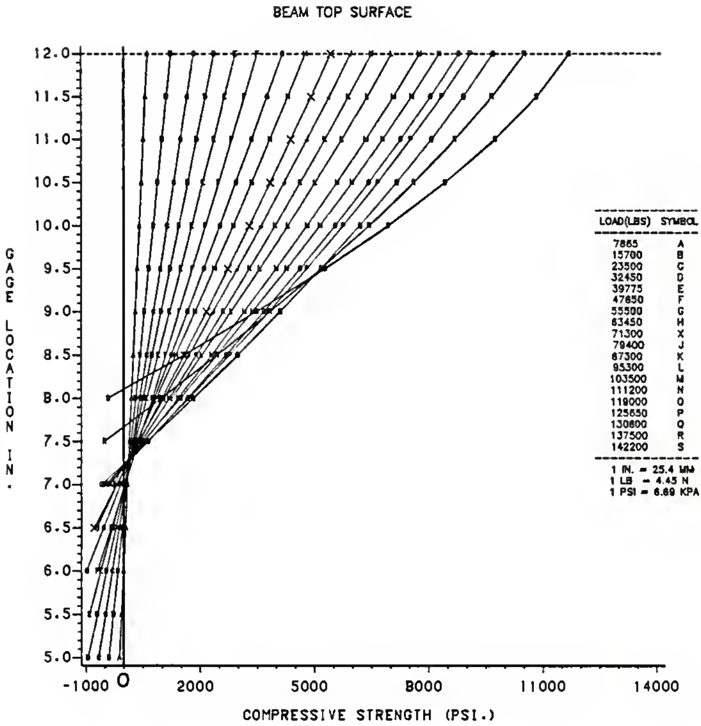

FIG. 5.20: COMPRESSIVE STRESS BLOCK OF BEAM 1
BASED ON CUBIC REGRESSION MODEL
AND LINEAR STRAIN ASSUMPTION

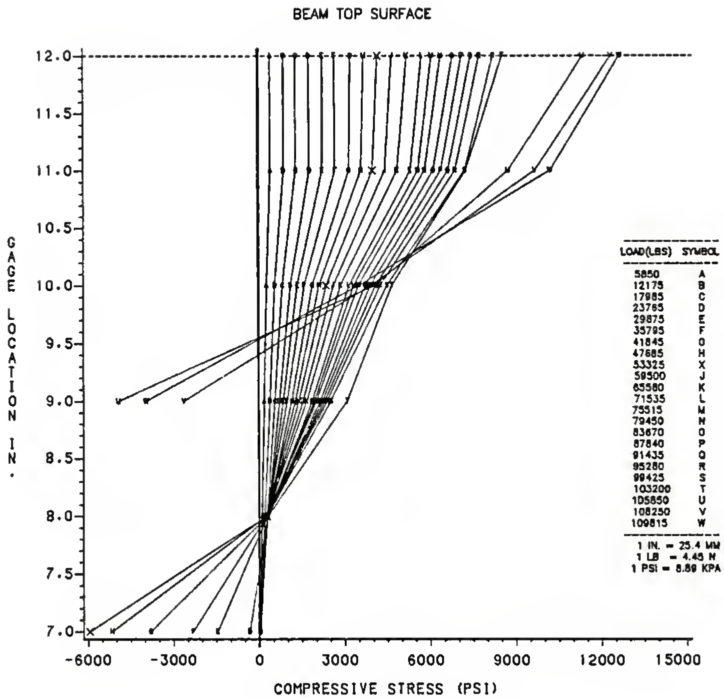

FIG. 5.21: GAGE LOCATIONS VS. AVERAGE COMPRESSIVE STRESS FOR BEAM 2 BASED ON CUBIC REGRESSION MODEL
(AVERAGE OF SIDE 1 AND SIDE 2)

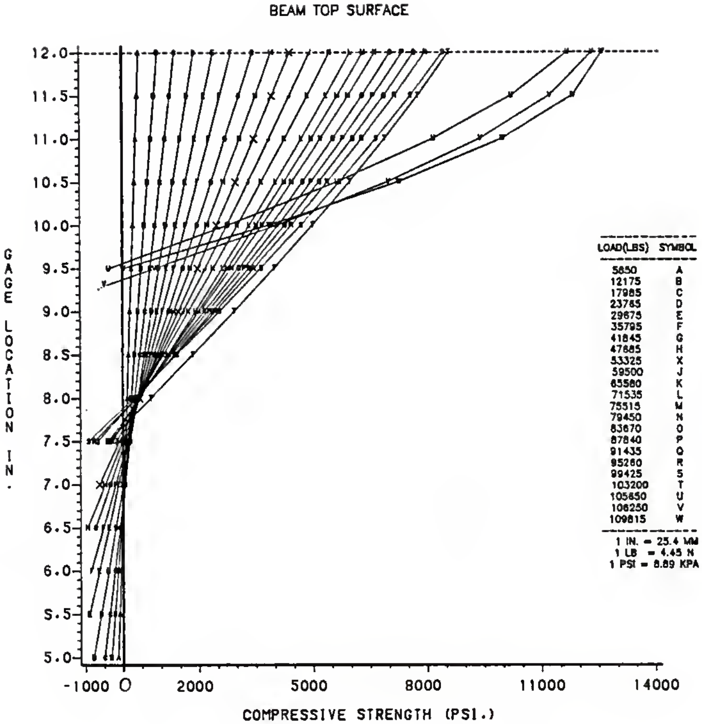

FIG. 5.22: COMPRESSIVE STRESS BLOCK OF BEAM 2
BASED ON CUBIC REGRESSION MODEL
AND LINEAR STRAIN ASSUMPTION

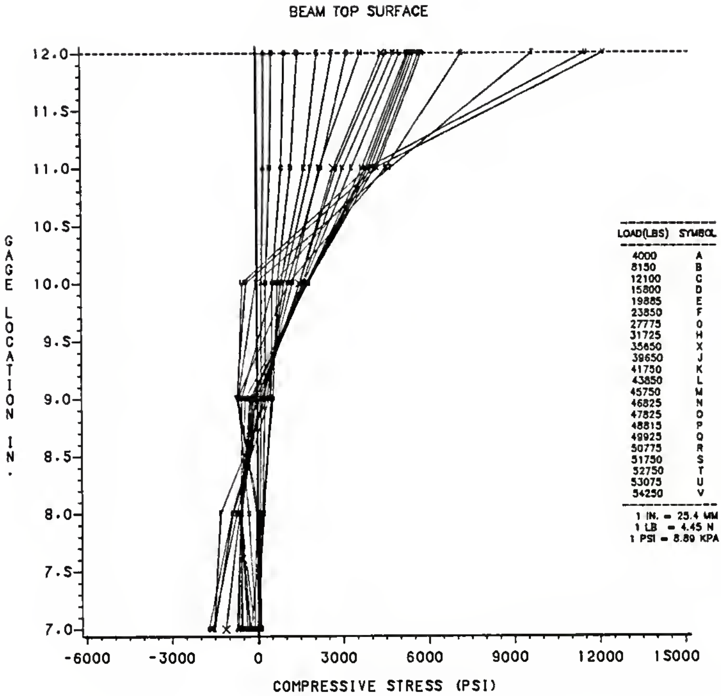

FIG. 5.23: GAGE LOCATIONS VS. AVERAGE COMPRESSIVE STRESS FOR BEAM 3 BASED ON CUBIC REGRESSION MODEL (AVERAGE OF SIDE 1 AND SIDE 2)

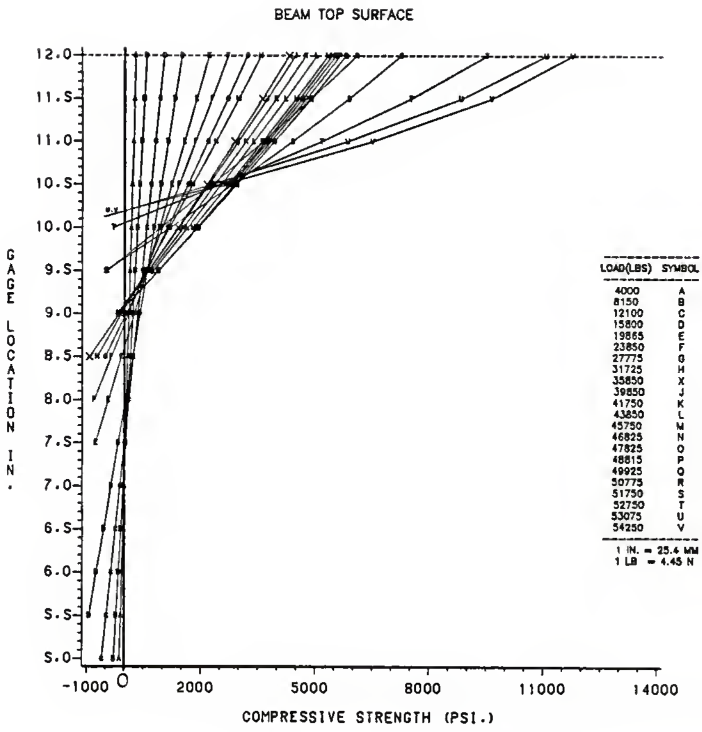

FIG. 5.24: COMPRESSIVE STRESS BLOCK OF BEAM 3
BASED ON CUBIC REGRESSION MODEL
AND LINEAR STRAIN ASSUMPTION

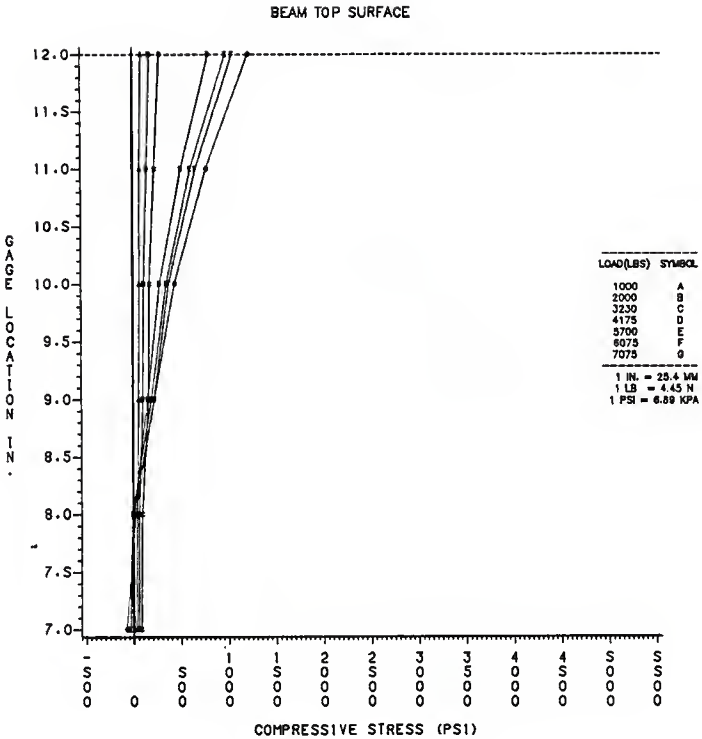

FIG. 5.25: GAGE LOCATIONS VS. AVERAGE COMPRESSIVE STRESS FOR BEAM 4 BASED ON CUBIC REGRESSION MODEL (AVERAGE OF SIDE 1 AND SIDE 2)

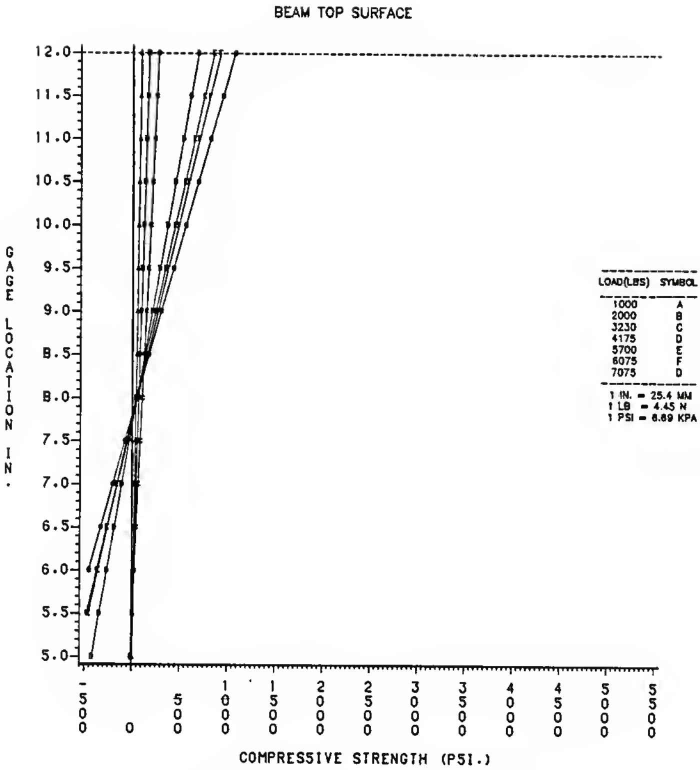

FIG. 5.26: COMPRESSIVE STRESS BLOCK OF BEAM 4
BASED ON CUBIC REGRESSION MODEL
AND LINEAR STRAIN ASSUMPTION

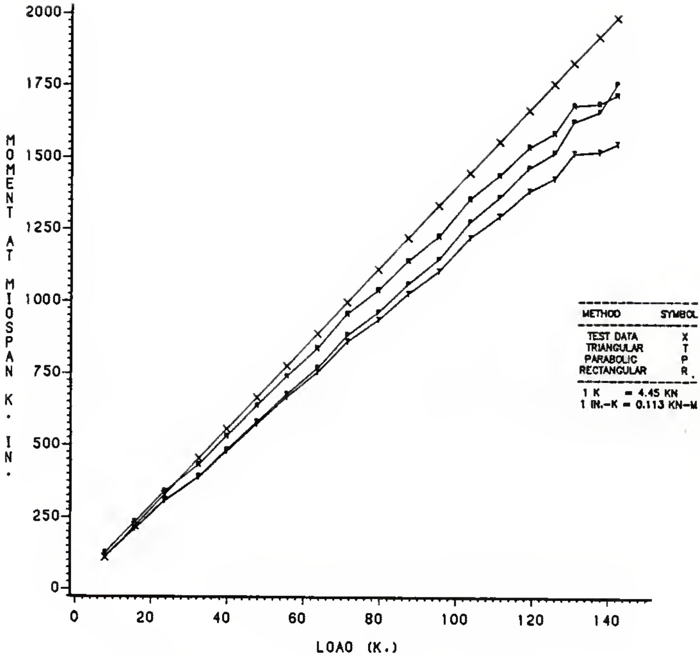

FIG. 5.27: MOMENT AT MIOSPAN VS. LOAD VALUE OF BEAM 1
(TEST MOMENT AND CALCULATED MOMENT USING PARABOLIC, TRIANGULAR AND RECTANGULAR STRESS BLOCKS)

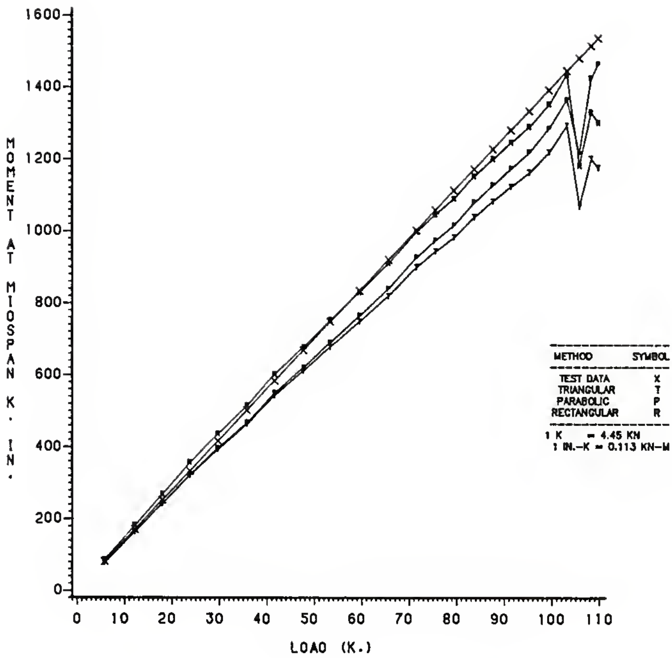

FIG. 5.28: MOMENT AT MIOSPAN VS. LOAO VALUE OF BEAM 2
(TEST MOMENT AND CALCULATED MOMENT USING PARABOLIC, TRIANGULAR AND RECTANGULAR STRESS BLOCKS)

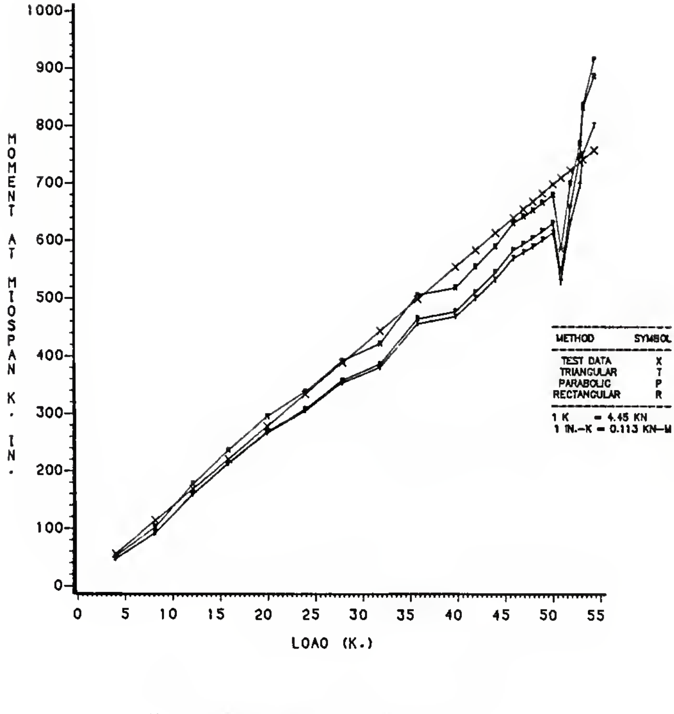

FIG. 5.29: MOMENT AT MIDSPAN VS. LOAD VALUE OF BEAM 3
(TEST MOMENT AND CALCULATED MOMENT USING PARABOLIC, TRIANGULAR AND RECTANGULAR STRESS BLOCKS)

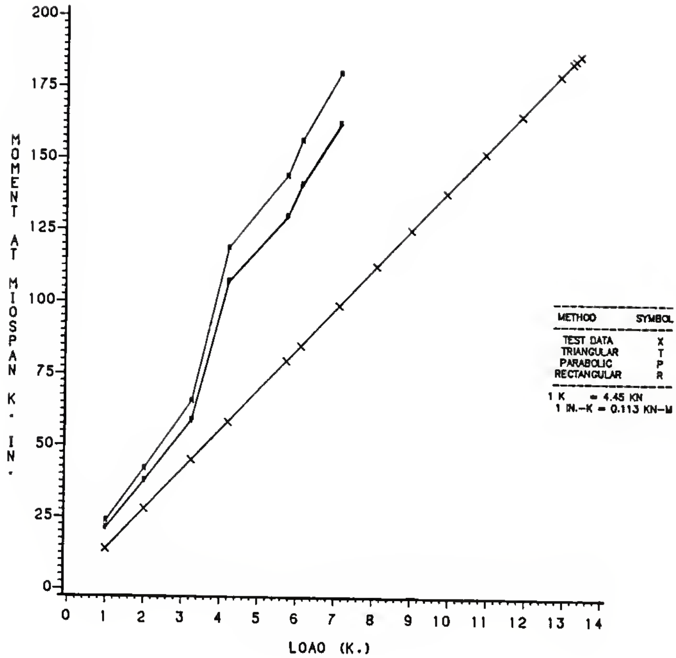

FIG. 5.30: MOMENT AT MIOSPAN VS. LOAO VALUE OF BEAM 4
(TEST MOMENT AND CALCULATED MOMENT USING PARABOLIC, TRIANGULAR AND RECTANGULAR STRESS BLOCKS)

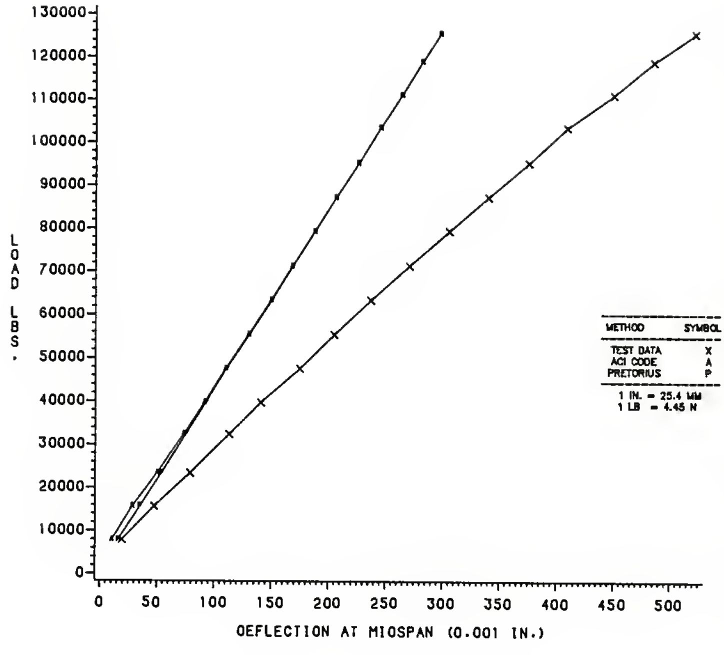

FIG. 5.31: LOAO VS. VERTICAL OEFLECTION
AT MIOSPAN OF BEAM 1

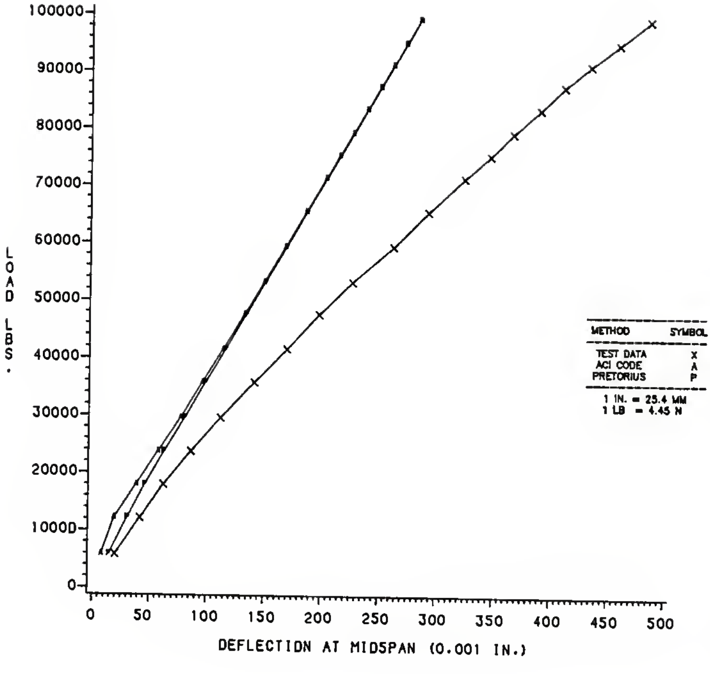

FIG. 5.32: LOAD VS. VERTICAL DEFLECTION
AT MIDSPAN OF BEAM 2

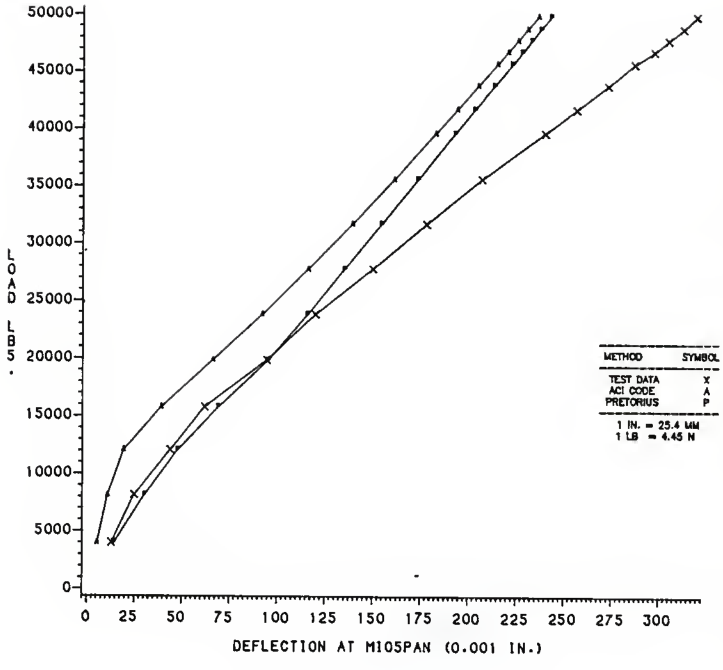

FIG. 5.33: LOAD VS. VERTICAL DEFLECTION
AT MIDSPAN OF BEAM 3

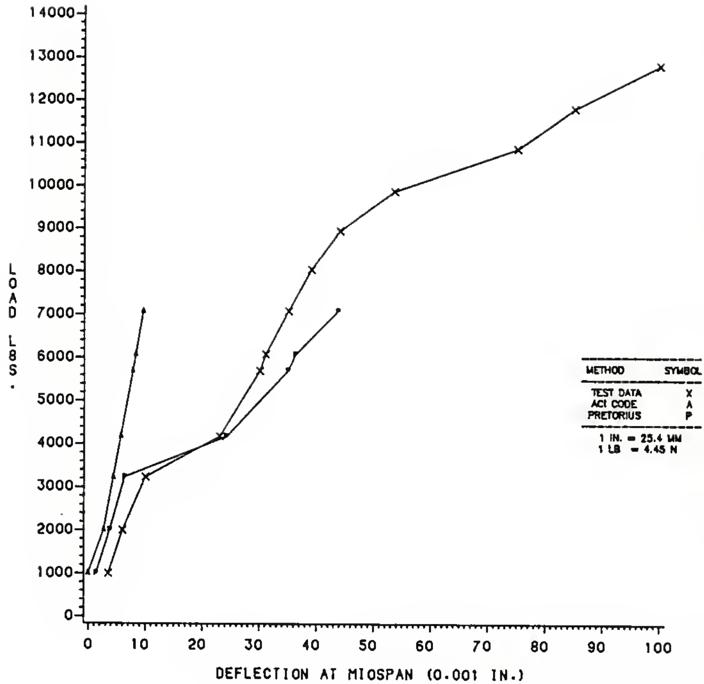

FIG. 5.34: LOAD VS. VERTICAL DEFLECTION
AT MIDSPAN OF BEAM 4

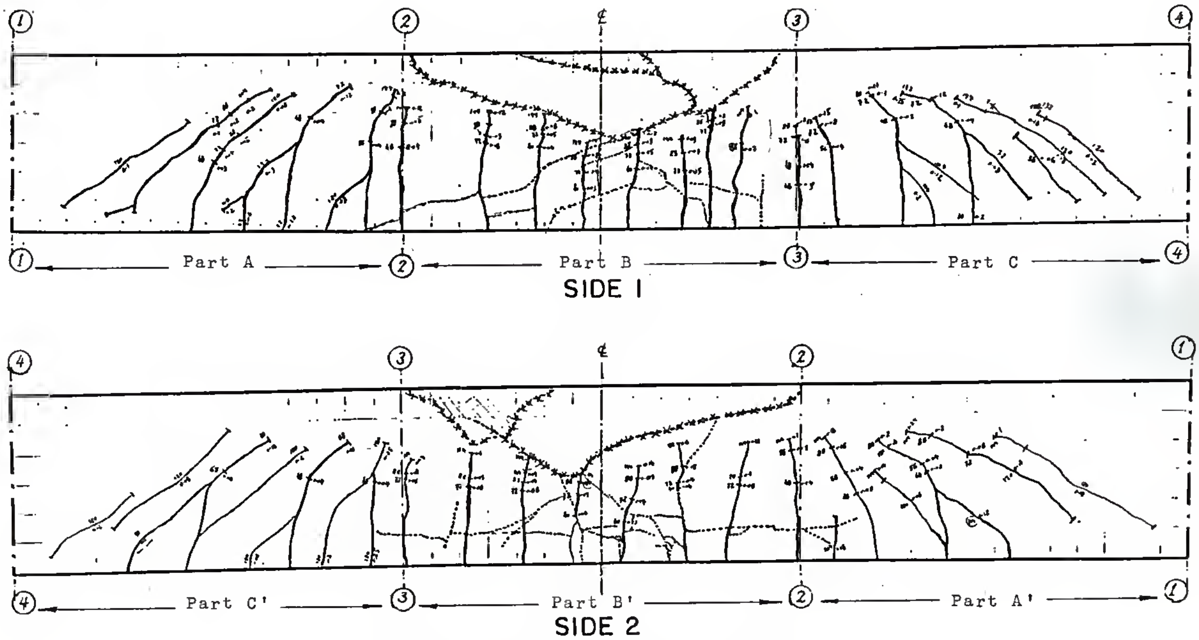

Fig. 5.35 Crack Pattern of Beam #1

(Side 1 and Side 2)

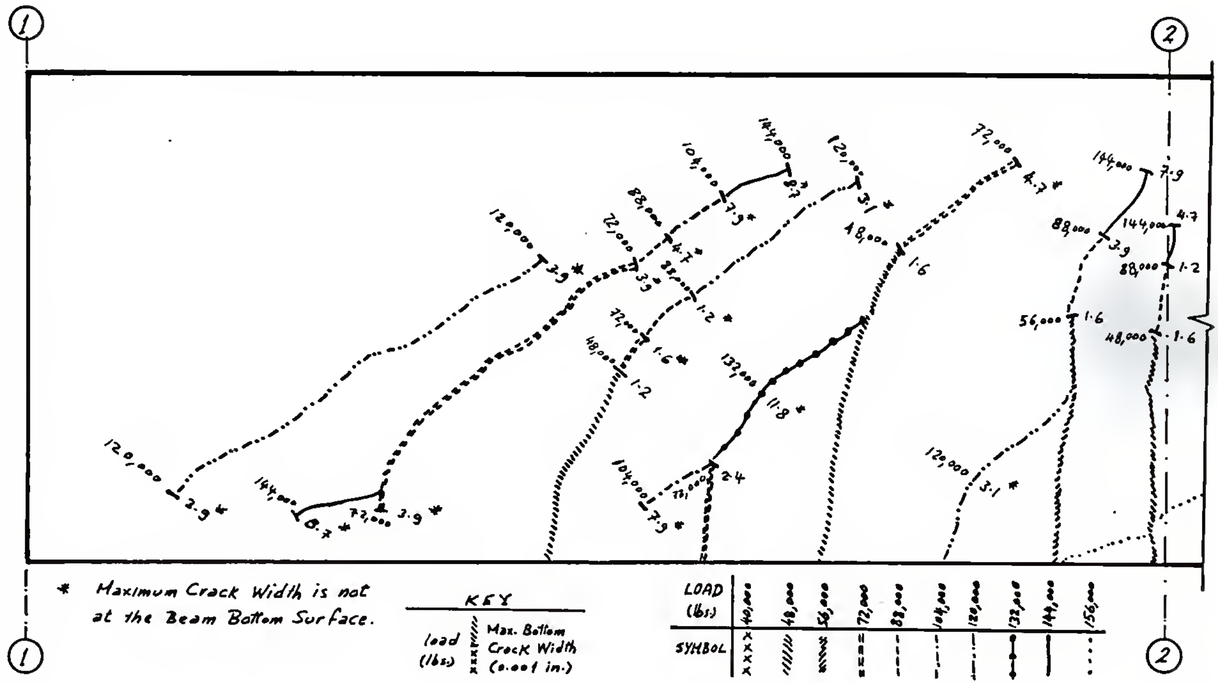

Fig. 5.36 Details of Crack Propagation of Beam #1

Side 1 Part A

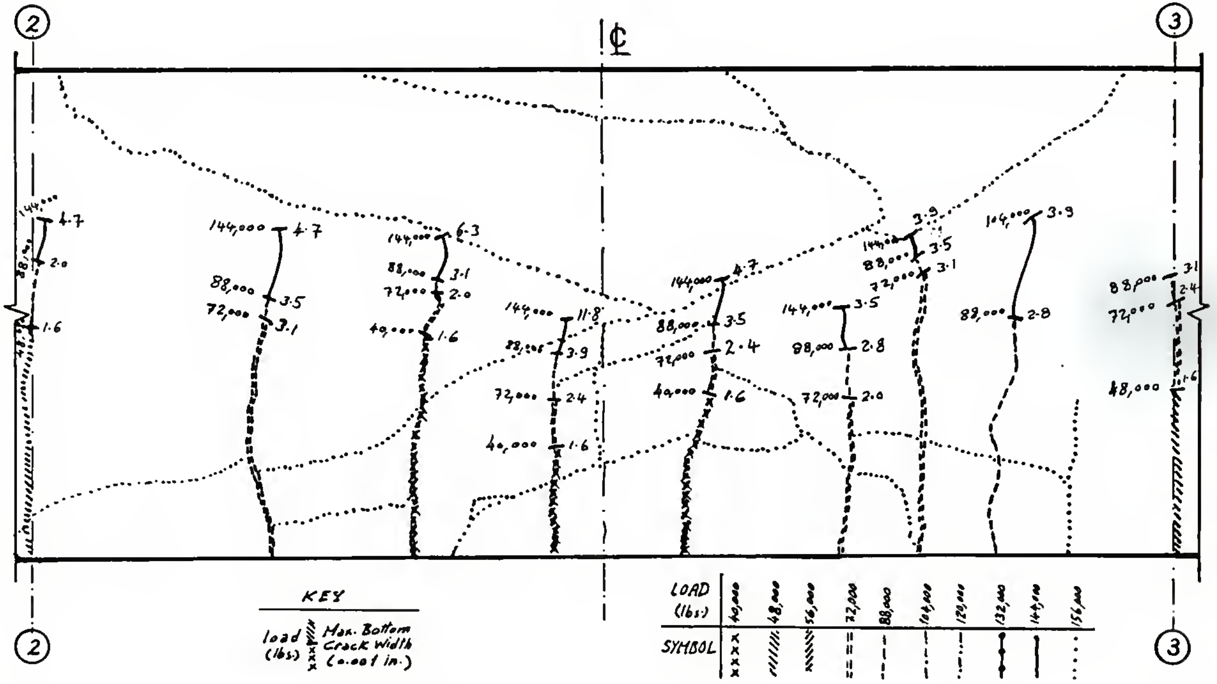

Fig. 5.37 Details of Crack Propagation of Beam #1
Side 1 Part B

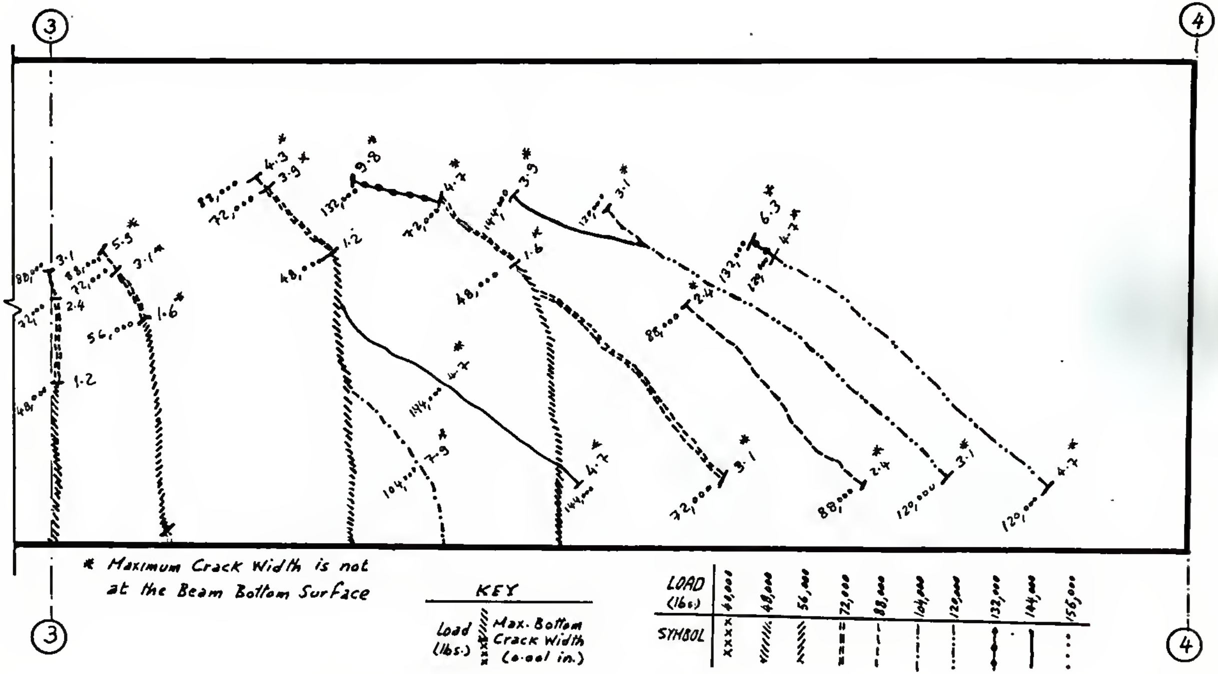

Fig. 5.38 Details of Crack Propagation of Beam #1

Side 1 Part c

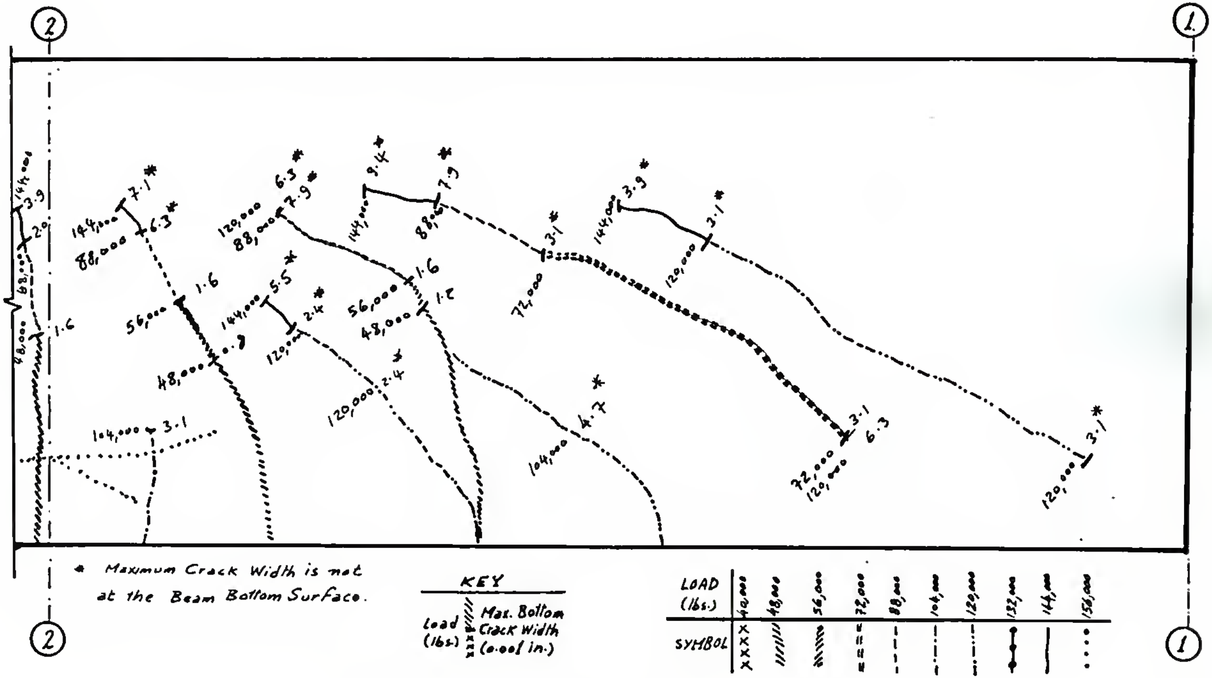

Fig. 5.39 Details of Crack Propagation of Beam #1
Side 2 Part A'

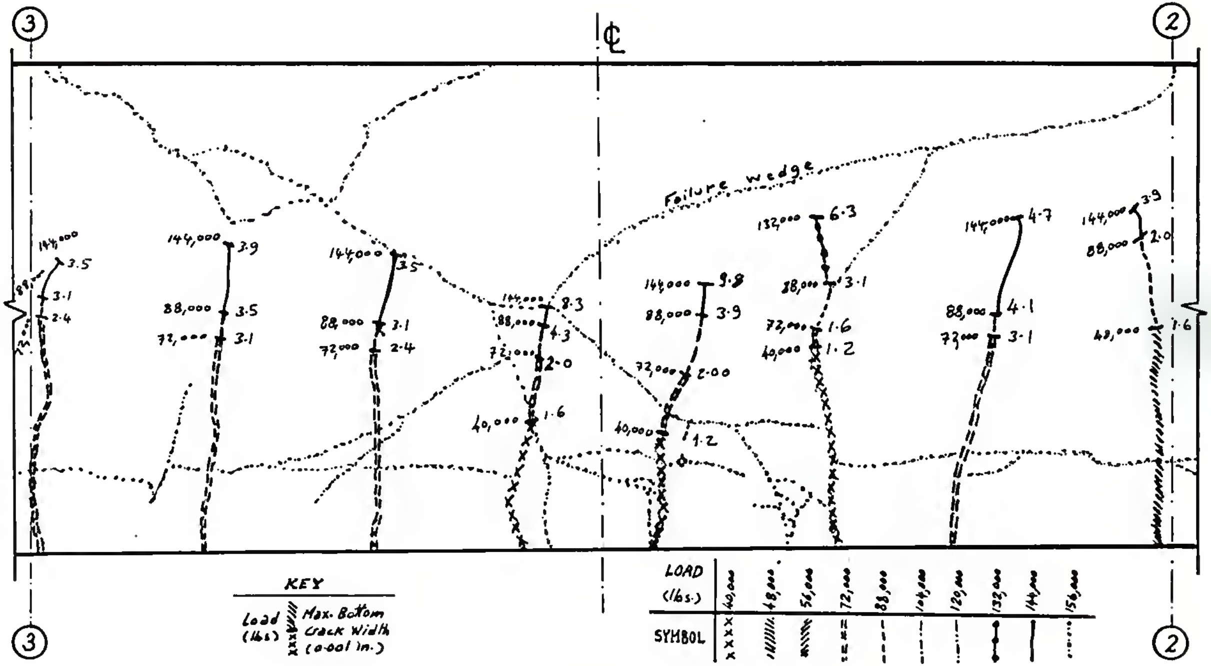

Fig. 5.40 Details of Crack Propagation of Beam #1
Side 2 Part B'

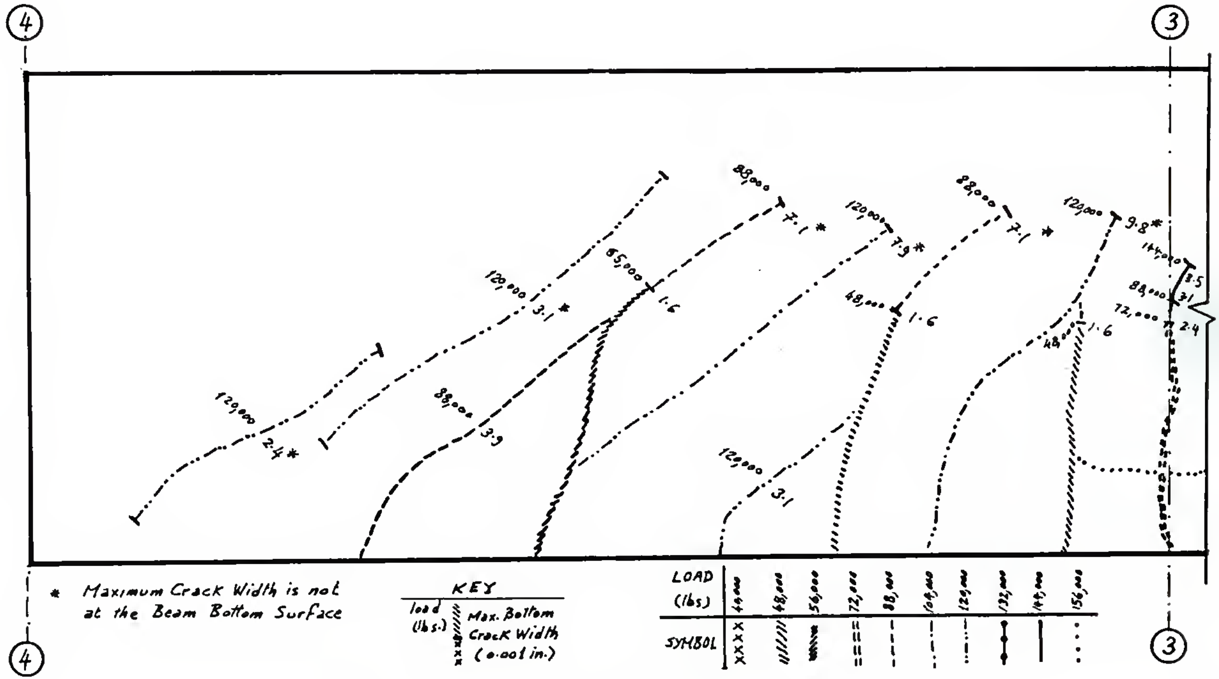

Fig. 5.41 Details of Crack Propagation of Beam #1
Side 2 Part C'

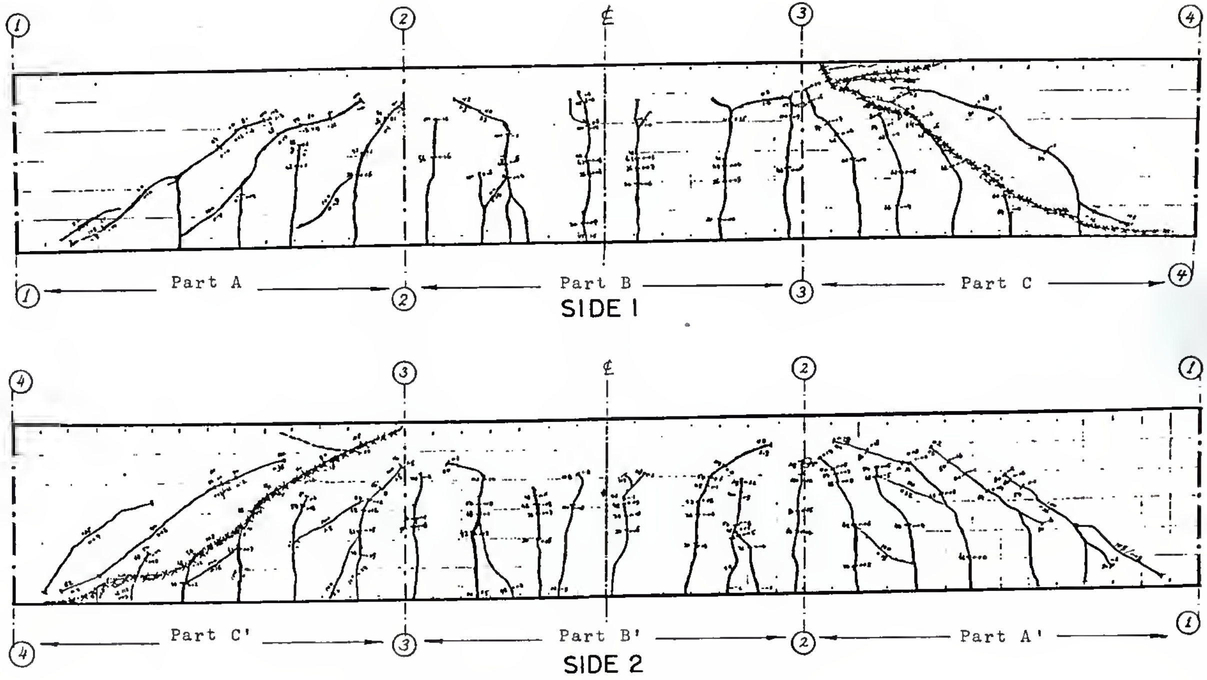

Fig. 5.42 Crack Pattern of Beam #2
(Side 1 and Side 2)

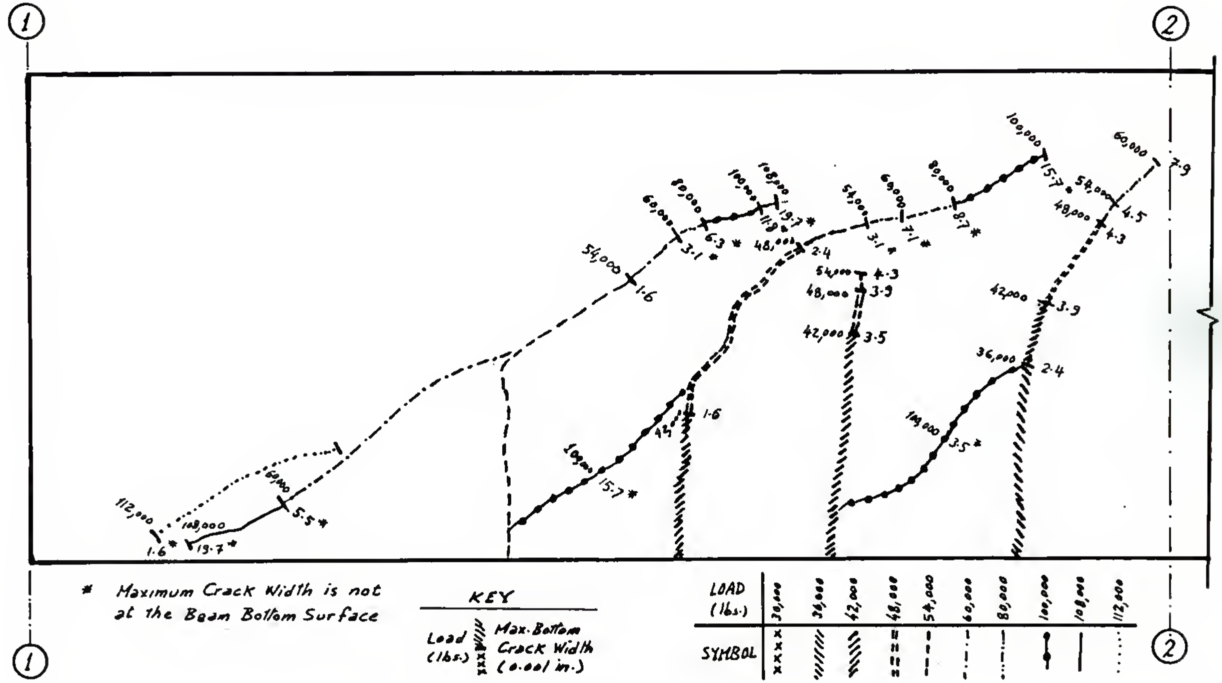

Fig. 5.43 Details of Crack Propagation of Beam #2
Side 1 Part A

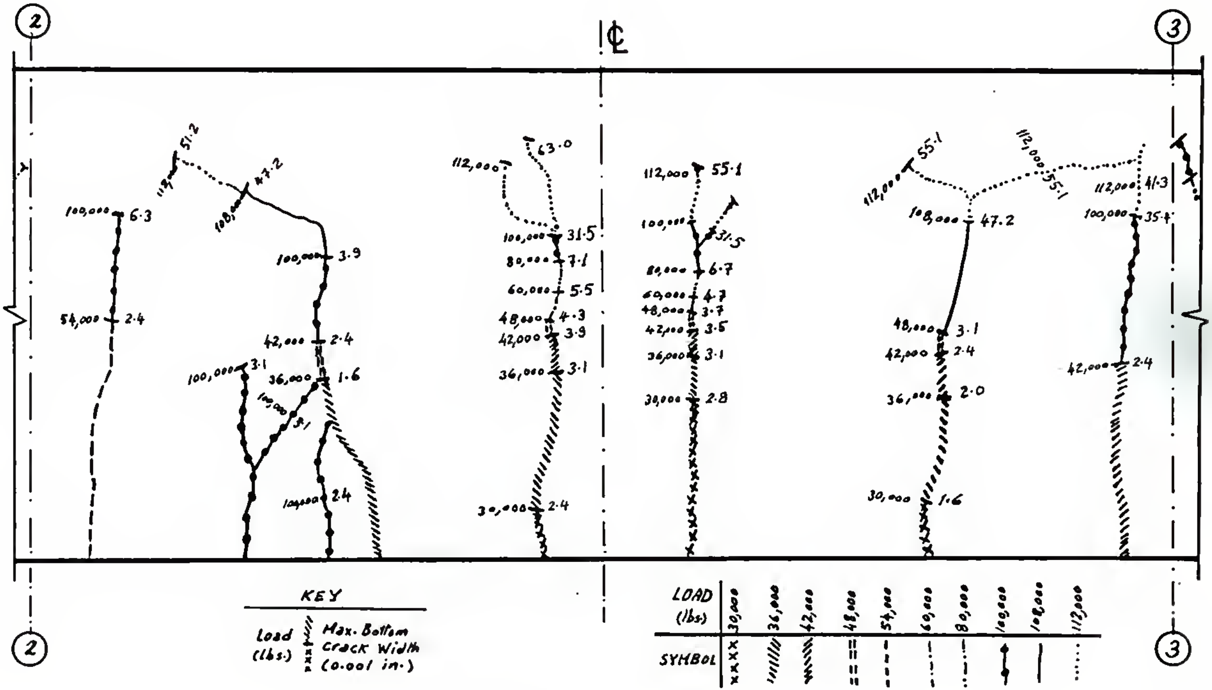

Fig: 5.44 Details of Crack Propagation of Beam #2

Side 1 Part B

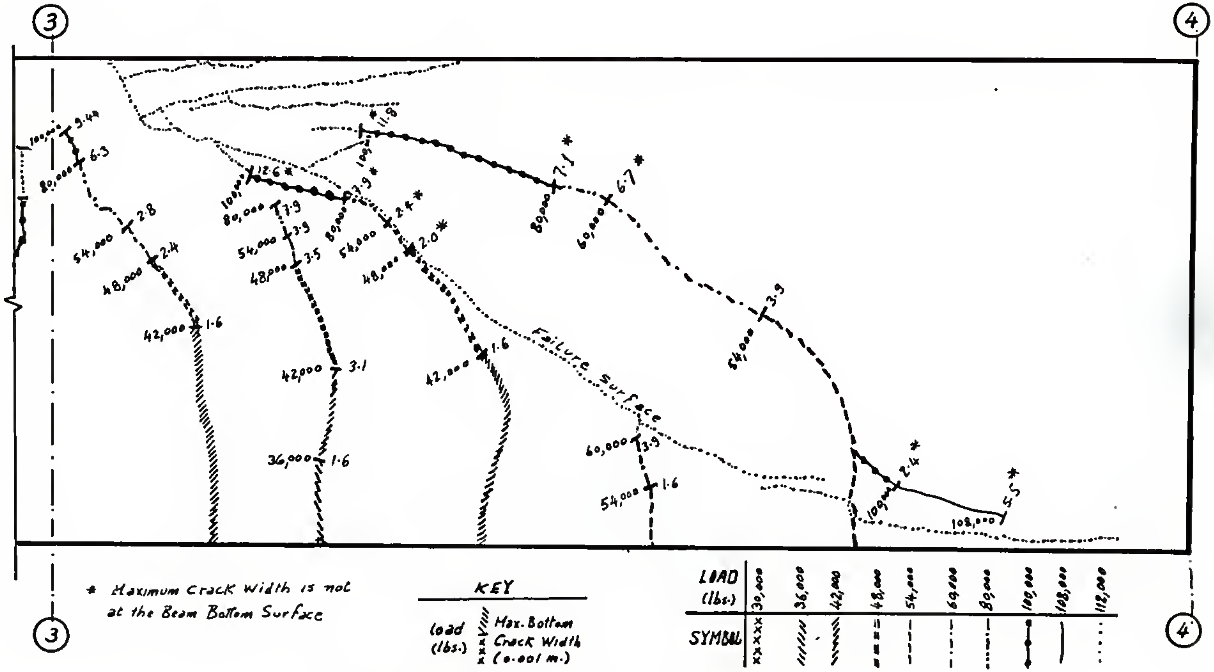

Fig. 5.45 Details of Crack Propagation of Beam #2

Side 1 Part C

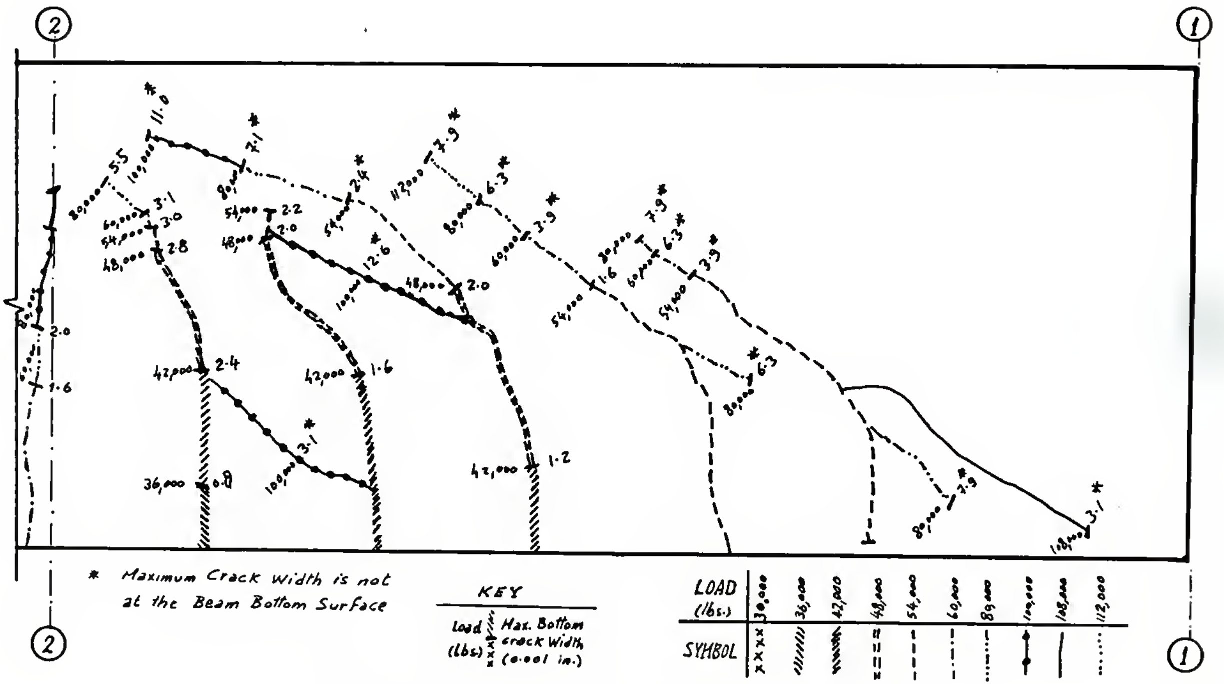

Fig. 5.46 Details of Crack Propagation of Beam #2

Side 2 Part A'

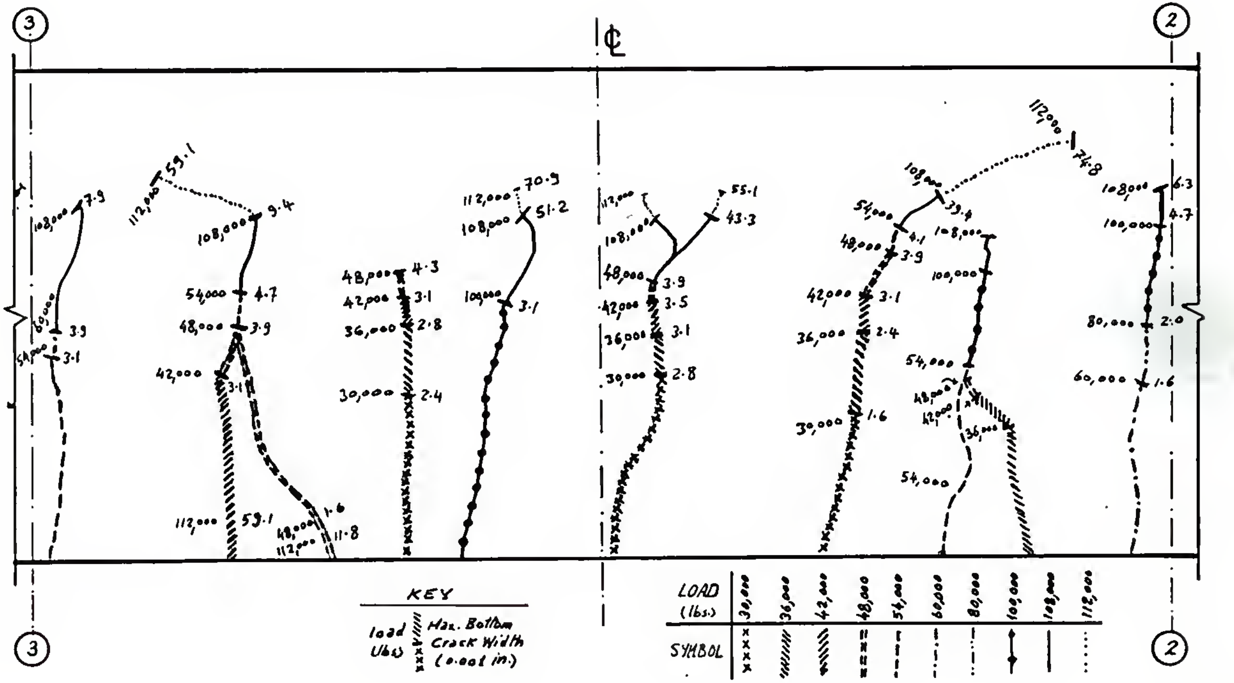

Fig. 5.47 Details of Crack Propagation of Beam #2

Side 2 Part B'

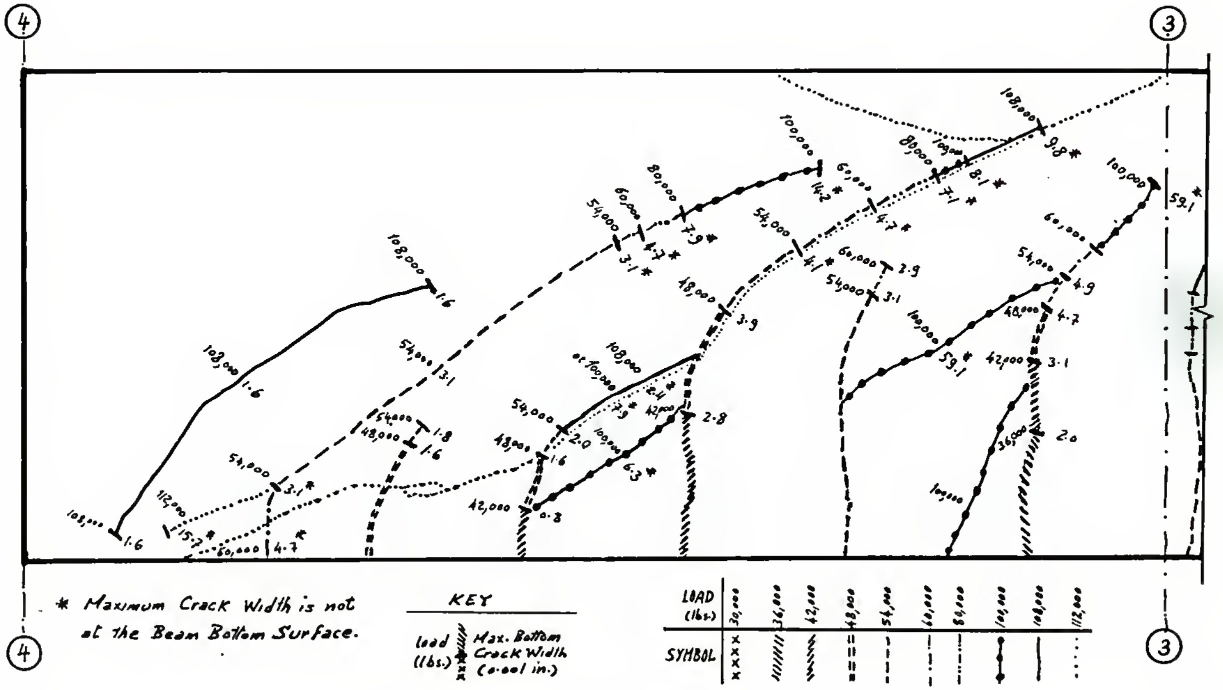

Fig. 5.48 Details of Crack Propagation of Beam #2

Side 2 Part C'

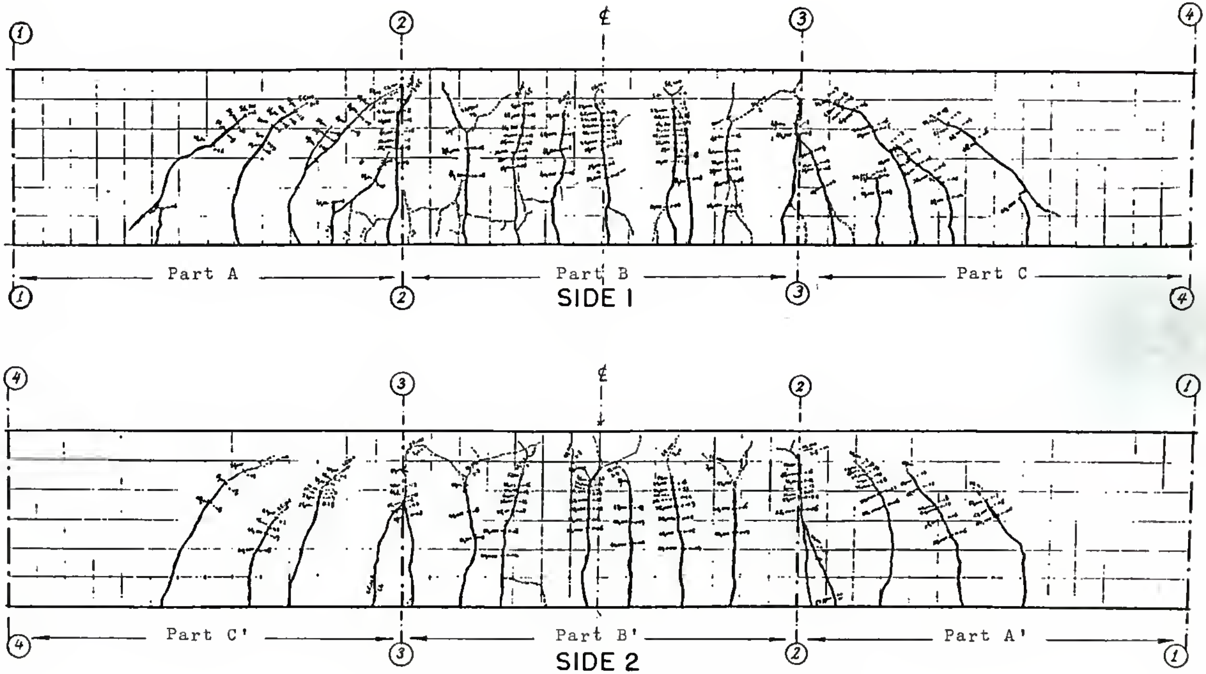

Fig. 5.49 Crack Pattern of Beam #3
(Side 1 and Side 2)

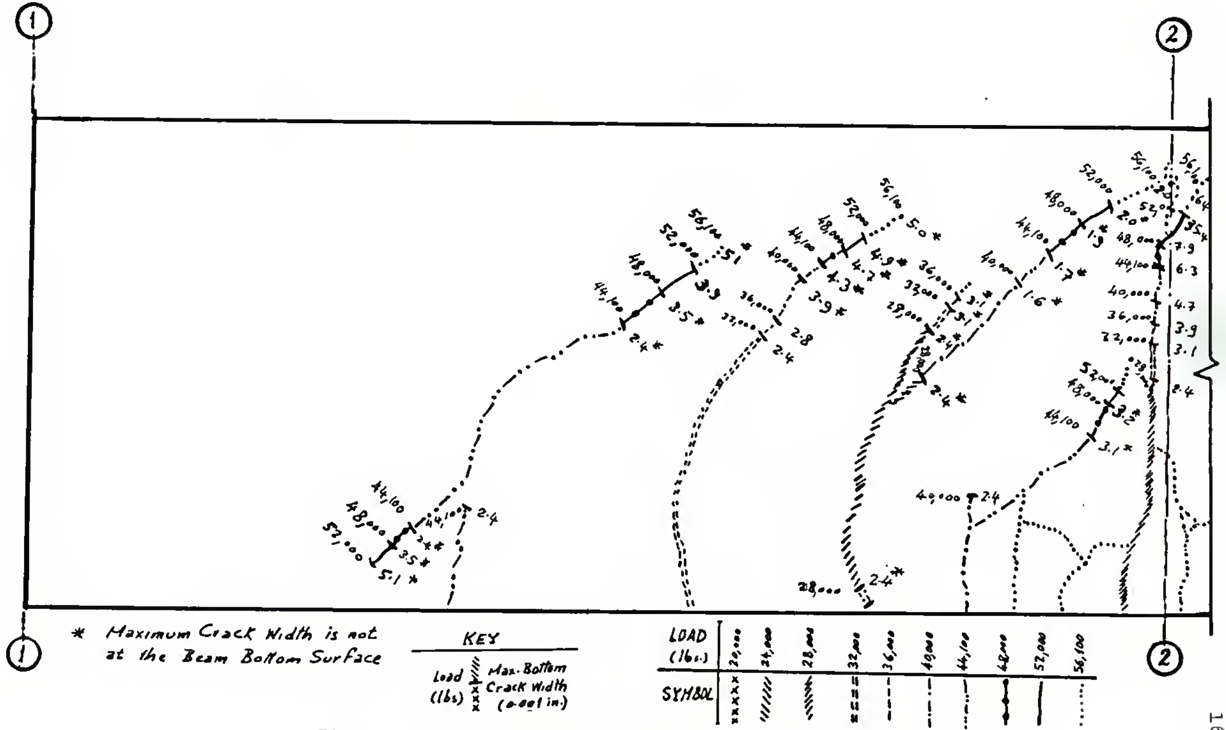

Fig. 5.50 Details of Crack Propagation of Beam #3
Side 1 Part A

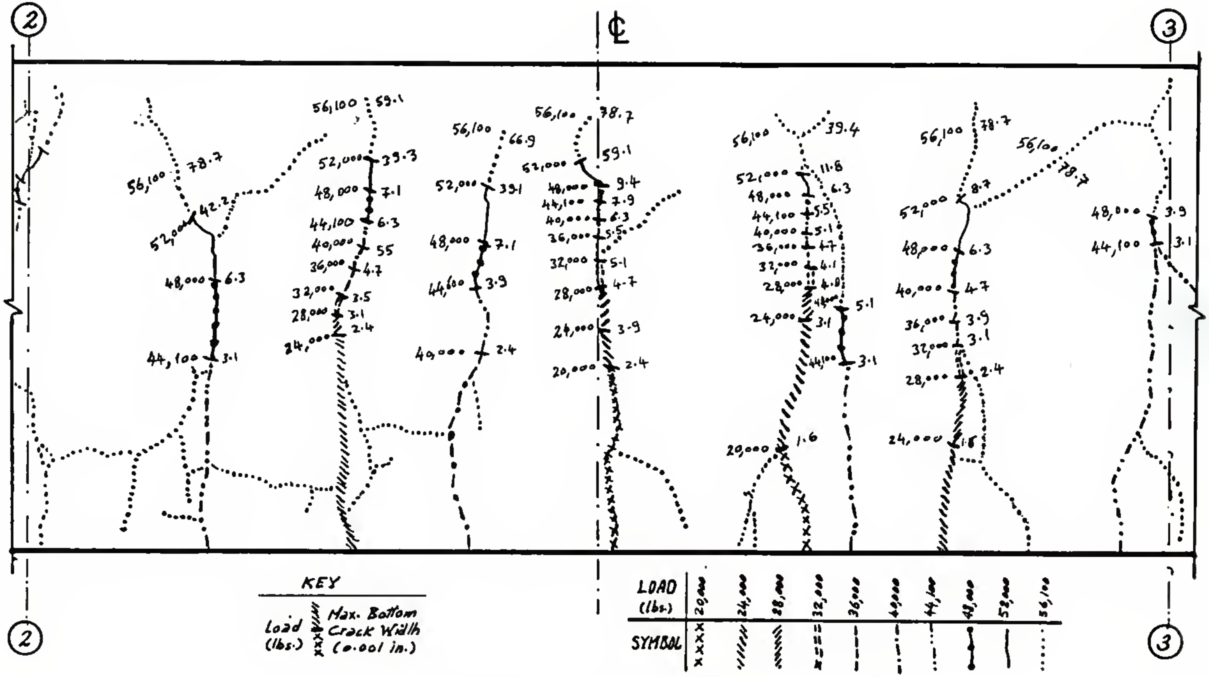

Fig. 5.51 Details of Crack Propagation of Beam #3

Side 1 Part B

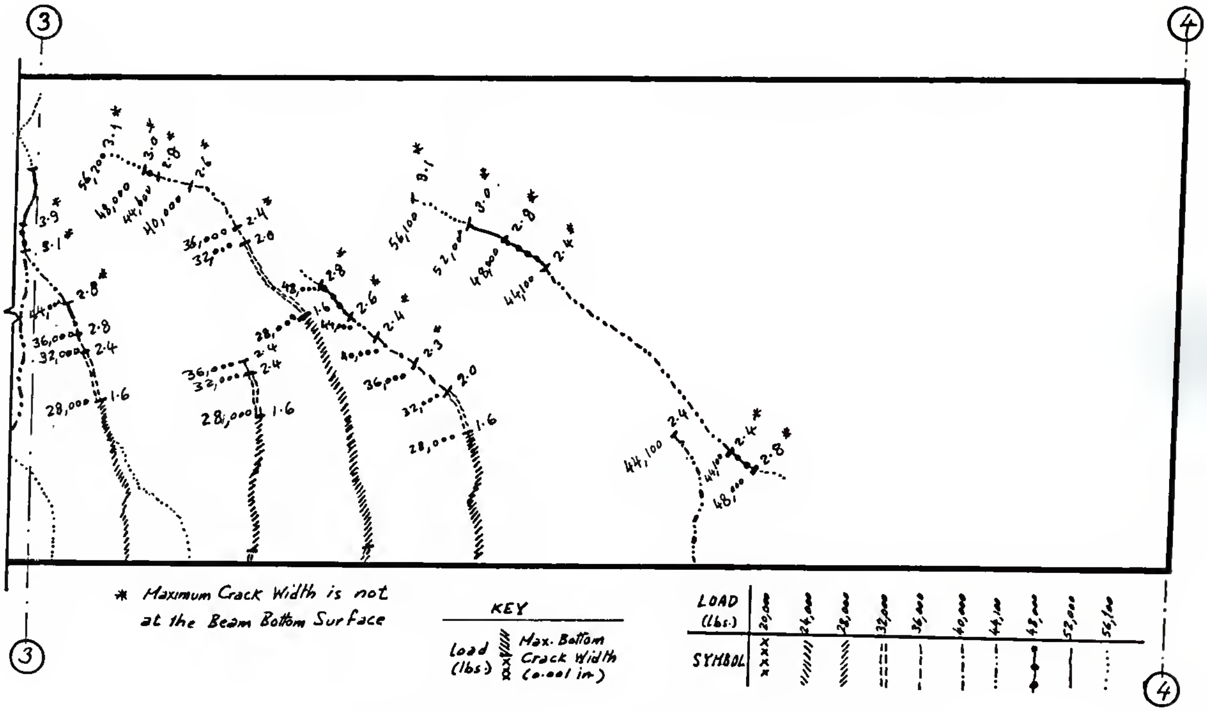

Fig. 5.52 Details of Crack Propagation of Beam #3

Side 1 Part C

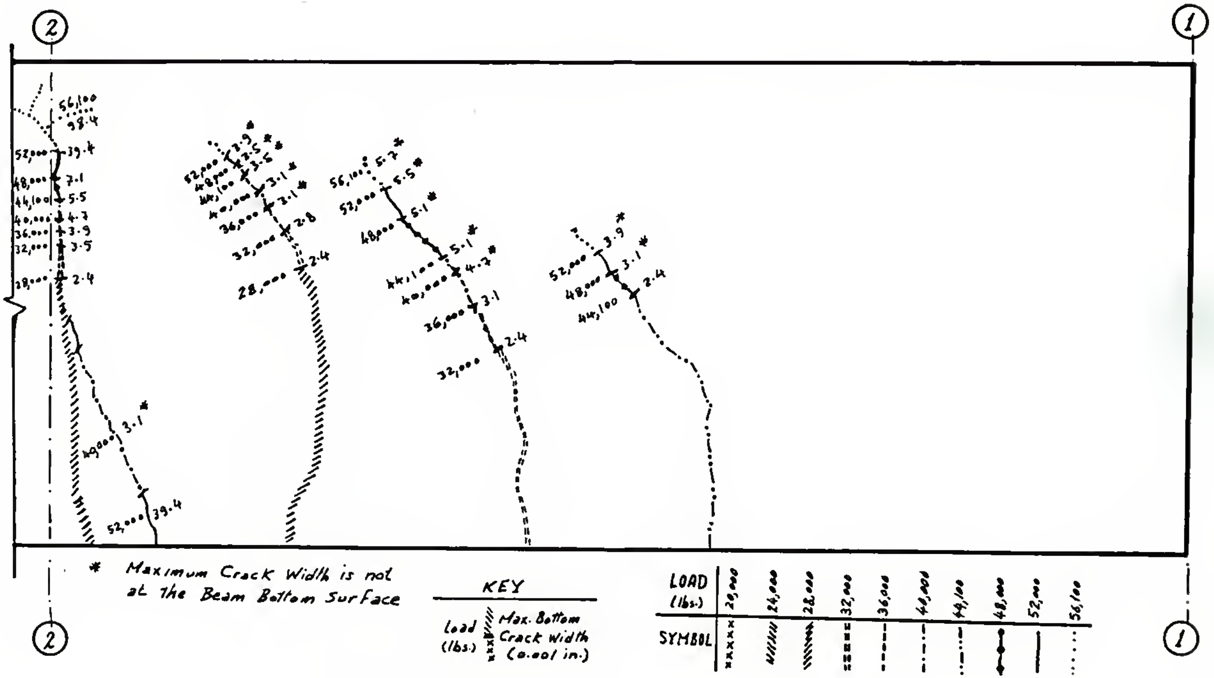

Fig. 5.53 Details of Crack Propagation of Beam #3
Side 2 Part A'

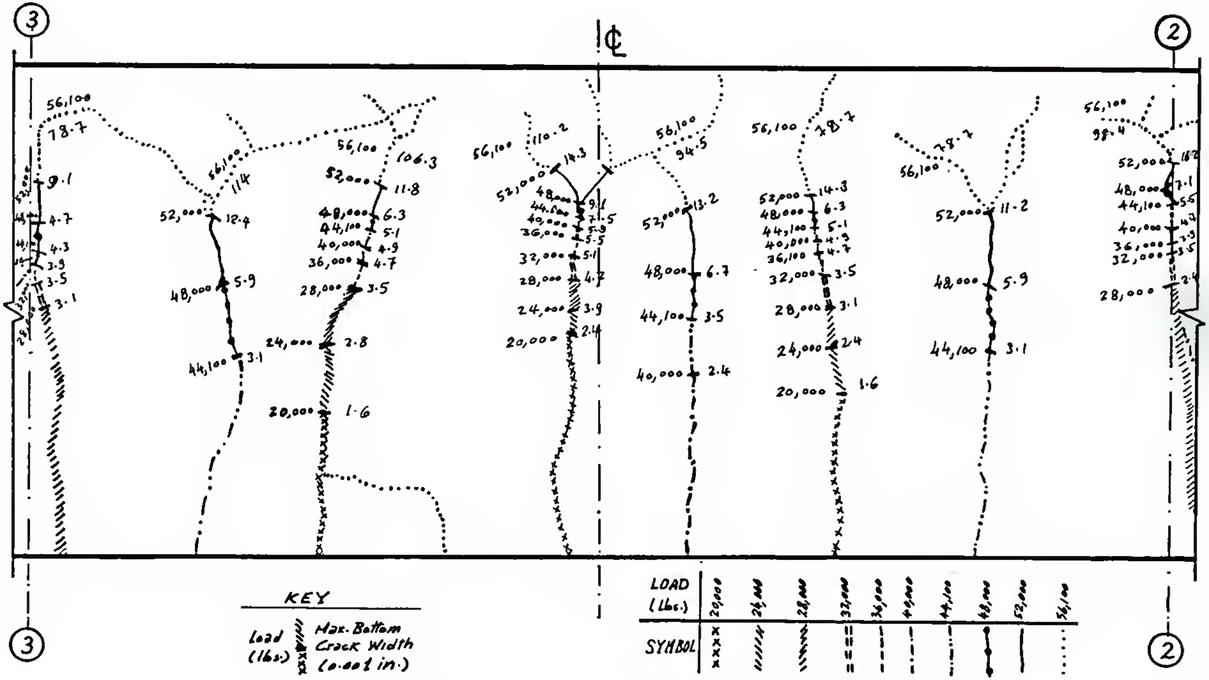

Fig. 5.54 Details of Crack Propagation of Beam #3
Side 2 Part B'

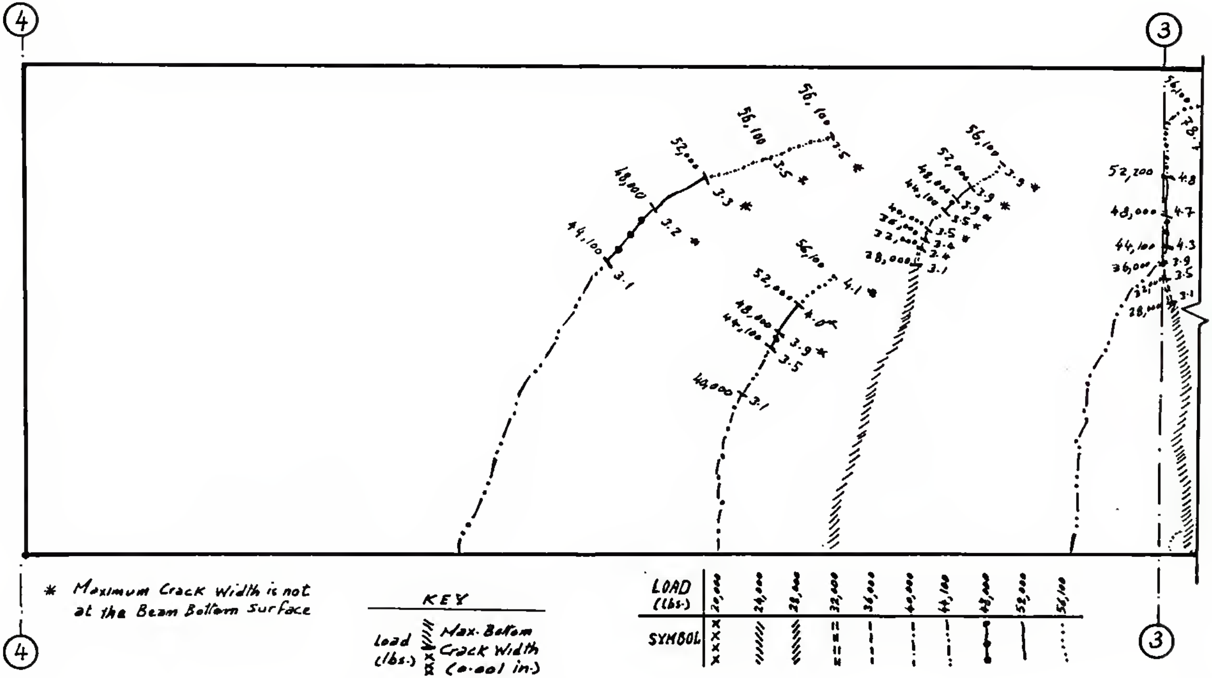

Fig. 5.55 Details of Crack Propagation of Beam #3

Side 2 Part C'

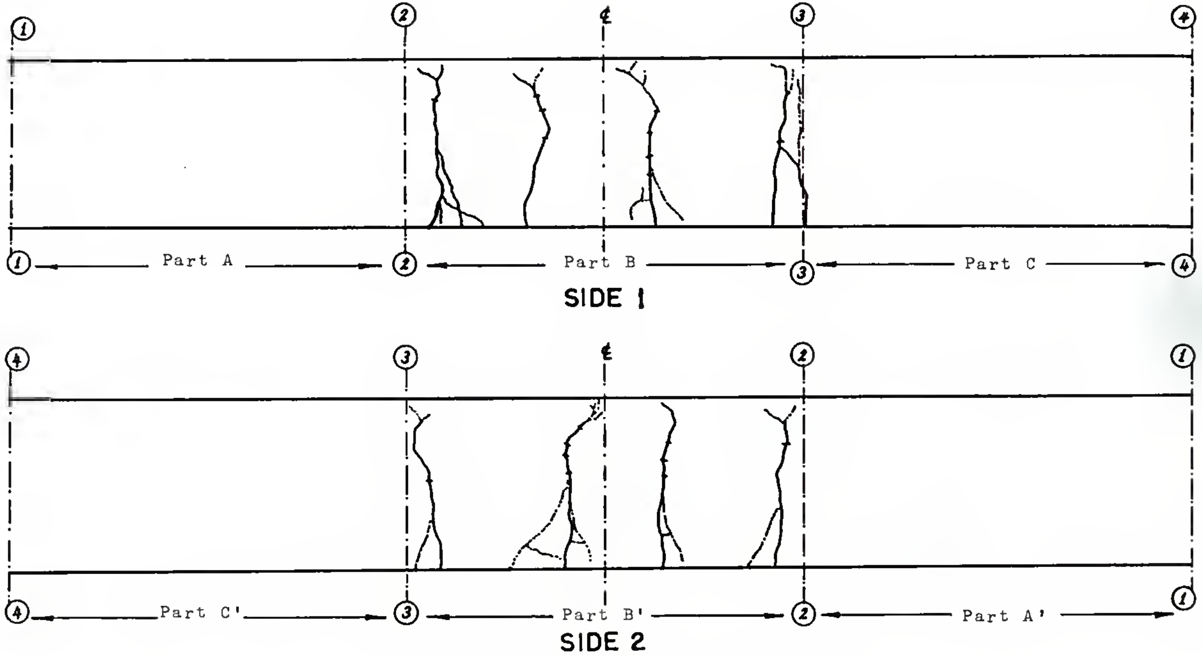

Fig. 5.56 Crack Pattern of Beam #4

(Side 1 and Side 2)

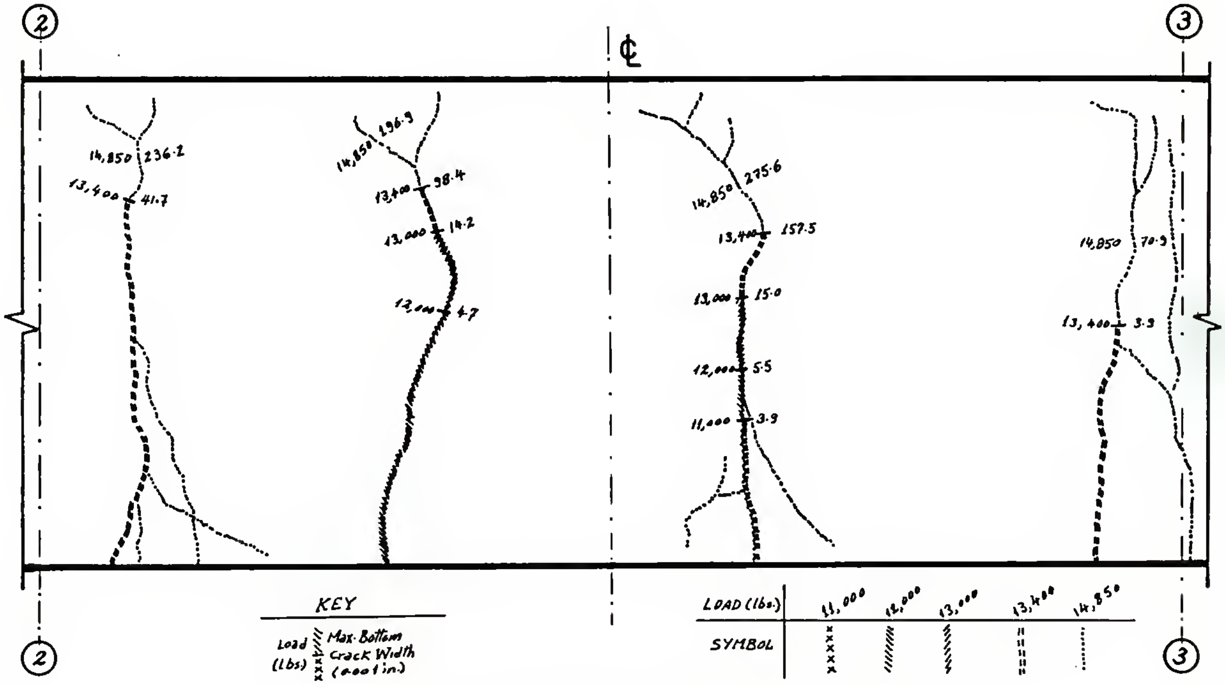

Fig. 5.57 Details of Crack Propagation of Beam #4
Side 1 Part B

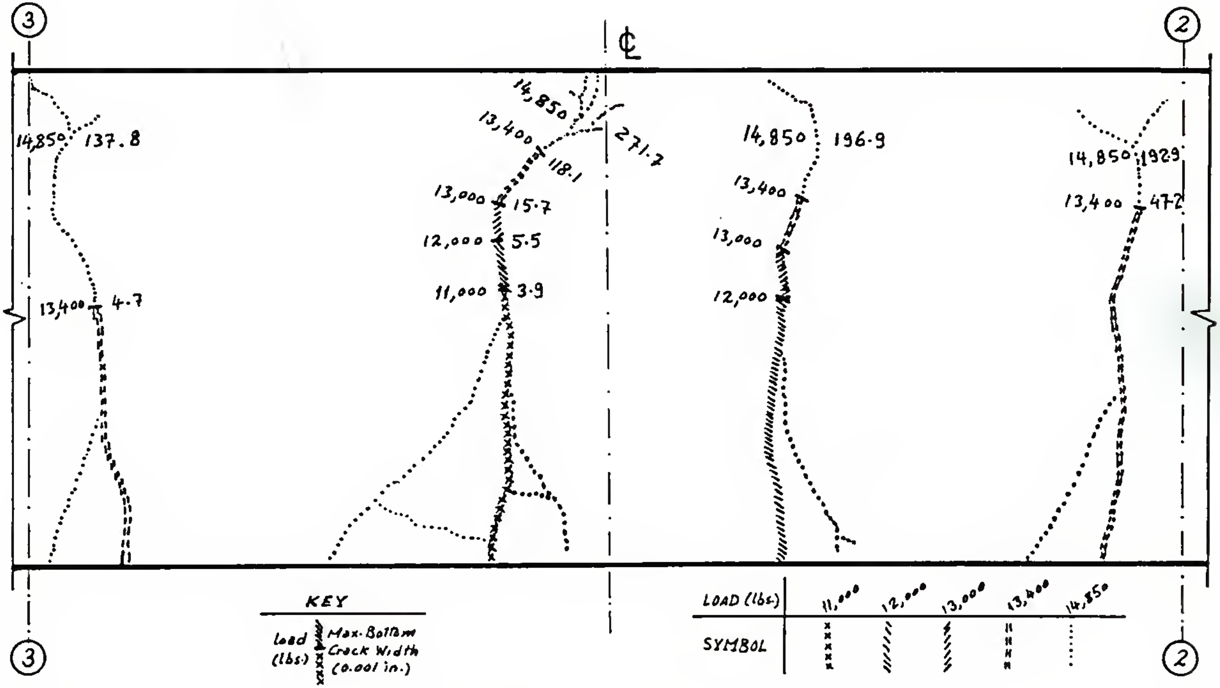

Fig. 5.58 Details of Crack Propagation of Beam #4

Side 2 Part B'

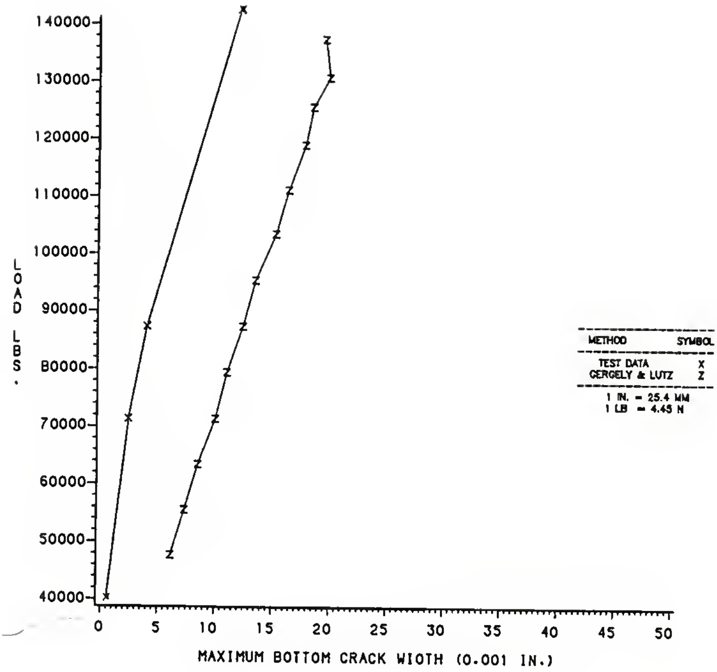

FIG. 5.59: LOAD VS. MAXIMUM BOTTOM CRACK WIDTH
OF BEAM 1

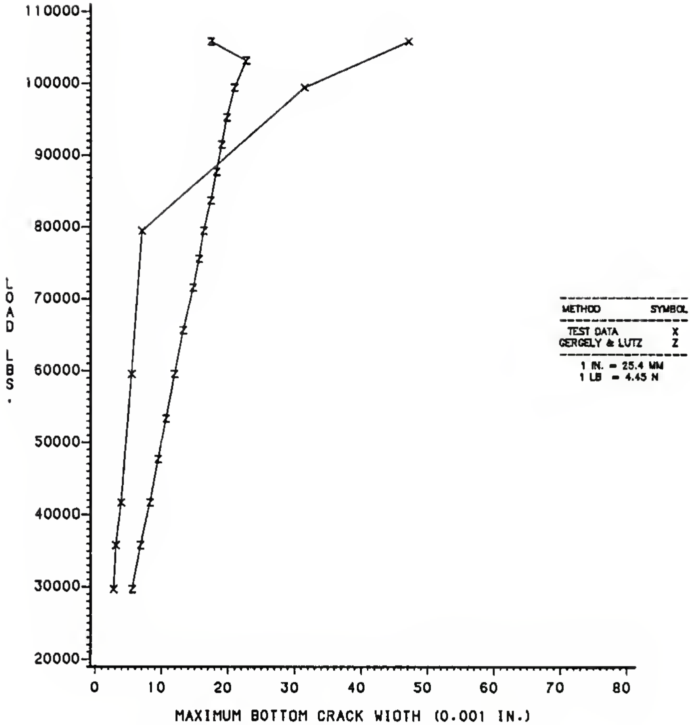

FIG. 5.60: LOAD VS. MAXIMUM BOTTOM CRACK WIDTH
OF BEAM 2

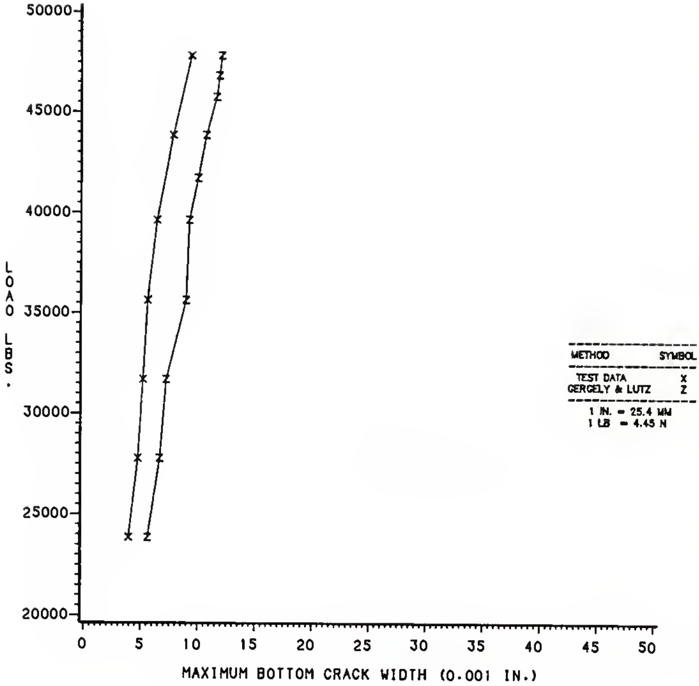

FIG. 5.61: LOAD VS. MAXIMUM BOTTOM CRACK WIDTH OF BEAM 3

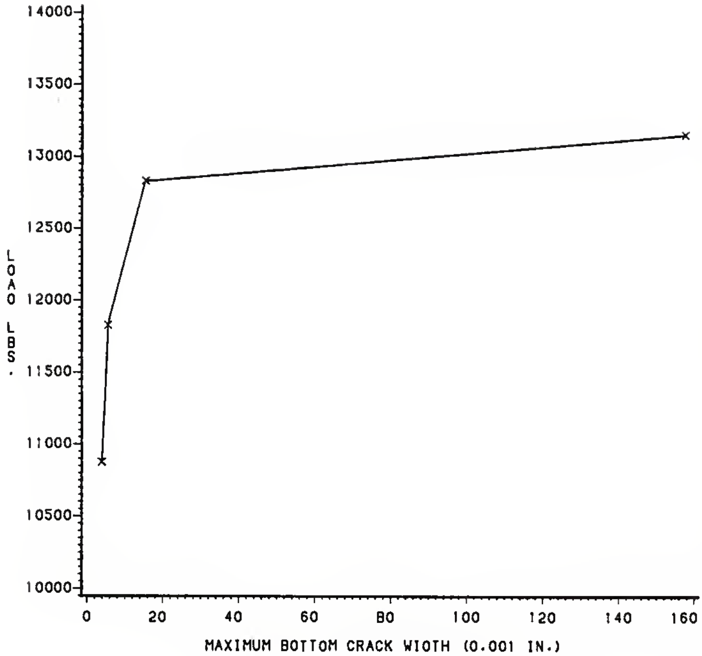

FIG. 5.62: LOAO VS. MAXIMUM BOTTOM CRACK WIOTH
OF BEAM 4
(1 IN. = 25.4 MM, 1 LB = 4.45 N)

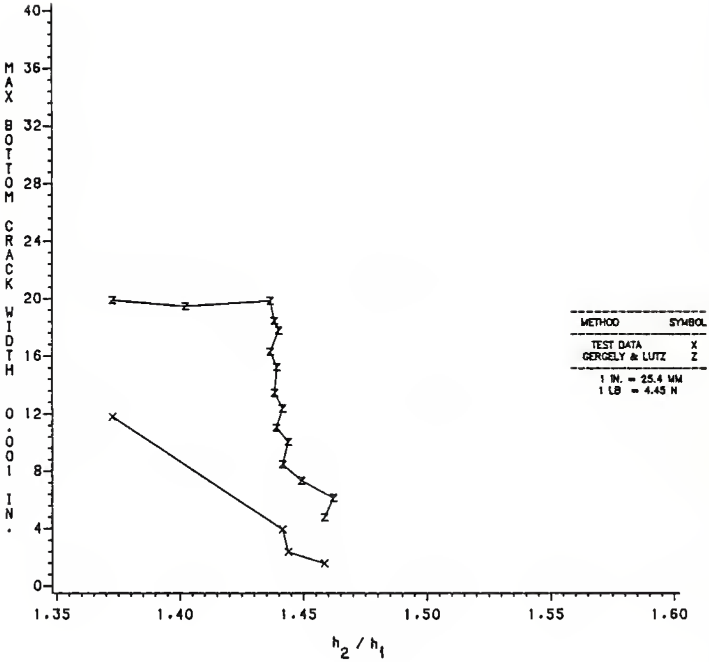

FIG. 5.63: MAXIMUM BOTTOM CRACK WIDTH VS. h_2 / h_1
OF BEAM 1

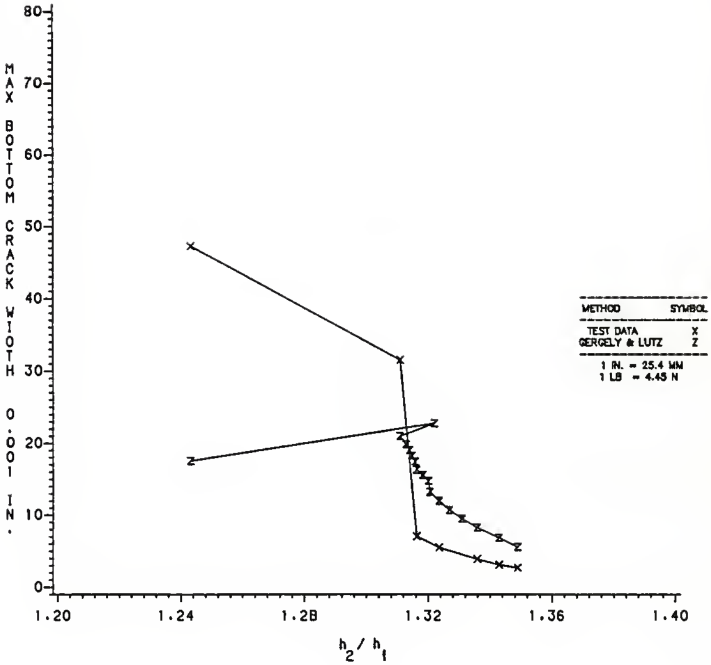

FIG. 5.64: MAX. BOTTOM CRACK WIDTH VS. h_2 / h_1 OF BEAM 2

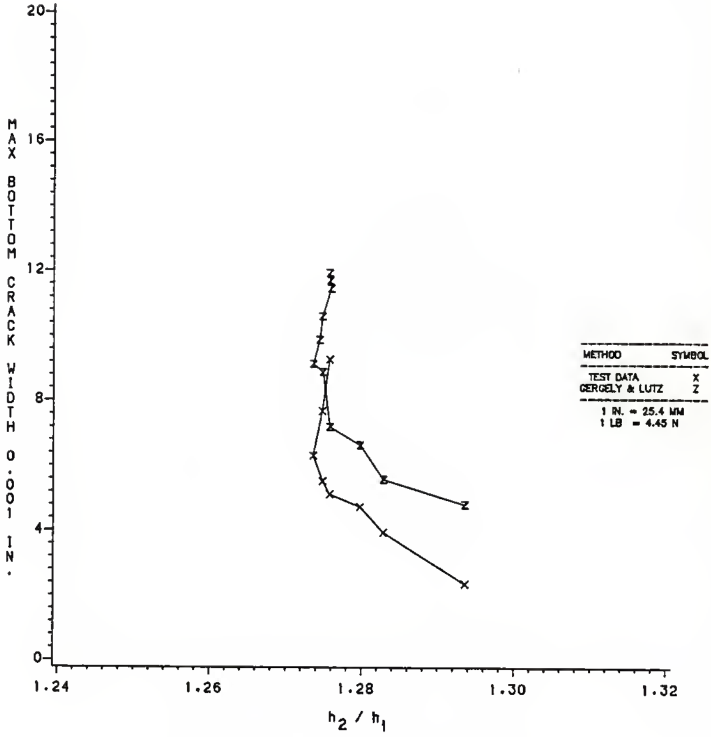

FIG. 5.65: MAX. BOTTOM CRACK WIDTH VS. h_2/h_1 OF BEAM 3

APPENDIX IV

NOTATION

a	$= \beta_a . c$	= depth of rectangnlar stress block.
A	$= A_e / m$	= Average effective concrete area aronnd a reinforcing bar.
A_e	$= 2b(t-d)$	= effective area of concrete aronnd reinforcement.
A_s		= area of tension reinforcement.
A_v		= area of shear reinforcement.
b		= width of beam.
c	$= k\ d$	= depth of nentral axis.
C		= compressive force in concrete.
d		= effective depth.
E_c		= secant modnlns of elaslicity of concrete.
E_s		= modnlns of elasticity of steel.
f_c		= streas in concrete at service load conditions.
f'_c		= compreasive strength of concrete.
f_r		= modnlns of rnptnre of concrete.
f_s		= stress in ateel at service load conditions.
f_y		= yield atress.
h_1		$= (1 - k)d$
h_2		$= t - k\ d$
I_{cr}		= moment of inertia of cracked transformed section.
I_e		= effective moment of inertia.
I_g		= gross moment of inertia.
k		= ratio of the nentral axis depth to the effective depth of beam.

L = span measured from support center lines.

m = number of steel bars.

n = modular ratio, E_s / E_c.

P = total load applied on beam.

R = h_2 / h_1

s = stirrup spacing.

t = total depth of beam.

t_b = bottom cover measured from the center of lowest bar.

T = tensile force attributable to the tension reinforcement.

V_c = shear force attributable to concrete.

V_n = ultimate shear force.

V_s = shear force attributable to stirrups.

w = maximum bottom crack width.

w/c = water - cement ratio in concrete mixture, by weight.

$\bar{y}$ = distance from the compression force C to the neutral axis.

Y_{ct} = lever arm of the internal moment of beam.

y_t = distance from the neutral axis to extreme fiber of concrete in tension.

ϵ_c = concrete strain under service load conditions.

ϵ_{cu} = concrete strain at the ultimate stress.

ϵ_y = steel strain at the yield point.

β_a = coefficient depends on support condition.

β_1 = a / c = ratio of depth of rectangular distribution to the depth of neutral axis.

Δ = vertical deflection.

ρ = steel ratio.

ACKNOWLEDGEMENTS

Many friends and colleagues have helped me successfully complete my investigation. Some have been by my side every step of the way, others have assisted me at different stages of my work. Everyone has my heart-felt-thanks, but a few people are outstanding. They are listed below.

A large thank you to Dr. Stuart E. Swartz, for his help, guidance, and attention above and beyond what is necessary for a major professor. The knowledge he passes on to his students stays with them for years to come.

A thank you to Dr. Robert R. Snell, Head of the Department of Civil Engineering, for his faith in my work and showing this faith with financial backing. Yes, computer time is expensive but I feel the results are worth it. Without his help, this project would not have been completed.

A thank you to Mr. David Abell of the Quartzite Stone Company, Inc. for his donation of quartzite for this project. Also a thank you to the Sika Company of Lyndhurst, New Jersey, for their generous donation of superplasticizer.

Thanks To Mr. Ali Nikaeen for the care he took in his ground-breaking work that provided a guide for me. Also to Mr. Tarek Refai for his help.

Special thanks go to Dr. Best, Dr. Cooper, Dr. Hn, Dr. Hodges, Dr. Williams, Mr. Jeff Crabb for all their care and help when I needed it.

Thanks are for Rnssell L. Gillespie, civil engineering technician, withont his help - no telling what wonld have happened in the lab. And a thank yon for Peggy Selvidge and Rosemary Visser.

And last bnt not by any means the least, to Cheryl Shakbona who helped me in any way she could. Without her help, nothing would have been the same. Thank you.

THE STRUCTURAL BEHAVIOR AND CRACK PATTERNS OF HIGHER STRENGTH CONCRETE BEAMS

BY

ABDEL-AZIZ A. MAKKAWY

B.S., CAIRO UNIVERSITY, 1979

AN ABSTRACT OF A MASTER'S THESIS

SUBMITTED IN PARTIAL FULFILLMENT

OF THE REQUIREMENTS FOR THE DEGREE

MASTER OF SCIENCE

DEPARTMENT OF CIVIL ENGINEERING

KANSAS STATE UNIVERSITY

MANHATTAN, KANSAS

1986

ABSTRACT

The many differences in conclusions about the behavior of higher strength concrete make it appropriate for further investigation. The study of the shape of compressive stress block, the ultimate concrete strain, the vertical deflection and the crack propagation and width are the main objectives to be investigated in this research.

Concrete with nominal compressive strength of 12,000 psi was used to build four reinforced beams with a span of seven feet and a cross - sectional dimension of 8 inch x 12 inch. The beams were reinforced with grade 60 steel reinforcing bars. Four different steel ratios; ρ_b, 0.59 ρ_b, 0.26 ρ_b and 0.07 ρ_b were used for the different beams.

From the test results it was concluded that the rectangular stress block can be used in moment calculations for higher strength concrete beams. Test data indicated that the ultimate strain for higher strength concrete was always in the range of 0.0023 to 0.003 in./in. Both the ACI approach and Pretorius approach for calculating vertical deflection are not conservative. It is also concluded that the Gergely and Lutz formula for maximum bottom crack width gives conservative values for higher strength concrete.